

# Parity- and time-reversal-violating nuclear forces

J. de Vries<sup>1,2</sup>, E. Epelbaum<sup>3</sup>, L. Girlanda<sup>4,5</sup>, A. Gnech<sup>6</sup>, E. Mereghetti<sup>7</sup>,  
M. Viviani<sup>8,\*</sup>,

<sup>1</sup> *Amherst Center for Fundamental Interactions, Department of Physics, University of Massachusetts, Amherst, MA, USA*

<sup>2</sup> *RIKEN BNL Research Center, Brookhaven National Laboratory, Upton, New York, NY, USA*

<sup>3</sup> *Ruhr-Universität Bochum, Fakultät für Physik und Astronomie, Institut für Theoretische Physik II, Bochum, Germany*

<sup>4</sup> *Department of Mathematics and Physics, University of Salento, Lecce, Italy*

<sup>5</sup> *INFN-Lecce, Lecce, Italy*

<sup>6</sup> *Gran Sasso Science Institute, L'Aquila, Italy*

<sup>7</sup> *Theoretical Division, Los Alamos National Laboratory, Los Alamos, NM, USA*

<sup>8</sup> *INFN-Pisa, Pisa, Italy*

emails: M. Viviani

INFN-Pisa, Largo B. Pontecorvo 3, I-56127 Pisa, Italy  
michele.viviani@pi.infn.it

## ABSTRACT

Parity-violating and time-reversal conserving (PVTC) and parity-violating and time-reversal-violating (PVTV) forces in nuclei form only a tiny component of the total interaction between nucleons. The study of these tiny forces can nevertheless be of extreme interest because they allow to obtain information on fundamental symmetries using nuclear systems. The PVTC interaction derives from the weak interaction between the quarks inside nucleons and nuclei and the study of PVTC effects opens a window on the quark-quark weak interaction. The PVTV interaction is sensitive to more exotic interactions at the fundamental level, in particular to strong CP violation in the Standard Model Lagrangian, or even to exotic phenomena predicted in various beyond-the-Standard-Model scenarios. The presence of these interactions can be revealed either by studying various asymmetries in polarized scattering of nuclear systems, or by measuring the presence of non-vanishing permanent electric dipole moments of nucleons, nuclei and diamagnetic atoms and molecules. In this contribution, we review the derivation of the nuclear PVTC and PVTV interactions within various frameworks. We focus in particular on the application of chiral effective field theory, which allows for a more strict connection with the fundamental interactions at the quark level. We investigate PVTC and PVTV effects induced by these potential on several few-nucleon observables, such as the longitudinal asymmetry in proton-proton scattering and radiative neutron-proton capture, and the electric dipole moments of the deuteron and the trinucleon system.

**Keywords:** Fundamental symmetries in nuclei, nuclear forces, effective field theory, chiral perturbation theory, few-body systems

## 1 INTRODUCTION

The interaction between nucleons is at the heart of nuclear physics and has been a subject of great scientific interest since many decades. The strong nuclear forces have their origin in the residual interaction between quarks and gluons inside colorless nucleons and are described by quantum chromodynamics (QCD). The resulting parity-conserving, time-reversal-conserving (PCTC) nuclear interactions are known to exhibit a complicated pattern with a delicate interplay of strongly state-dependent repulsive and attractive pieces. While the nucleon-nucleon (NN) scattering data below the pion production threshold can nowadays be accurately described by modern NN potentials, the (weaker) three-nucleon (3N) forces and the electromagnetic interactions (EM) between the nucleons, known to play an important role in the nuclear structure and dynamics, are not so well understood and subject of active research. The current status of PCTC nuclear forces is reviewed in other contributions to this topical issue.

In addition to the bulk PCTC interactions mentioned above, nuclear forces also feature much tinier components, which originate from the weak forces between quarks and/or physics beyond the standard model (BSM) and whose strength is smaller than that of the strong and EM interactions by many orders of magnitude. These tiny components are, nevertheless, extremely interesting since investigation of their effects may shed new light on fundamental symmetries and BSM physics. While effects of such exotic PCTC components are, of course, completely overwhelmed by the strong and EM nuclear forces, parity- (P) violating and/or time-reversal- (T) violating nuclear interactions can be determined by measuring specific observables which would vanish if these symmetries were conserved. In this contribution, we review the theory of parity-violating, time-reversal-conserving (PVTC) and parity-violating, time-reversal-violating (PVTV) nuclear forces and discuss selected applications.

Starting from the fifties of the last century, a wide variety of phenomenological models have been developed to describe nuclear forces, the most prominent utilizing the one-boson exchange picture, see Ref. [1] and references therein. More recently, the development of chiral effective field theory ( $\chi$ EFT) [2] has given a new impetus to the derivation of nuclear interactions [3, 4, 5]. The  $\chi$ EFT approach utilizes the spontaneously broken approximate  $SU(2)_L \times SU(2)_R$  chiral symmetry of QCD<sup>1</sup> in order to describe low-energy dynamics of pions, the (pseudo-) Goldstone bosons of the spontaneously broken axial generators, in a systematic and model-independent fashion within the framework of the effective chiral Lagrangian [6, 7, 8, 9, 10, 11], see Refs. [12, 13, 14] for review articles. Owing to the derivative nature of the Goldstone boson interactions, the scattering amplitude in the pion- and single-baryon sectors can be calculated via a perturbative expansion in powers of  $Q/\Lambda_\chi$ , where  $Q$  refers to momenta of the order of the pion mass  $m_\pi$  and  $\Lambda_\chi \sim m_\rho \sim 1$  GeV denotes the chiral symmetry breaking scale, with  $m_\rho$  the  $\rho$ -meson mass. The effective Lagrangian involves (an infinite number of) all possible hadronic interactions compatible with the symmetries of QCD, which are naturally organized according to the number of derivatives and/or quark or pion mass insertions.<sup>2</sup> Every term in the effective Lagrangian is multiplied with a coefficient, whose strength is not fixed by the symmetry. These so-called low-energy constants (LECs) can be determined by fits to experimental data and/or obtained from lattice QCD simulations, see [13, 14] and references therein. At every order in the  $Q/\Lambda_\chi$ -expansion, only a finite number of terms from the effective Lagrangian contributes to the scattering amplitude. The resulting framework, commonly referred to as chiral perturbation theory ( $\chi$ PT), is nowadays widely applied to analyze low-energy processes in the Goldstone boson and single-nucleon sectors. It has also been

<sup>1</sup> Here and in what follows, we restrict ourselves to the two-flavor case of the light up and down quarks unless specified otherwise.

<sup>2</sup> In the isospin limit, the quark and pion masses are related to each other via  $m_\pi^2 = 2Bm_q + \mathcal{O}(m_q^2)$ , where  $B$  is a constant proportional to the quark condensate  $\langle 0|\bar{u}u|0\rangle = \langle 0|\bar{d}d|0\rangle$ .

generalized to study few- and many-nucleon systems, where certain resummations beyond perturbation theory are necessary in order to dynamically generate the ultrasoft scale associated with nuclear binding. According to [2], the breakdown of the perturbative expansion for the NN scattering amplitude is traced back to enhanced contributions of ladder diagrams, i.e. Feynman diagrams that become infrared divergent in the static limit of infinitely heavy nucleons. The simplest and natural way to resum enhanced ladder diagrams is provided by solving the nuclear Schrödinger equation. The framework therefore essentially reduces to the conventional quantum mechanical  $A$ -body problem. The corresponding nuclear forces and current operators are defined in terms of non-iterative parts of the scattering amplitude, which are free from the above mentioned enhancement. They can be derived from the effective chiral Lagrangian in a systematically improvable way via a perturbative expansion in powers of  $Q/\Lambda_\chi$  [4, 5]. Assuming the scaling of few-nucleon contact operators according to naive dimensional analysis<sup>3</sup>, the PCTC interactions are dominated by the pairwise NN force, which receives its dominant contribution at order  $(Q/\Lambda_\chi)^\nu$  with  $\nu = 0$ , defined to be the leading order (LO). Parity conservation forbids the appearance of nuclear forces at order  $\nu = 1$ , so that the next-to-leading order (NLO) contribution to the PCTC NN potential appears at order  $\nu = 2$ . Next-to-next-to-leading order (N<sup>2</sup>LO) has  $\nu = 3$  and so on. PCTC three- and four-nucleon forces are suppressed and start contributing at orders  $\nu = 3$  (N<sup>2</sup>LO) and  $\nu = 4$  (N<sup>3</sup>LO), respectively. Presently, the chiral expansion of the PCTC NN force has been pushed to order  $\nu = 5$  (N<sup>4</sup>LO) [16, 17, 18, 19], while many-nucleon interactions have been worked out up through N<sup>3</sup>LO, see [4, 5] and references therein. We further emphasize that a number of alternative formulations of  $\chi$ EFT for nuclear systems have been proposed [20, 21, 22, 23, 24, 25], see also Refs. [26, 27, 28, 29, 30, 31] for a related discussion.

Another framework to analyze nuclear systems at very low energies is based on the so-called pionless formulation of EFT, see Refs. [32, 33, 31] for review articles. It is valid at momenta well below the pion mass, at which the pionic degrees of freedom can be integrated out. In the resulting picture, nucleons interact with each other solely through short-range contact two- and many-body forces. This formulation is considerably simpler than  $\chi$ EFT both at the conceptual and practical levels, and has been successfully applied to study e.g. Efimov physics and universality in few-body systems near the unitary limit, low-energy properties of halo-nuclei and reactions of astrophysical relevance, see Refs. [32, 33, 31] and references therein.

In this paper we focus on the PVTC and PVTV interactions in the frameworks of  $\chi$ EFT and pionless EFT. We also outline various meson-exchange models frequently adopted to analyze the results for some PVTC and PVTV observables. In the subsections below, we briefly discuss the origin of the PVTC and PVTV interactions and summarize the current experimental and theoretical status of research along these lines.

## 1.1 The PVTC interaction

The PVTC component of the nuclear force is governed by the weak interaction between the quarks inside the nucleons (and pions). Studying such effects, therefore, opens a window on the so-called “pure” hadronic weak interaction (HWI) [34, 35, 36, 37, 38]. This part of the weak interaction is far less known experimentally.

<sup>3</sup> Notice that for systems near the unitary limit corresponding to the infinitely large scattering length (such as e.g. the NN systems in the S-waves), the scattering amplitude exhibits a certain amount of fine tuning beyond naive dimensional analysis. The expansion of the scattering amplitude does, therefore, not necessarily coincide with the expansion of nuclear potentials [15].

A number of experiments aimed at studying PVTC in low-energy processes involving few-nucleon systems have been completed/are being planned at cold-neutron facilities, such as the Los Alamos Neutron Science Center (LANSCE), the National Institute of Standards and Technology (NIST) Center for Neutron Research, the Spallation Neutron Source (SNS) at Oak Ridge National Laboratory, and the European Spallation Source (ESS) in Lund. The primary objective of this experimental program is to determine the LECs which appear in the PVTC nuclear potentials. For a recent review of the current status of experiments along this line and the impact of anticipated results see Ref. [39].

PVTC nuclear forces have already been analyzed in the framework of  $\chi$ EFT [40, 41, 42]. The LO PVTC NN force is driven by the one-pion-exchange term with  $\nu = -1$ , while the NLO terms with  $\nu = 1$  emerge from two-pion-exchange diagrams and NN contact interactions<sup>4</sup>. In Ref. [44], it was shown that the PVTC NN potential involves only five independent contact operators at this order corresponding to five S-P transition amplitudes at low energies [45]. Including the PVTC pion-nucleon coupling constant  $h_{\pi}^1$ , the NN potential at NLO thus contains six LECs which need to be determined from experimental data. At N<sup>2</sup>LO one has to take into account five additional LECs, which determine the strength of the subleading PVTC pion-nucleon interactions [46].

In pionless EFT, the LO PVTC NN potential is completely described in terms of the already mentioned five contact terms [36, 47]. The large- $N_c$  scaling of PVTC NN contact interactions was analyzed in Refs. [48, 47]. These studies suggest that three out of five PVTC contact interactions are suppressed by a factor of  $(1/N_c)^2$  or by the factor  $\sin^2 \theta_W \approx 0.23$ , see also a related discussion in [49]. If the large- $N_c$  scaling persists to the physically relevant case of  $N_c = 3$ , the pionless potential at LO should be dominated by only 2 LECs [39]. Unfortunately, the currently available experimental data do not allow one to draw definitive conclusions on whether the suggested large- $N_c$  hierarchy of PVTC contact interactions is indeed realized in Nature.

Regarding the various meson-exchange models developed to describe the PVTC interaction, we will mainly discuss the model proposed by Desplanques, Donoghue, and Holstein (DDH) [50] which includes pion and vector-meson exchanges with seven unknown meson-nucleon PVTC coupling constants.

## 1.2 The PVTV interaction

PVTV nuclear forces originate from more exotic sources at the fundamental level, which include the so-called  $\theta$ -term in the Standard Model (SM) Lagrangian [51], or even BSM interactions [52]. Due to the CPT theorem, any PVTV interaction also violates the CP symmetry, where C refers to charge conjugation. CP violation is a key ingredient for the dynamical generation of a matter-antimatter asymmetry in the Universe [53]. The SM with three generations of quarks has a natural source of CP-violation in the phase of the Cabibbo-Kobayashi-Maskawa (CKM) quark mixing matrix. This mechanism is however not sufficient for explaining the observed asymmetry [54].

The phase of the CKM matrix also does not contribute sizably to the nuclear PVTV interaction. For example, let us consider the electric dipole moment (EDM) of a system of particles. A nonzero permanent EDM of a particle or a system of particles necessarily involves the breaking of the parity and time-reflection symmetries. EDMs of the electron, nucleons and nuclei are mostly sensitive to P- and T-violating flavor-diagonal interactions. To induce a non-zero EDM, on the other hand, the phase of the CKM requires contributions from all three generations of quarks, including heavy quarks, leading to a large suppression [52, 55, 56, 57]. For example, the expected size of the nucleon EDM based on the CKM

<sup>4</sup> Notice that PVTC hadronic interactions involve a typical suppression factor of  $\sim G_F M_{\pi}^2 \sim 10^{-7}$  as compared to PCTC vertices [43].

mechanism in the SM is  $|d_N^{\text{CKM}}| \sim 10^{-18} e \text{ fm}$  [58, 59]. Therefore, any observed permanent EDM of an atomic or nuclear system larger in magnitude than the expected size within the SM would highlight PVTV effects beyond the CKM mixing matrix. The present experimental upper bounds on the EDMs of neutron and proton are  $|d_n| < 3.0 \cdot 10^{-13} e \text{ fm}$  [60, 61] and  $|d_p| < 2.0 \cdot 10^{-12} e \text{ fm}$ , where the proton EDM has been inferred from a measurement of the diamagnetic  $^{199}\text{Hg}$  atom [62] using a calculation of the nuclear Schiff moment [63]. For the electron, the most recent upper bound is  $|d_e| < 1.1 \cdot 10^{-16} e \text{ fm}$  [64], derived from the EDM of the ThO molecule. In all cases, the current experimental sensitivities are orders of magnitude away from CKM predictions.

$\chi\text{EFT}$  allows to derive PVTV nuclear forces in a systematic and model independent way. To this aim, the PCTC effective chiral Lagrangian has to be extended to include all possible PVTV terms classified according to their chiral dimension. Some of these terms are induced, at the microscopic level, by the SM mechanisms discussed above. The effective chiral Lagrangian induced by the  $\theta$ -term is discussed in Refs. [65, 66]. BSM theories such as supersymmetry, multi-Higgs scenarios, left-right symmetric model *etc.* would give rise to additional PVTV sources of dimension six (and higher) in the quark-gluon Lagrangian [67]. The  $\chi\text{EFT}$  Lagrangians originating from these sources were derived in Refs. [68, 69]. Various terms in the resulting effective chiral Lagrangian possess different scaling with respect to the underlying microscopic PVTV sources.  $\chi\text{EFT}$  can thus be used to establish relations between the fundamental PVTV mechanisms and specific terms in the nuclear potentials and, accordingly, specific pattern in the corresponding nuclear observables [65, 68, 69]. In principle, this offers the possibility to identify the fundamental sources of time-reversal violation and to shed light on some of the BSM scenarios, provided the corresponding LECs in the effective Lagrangian can be determined from Lattice QCD calculations or experimental data [70, 71].

In the framework of  $\chi\text{EFT}$ , the PVTV NN potential was derived up to  $\text{N}^2\text{LO}$  including one- and two-pion exchange contributions and the corresponding contact interactions [72, 73]. Subsequent works showed the presence in the PVTV Lagrangian of a three-pion term [68], which was for the first time included in the calculations in Ref. [66]. This term also generates a PVTV 3N force at NLO, which contributes to the  $^3\text{H}$  and  $^3\text{He}$  EDM. The calculation reported in Ref. [66] was also the first one carried out using solely the interactions derived in  $\chi\text{EFT}$ . More precisely, the PVTV potential at NLO was used in combination with the  $\text{N}^2\text{LO}$  PCTC potentials from Ref. [74]. Finally, in Ref. [75], the EDM of deuteron and trinucleons was studied using the  $\chi\text{EFT}$  PVTV potential up to  $\text{N}^2\text{LO}$  along with the  $\text{N}^4\text{LO}$  PCTC potential of Ref. [18]. In this paper, it was also shown that the  $\text{N}^2\text{LO}$  contribution to the PVTV 3N force generated by the three-pion interaction vanishes. The LO  $\chi\text{EFT}$  PVTV potential has also been applied in combination with many-body methods to calculate Schiff moments of heavy nuclei [76].

Currently, no direct limits on EDMs of light nuclei have been established. However, experiments are planned to measure the EDM of protons and light nuclei in dedicated storage rings [77, 78, 79, 80, 81, 82]. This new approach could reach an accuracy of  $\sim 10^{-16} e \text{ fm}$ , although this has to be established in practice. If successful, these experiments would lead to a great improvement in the hadronic sector of EDM searches. A measurement of a non-vanishing EDM of this magnitude would provide evidence of a PVTV source beyond the CKM mechanism. However, a single measurement would be insufficient to identify the source of PVTV. For this reason, experiments with various light nuclei such as  $^2\text{H}$ ,  $^3\text{H}$  and  $^3\text{He}$  are planned. Such measurements would provide a complementary information needed to impose constraints on PVTV sources at the fundamental level.

A brief discussion of the PVTV potentials derived in the framework of the one-meson exchange model and in the pionless EFT approach will also be reported in this review.

### 1.3 Outline of the article

Our paper is organized as follow. In Section 2, we discuss the origins of PVTC and PVTV interactions at the fundamental level and list the relevant terms in the quark-gluon Lagrangian. In Section 3, we give the corresponding terms in the effective chiral Lagrangian and discuss the derivation of the PVTC and PVTV potentials in  $\chi$ EFT. In Section 4, we specifically focus on the contact few-nucleon interactions which enter the potentials in both chiral and pionless EFT formulations. We also discuss the expected hierarchy of the corresponding LECs as suggested by the large- $N_c$  analysis. Next, in Section 5, the various meson-exchange models developed to describe the PVTC and PVTV interactions will be summarized. Then, in Section 6, we report on a selected set of results for PVTC and PVTV observables in light nuclei up to  $A = 3$ . Finally, the main conclusions of this paper and future perspectives are summarized in section 7.

## 2 PARITY VIOLATION AND TIME-REVERSAL VIOLATION AT THE MICROSCOPIC LEVEL

Parity is violated in the SM of particle physics because of the different gauge interactions of left- and right-handed fermion fields. Only left-handed particles interact via  $SU(2)_L$  gauge interactions such that this part of the SM violates parity maximally. The remaining color and electromagnetic interactions conserve parity modulo the QCD vacuum angle which is discussed below. Parity violation was first observed in semileptonic charged current interactions in 1957 [83]. Twenty years later, in the late '70s, PVTC was observed in neutral current electron-nucleus scattering [84], providing a strong confirmation of the SM. Subsequent PVTC electron scattering experiments have quantitatively confirmed the SM picture [85]. In addition to PVTC in  $\beta$  decays and semileptonic neutral current processes, the SM predicts PVTC in weak interactions between quarks. At energies smaller than the masses of the  $W$  and  $Z$  bosons, these interactions can be represented by four-fermion operators. Right below the electroweak (EW) scale, and limiting ourselves to the lightest  $u$  and  $d$  quarks, the four-fermion Lagrangian is

$$\begin{aligned} \mathcal{L}_W = & -\frac{G_F}{\sqrt{2}} \left\{ \left( 1 - \frac{2}{3}s_w^2 \right) \bar{q}_L \gamma^\mu \tau_a q_L \bar{q}_L \gamma_\mu \tau_a q_L - \frac{2s_w^2}{3} \bar{q}_L \gamma^\mu \tau_3 q_L (\bar{q}_L \gamma_\mu q_L + \bar{q}_R \gamma_\mu q_R) \right. \\ & \left. - 2s_w^2 \left( \bar{q}_L \gamma^\mu \tau_3 q_L \bar{q}_L \gamma_\mu \tau_3 q_L - \frac{1}{3} \bar{q}_L \gamma^\mu \tau_a q_L \bar{q}_L \gamma_\mu \tau_a q_L \right) + \dots \right\}, \end{aligned} \quad (1)$$

where  $G_F$  is the Fermi coupling constant and  $s_w^2 \equiv \sin^2 \theta_W = 0.231$ , with  $\theta_W$  the Weinberg mixing angle.  $q_L$  and  $q_R$  denote the left-handed and right-handed doublets  $q_L^T = (u_L, d_L)$  and  $q_R^T = (u_R, d_R)$ , and the dots denote terms that conserve parity<sup>5</sup>. Eq. (1) was obtained assuming the CKM matrix to be the identity, that is  $V_{ud} = 1$ . The three operators in Eq. (1) all break parity, but have different transformation properties under chiral symmetry and isospin. We note that the isovector and isotensor terms (the second and third operators) given in Eq. (1) are suppressed by a factor  $s_w^2$  with respect to the isoscalar one.

The operators in Eq. (1) need to be evolved using the renormalization group equations (RGE) from the EW scale down to the QCD scale, and in this process they mix with additional PVTC operators [86]. After

<sup>5</sup> Here  $u$  and  $d$  denote the  $u$ - and  $d$ -quark Dirac fields, respectively. Moreover  $u_{R,L} = \frac{1 \pm \gamma^5}{2} u$ , etc.

the RGE evolution, the PVTC Lagrangian assumes the form

$$\begin{aligned}
 \mathcal{L}_{\text{PVTC}}^{\text{SM}} = & -\frac{G_F}{\sqrt{2}} \left\{ C_1^{\text{SM}} \bar{q}_L \gamma^\mu \tau_a q_L \bar{q}_L \gamma_\mu \tau_a q_L + C_2^{\text{SM}} \bar{q}_L \gamma^\mu q_L \bar{q}_L \gamma_\mu q_L + C_3^{\text{SM}} \bar{q}_L \gamma^\mu \tau_3 q_L \bar{q}_L \gamma_\mu q_L \right. \\
 & + C_4^{\text{SM}} (\bar{q}_L \gamma^\mu \tau_3 q_L \bar{q}_R \gamma_\mu q_R - \bar{q}_L \gamma^\mu q_L \bar{q}_R \gamma_\mu \tau_3 q_R) \\
 & + C_5^{\text{SM}} (\bar{q}_L^\alpha \gamma^\mu \tau_3 q_L^\beta \bar{q}_R^\beta \gamma_\mu q_R^\alpha - \bar{q}_L^\alpha \gamma^\mu q_L^\beta \bar{q}_R^\beta \gamma_\mu \tau_3 q_R^\alpha) \\
 & \left. + C_6^{\text{SM}} \left( \bar{q}_L \gamma^\mu \tau_3 q_L \bar{q}_L \gamma_\mu \tau_3 q_L - \frac{1}{3} \bar{q}_L \gamma^\mu \tau_a q_L \bar{q}_L \gamma_\mu \tau_a q_L \right) - (L \leftrightarrow R) \right\}, \quad (2)
 \end{aligned}$$

where in the SM, the coefficients  $C_i^{\text{SM}}$  are known functions of SM parameters as  $s_w$ , the strong coupling constant  $g_s$ , etc. Greek indices  $\alpha$  and  $\beta$  appearing as superscript in some of the quark fields in Eq. (2) specify color indices. They are only shown for cases where the color contractions are not obvious. Notice that the QCD evolution does not remedy the  $s_w^2$  suppression of the isospin-one and -two operators [86]. BSM physics that arises at scales well above the EW can be represented at the EW scale via gauge-invariant higher-dimensional operators [87, 67]. This framework is usually called the SM Effective Field Theory (SM-EFT). SM-EFT operators can induce new PVTC couplings of the  $W$  and  $Z$  bosons to left- and right-handed quarks, and new PVTC four-fermion operators. After evolving the effective operators from the EW to the QCD scale, the net effect of BSM PVTC SM-EFT operators is to modify the coefficients  $C_i^{\text{SM}}$  in Eq. (2) with respect to their SM values, namely in Eq. (2) one substitutes  $C_i^{\text{SM}} \rightarrow C_i^{\text{SM}+\text{BSM}}$ . We have focused so far on operators involving only the  $u$  and  $d$  quarks. Flavor-conserving ( $\Delta F = 0$ ) operators involving the  $s$  quark can also generate interesting contributions to hadronic P violation [88, 86], such as contributions to isospin-one operators that are not suppressed by  $s_w^2$ .

While P and C are maximally broken by the  $V - A$  structure of the SM, the breaking of CP is much more delicate. In the SM with three generations of quarks, CP is broken by the phase of the CKM matrix, which explains all the observed CP violation in the kaon [89, 90, 91], and  $B$  meson systems [92, 93]. Theoretical uncertainties are at the moment too large to definitively conclude whether the recently discovered CP violation in  $D$  decays [94] is compatible with the SM. The phase of CKM gives, on the other hand, unobservable contributions to flavor-diagonal CP violation, in particular to the neutron [95, 55, 59] and electron EDMs [96, 97, 98].

The second source of CP violation in the SM is the QCD  $\theta$  term [99, 51, 100]

$$\mathcal{L}_{\text{PVTV}}^\theta = -\theta \frac{g_s^2}{64\pi^2} \varepsilon^{\mu\nu\alpha\beta} G_{\mu\nu}^a G_{\alpha\beta}^a, \quad (3)$$

where  $g_s$  is the strong coupling constants and  $G_{\mu\nu}^a$  the gluon field tensors ( $a$  is a color index). The  $\theta$  term is a total derivative, but it contributes to physical processes through extended, spacetime-dependent field configurations known as instantons. CP violation from the QCD  $\theta$  term is intimately related to the quark masses. All phases of the quark mass matrix can be eliminated through non-anomalous  $SU(2)$  vector and axial rotations, except for a common phase  $\rho$ . The mass plus QCD  $\theta$  terms which are left are

$$\mathcal{L}_{\text{PVTV}}^{\text{mass}+\theta} = - (e^{i\rho} \bar{q}_L \mathcal{M} q_R + e^{-i\rho} \bar{q}_R \mathcal{M} q_L) - \theta \frac{g_s^2}{64\pi^2} \varepsilon^{\mu\nu\alpha\beta} G_{\mu\nu}^a G_{\alpha\beta}^a, \quad (4)$$

where  $\mathcal{M} = \text{diag}(m_u, m_d)$ . The parameters  $\rho$  and  $\theta$  are not independent. In  $\chi$ EFT, it is convenient to rotate  $\mathcal{L}_{PVTV}^{\text{mass}+\theta}$  into a complex mass term with an anomalous  $U(1)_A$  rotation, obtaining, after vacuum alignment [101],

$$\mathcal{L}_{PVTV}^{\text{mass}+\theta} = m_* \bar{\theta} \bar{q} i \gamma_5 q, \quad (5)$$

where

$$\bar{\theta} = \theta + n_f \rho, \quad m_* = \frac{m_u m_d}{m_u + m_d} = \frac{\bar{m}(1 - \epsilon^2)}{2}. \quad (6)$$

$n_f = 2$  is the number of light flavors, and the combinations of light quarks masses  $\bar{m}$  and  $\epsilon$  are  $2\bar{m} = m_u + m_d$ ,  $\epsilon = (m_d - m_u)/(m_d + m_u)$ . Eqs. (5) and (6) can be easily generalized to include strangeness.  $\bar{\theta}$  is a free parameter in the QCD Lagrangian, and one would expect  $\bar{\theta} = \mathcal{O}(1)$ . This would however lead to a large neutron EDM  $|d_n| \sim 10^{-3} \bar{\theta} e \text{ fm}$  [102, 103], ten orders of magnitude larger than the current limits,  $d_n < 3.0 \cdot 10^{-13} e \text{ fm}$  [61]. Therefore  $\bar{\theta} \lesssim 10^{-10}$ , the so-called strong CP problem.

The phase of the CKM and the QCD  $\bar{\theta}$  term are the only CP-violating parameters in the SM Lagrangian. They are however not sufficient to explain the observed matter-antimatter asymmetry of the Universe [104, 105, 106, 107], and it is therefore natural to think about CP-violating sources induced by BSM physics. The low-energy CP-violating operators relevant for EDMs have been cataloged in several works, e.g. Refs. [52, 108, 109, 110]. Ref. [68] considered all the low-energy operators that are induced by SM-EFT operators at tree level, retaining the two lightest quarks. Generalization to three flavors are given, for example, in Refs. [111, 112]. The most relevant  $SU(3)_c \times U(1)_{\text{em}}$ -invariant purely hadronic operators induced by dimension-six SM-EFT operators are

$$\begin{aligned} \mathcal{L}_{PVTV}^{6,\text{hadr}} = & \frac{g_s \tilde{C}_G}{6v^2} f^{abc} \epsilon^{\mu\nu\alpha\beta} G_{\alpha\beta}^a G_{\mu\rho}^b G_{\nu}^{c\rho} - \frac{1}{2v^2} (\bar{q} [d_E] i\sigma^{\mu\nu} \gamma_5 q e F_{\mu\nu} + \bar{q} [d_{CE}] i\sigma^{\mu\nu} g_s G_{\mu\nu} \gamma_5 q) \\ & - \frac{4G_F}{\sqrt{2}} \left\{ \Sigma_1^{(ud)} (\bar{d}_L u_R \bar{u}_L d_R - \bar{u}_L u_R \bar{d}_L d_R) + \Sigma_2^{(ud)} (\bar{d}_L^\alpha u_R^\beta \bar{u}_L^\beta d_R^\alpha - \bar{u}_L^\alpha u_R^\beta \bar{d}_L^\beta d_R^\alpha) \right\} \\ & - \frac{4G_F}{\sqrt{2}} \left\{ \Xi_1^{(ud)} \bar{d}_L \gamma^\mu u_L \bar{u}_R \gamma_\mu d_R + \Xi_2^{(ud)} \bar{d}_L^\alpha \gamma^\mu u_L^\beta \bar{u}_R^\beta \gamma_\mu d_R^\alpha \right\}, \quad (7) \end{aligned}$$

where  $f^{abc}$  are the structure constants of the Lie algebra of the color  $SU(3)$  group,  $[d_E]$  and  $[d_{CE}]$  are matrices in flavor space,  $[d_E] = \text{diag}(m_u \tilde{c}_\gamma^{(u)}, m_d \tilde{c}_\gamma^{(d)})$  and  $[d_{CE}] = \text{diag}(m_u \tilde{c}_g^{(u)}, m_d \tilde{c}_g^{(d)})$ . The coefficients  $\tilde{C}_G$ ,  $\tilde{c}_{\gamma,g}^{(q)}$ ,  $\Sigma_{1,2}^{(ud)}$  and  $\Xi_{1,2}^{(ud)}$  are dimensionless and scale as  $(v/\Lambda_X)^2$ , where  $v = 246 \text{ GeV}$  is the Higgs vacuum expectation value, and  $\Lambda_X$  is the scale of new physics. The Weinberg three-gluon, the quark EDM (qEDM), and the chromo-EDM (qCEDM) operators (the first, second, and third term given in Eq. (7), respectively) have received the most attention in the literature [52, 113]. They can be written directly in terms of  $SU(3)_c \times SU(2)_L \times U(1)_Y$ -invariant operators at the EW scale, and receive corrections by a variety of CP-violating operators in the SM-EFT, involving heavy SM fields. The four-quark operators, given in the second line of Eq. (7), can also be expressed in terms of gauge-invariant operators at the EW scale, and they arise, for example, in leptoquark models, see [114, 115]. The four-quark operators, given in the third line of Eq. (7), are on the other hand induced by right-handed couplings of quarks to the  $W$  boson [116, 68], and are generated, for example, in left-right symmetric models.



While all operators in Eqs. (5) and (7) violate P and CP symmetry, they transform differently under isospin and chiral rotations. As such, the operators induce different  $\chi$ EFT Lagrangians at lower energies, and different hierarchies of CP-violating hadronic and nuclear observables such as EDMs or scattering observables.

### 3 PVTC AND PVTV CHIRAL POTENTIALS

In this section, we discuss the derivation of the PVTC and PVTV NN and 3N potentials within the framework of  $\chi$ EFT. In the first and second subsections we briefly review the properties of the PVTC and PVTV chiral Lagrangians. In subsection 3.3, we present briefly two methods used to derive the potentials starting from a Lagrangian. Finally, in the last two subsections, we present the PVTC and PVTV chiral potentials, respectively.

In order to discuss hadronic observables such as nuclear EDMs or PVTC asymmetries in  $pp$  scattering, the quark-level PVTC and PVTV Lagrangians of Eqs. (2) and (7) need to be matched onto nuclear EFTs, such as chiral EFT and pionless EFT. Due to the nonperturbative nature of QCD at low energy, this matching cannot be done in perturbation theory. Nevertheless, the approximate chiral and isospin symmetries of the QCD Lagrangian provide an organizing principle for low-energy interactions, see [12, 13, 14] for review articles.

Let us first introduce the nucleon and pion fields. The (relativistic) nucleon field  $N(x)$  is considered to be an isospin doublet

$$N(x) = \begin{pmatrix} p(x) \\ n(x) \end{pmatrix}, \quad (8)$$

where  $p(x)$  ( $n(x)$ ) is the proton (neutron) field. The pion fields are given in ‘‘Cartesian’’ coordinates  $\pi_a$ ,  $a = 1, 2, 3$ , where

$$\pi_1(x) = \frac{\pi^{(+)}(x) + \pi^{(-)}(x)}{\sqrt{2}}, \quad \pi_2(x) = \frac{i(\pi^{(+)}(x) - \pi^{(-)}(x))}{\sqrt{2}}, \quad \pi_3(x) = \pi^{(0)}(x), \quad (9)$$

$\pi^{(+)}(x)$ ,  $\pi^{(-)}(x)$ , and  $\pi^{(0)}(x)$  being the fields associated to the three charge states of the pion. The pion fields in Cartesian coordinates are collectively denoted by  $\vec{\pi}(x)$ . We use the  $2 \times 2$  matrices  $\tau_a$ ,  $a = 0, \dots, 3$ , where  $\tau_0$  is the identity matrix, while  $\tau_a$ ,  $a = 1, \dots, 3$  are the Pauli matrices acting on the isospin degrees of freedom (often indicated cumulatively as  $\vec{\tau}$ ). For example,  $\vec{\tau} \cdot \vec{\pi}(x) = \sum_{a=1}^3 \tau_a \pi_a(x)$ . Sometimes the  $a = 3$  component will be denoted as the ‘‘z’’ component, i.e.  $\pi_3 \equiv \pi_z$ , etc., in our notation. Finally, we denote the nucleon (pion) mass by  $M$  ( $m_\pi$ ).

In some cases, we will perform a non-relativistic reduction of the nucleon field  $N(x)$  and use  $N_r(x)$

$$N_r(x) = \begin{pmatrix} p_r(x) \\ n_r(x) \end{pmatrix}, \quad (10)$$

where  $p_r(x)$  ( $n_r(x)$ ) is the two component Pauli spinor representing the static proton (neutron) field. Effects of the anti-nucleon degrees of freedom are taken into account in the form of  $1/M$  relativistic corrections to the vertices. The coefficient of the annihilation operator reduces to  $\chi_s \exp(i\mathbf{p} \cdot \mathbf{x})$ , where  $\chi_s$  is a spinor describing a spin state with  $z$ -projection  $s = \pm \frac{1}{2}$ .

The main “building block” to construct the chiral Lagrangian is the  $SU(2)$  pionic matrix field  $U(x)$ , often written as (but its definition is not unique) [12]

$$U(x) = e^{\frac{i}{f_\pi} \vec{\pi}(x) \cdot \vec{\tau}}, \quad (11)$$

where  $f_\pi \approx 92.4$  MeV is the pion decay constant. Another low energy constant frequently entering the chiral Lagrangian is the axial coupling constant  $g_A \approx 1.29$ . Following the standard convention, we give here the effective value that takes into account the Goldberger-Treiman discrepancy and is extracted from the empirical value of the pion-nucleon coupling constant. The effective chiral Lagrangian is constructed in terms of  $N(x)$  and  $U(x)$  and therefore contains vertices with arbitrary number of pion fields. In the following, we will retain explicitly only relevant terms with the minimum number of pion fields, obtained by expanding  $U(x)$  in powers of the pion field. Additional terms with a larger number of pion fields will only contribute to the PVTC and PVTV potential at higher orders in the chiral expansion. For an introduction to the chiral Lagrangians and their building blocks, the reader is referred to Refs. [12, 13, 14] and references therein.

Each term of the chiral Lagrangian will be classified by the so-called “chiral order”. Each four-gradient of the pion matrix field or a multiplication by a pion mass increases the order of the term by one. Four-gradients acting on nucleon fields are more difficult to classify, since the time derivative brings down a factor proportional to the nucleon mass. An easier counting is obtained using the non-relativistic heavy baryon perturbation theory [117, 12], which was used in the derivation of the PVTC potential in [46] and of the PVTV potential in [72]. In the following, we will use both the relativistic and nonrelativistic nucleon fields.

For the sake of completeness, we report first of all the terms of the PCTC Lagrangian that contribute to the PVTC and PVTV potentials up to the order we are interested in. In  $SU(2)$   $\chi$ PT, the PCTC Lagrangian can be conveniently organized in sectors with different numbers of pions and nucleons (below we give the explicit expression for the relevant terms in the  $\pi N$  Lagrangian only).

$$\begin{aligned} \mathcal{L}_{PCTC} &= \mathcal{L}_{PCTC,\pi N} + \mathcal{L}_{PCTC,NN} + \mathcal{L}_{PCTC,\pi\pi} + \dots, \quad (12) \\ \mathcal{L}_{PCTC,\pi N} &= \bar{N} \left[ -\frac{1}{4f_\pi^2} (\vec{\tau} \times \vec{\pi}) \cdot \partial_\mu \vec{\pi} \gamma^\mu - \frac{g_A}{2f_\pi} (\vec{\tau} \cdot \partial_\mu \vec{\pi}) \gamma^\mu \gamma^5 \right. \\ &\quad + 4c_1 m_\pi^2 \left( 1 - \frac{\vec{\pi}^2}{2f_\pi^2} \right) + \frac{c_2}{f_\pi^2} \left( \partial_0 \vec{\pi} \cdot \partial_0 \vec{\pi} + \frac{1}{M} \partial_0 \vec{\pi} \cdot \partial_i \vec{\pi} \gamma^0 i \overleftrightarrow{\partial}^i \right) \\ &\quad \left. + \frac{c_3}{f_\pi^2} \partial_\mu \vec{\pi} \cdot \partial^\mu \vec{\pi} - \frac{c_4}{2f_\pi^2} (\vec{\tau} \cdot \partial_\mu \vec{\pi} \times \partial_\nu \vec{\pi}) \sigma^{\mu\nu} + \dots \right] N \quad (13) \end{aligned}$$

where “ $\dots$ ” in the previous expression denotes terms of higher order and/or more pions fields of no interest here. Above  $\overleftrightarrow{\partial}^\mu \equiv \overrightarrow{\partial}^\mu - \overleftarrow{\partial}^\mu$  and  $\sigma^{\mu\nu} = \frac{i}{2} [\gamma^\mu, \gamma^\nu]$ . The parameters  $c_{i=1-4}$  are LECs appearing in the Lagrangian of order  $Q^2$ . They have dimension of the inverse of an energy. For a complete discussion of the terms appearing in the Lagrangians  $\mathcal{L}_{PCTC,\pi N}$ ,  $\mathcal{L}_{PCTC,NN}$ , and  $\mathcal{L}_{PCTC,\pi\pi}$ , etc., see Refs. [12, 118].

### 3.1 The PVTC chiral Lagrangian

The effective chiral Lagrangian that involves contributions from the weak sector of the SM was first discussed in the seminal paper by Kaplan and Savage [88] and subsequently revisited in Refs. [119, 40, 46, 42]. Also the PVTC Lagrangian can be conveniently organized in sectors with different numbers of

pions and nucleons, explicitly

$$\mathcal{L}_{PVTC} = \mathcal{L}_{PVTC,\pi N} + \mathcal{L}_{PVTC,NN} + \mathcal{L}_{PVTC,\pi\pi\pi} + \dots, \quad (14)$$

$$\mathcal{L}_{PVTC,\pi N} = \mathcal{L}_{PVTC,\pi N}^{(0)} + \mathcal{L}_{PVTC,\pi N}^{(1)} + \dots, \quad (15)$$

$$\mathcal{L}_{PVTC,NN} = \mathcal{L}_{PVTC,NN}^{(1)} + \mathcal{L}_{PVTC,NN}^{(3)} + \dots, \quad (16)$$

$$\mathcal{L}_{PVTC,\pi\pi\pi} = \mathcal{L}_{PVTC,\pi\pi\pi}^{(2)} + \dots, \quad (17)$$

where the superscript ( $n$ ) denotes the chiral order of each piece. The pion-nucleon interaction terms are collected in  $\mathcal{L}_{PVTC,\pi N}$  and those entering the PVTC potential up to  $Q^1$  are the following [88, 46]

$$\begin{aligned} \mathcal{L}_{PVTC,\pi N}^{(0)} &= \frac{h_\pi^1}{\sqrt{2}} \bar{N} (\vec{\pi} \times \vec{\tau})_z N, \\ \mathcal{L}_{PVTC,\pi N}^{(1)} &= -\frac{h_V^0}{2f_\pi} \bar{N} \gamma^\mu \partial_\mu (\vec{\tau} \cdot \vec{\pi}) N - \frac{h_V^1}{f_\pi} \bar{N} \gamma^\mu N \partial_\mu \pi_z \\ &\quad - \frac{2h_V^2}{f_\pi} \sum_{a,b} \mathcal{I}_{ab} \partial_\mu \pi_a \bar{N} \gamma^\mu \tau_b N - \frac{h_A^1}{f_\pi^2} \bar{N} \gamma^\mu \gamma^5 N (\vec{\pi} \times \partial_\mu \vec{\pi})_z \\ &\quad + \frac{h_A^2}{f_\pi^2} \sum_{a,b=1}^3 \mathcal{I}_{ab} \bar{N} \left( (\vec{\pi} \times \partial_\mu \vec{\pi})_a \tau_b + \partial_\mu \pi_a (\vec{\pi} \times \vec{\tau})_b \right) \gamma^\mu \gamma^5 N, \end{aligned} \quad (18)$$

where

$$\mathcal{I}_{ab} = \begin{pmatrix} -1 & 0 & 0 \\ 0 & -1 & 0 \\ 0 & 0 & +2 \end{pmatrix}. \quad (20)$$

The parameters  $h_\pi^1$  and  $h_{V,A}^{\Delta I}$  are unknown LECs. The superscript  $\Delta I$  labels the rank of the corresponding isospin tensor. The LECs can be estimated by naive dimensional analysis (NDA) [88, 40, 46, 42]

$$h_\pi^1 \sim G_F f_\pi \Lambda_\chi \sim 10^{-6}, \quad h_{V,A}^{\Delta I} \sim \frac{f_\pi}{\Lambda_\chi} h_\pi^1 \sim 10^{-7}, \quad (21)$$

where  $\Lambda_\chi = 4\pi f_\pi \sim 1.2$  GeV is the typical scale of the strong interaction. Eq. (21) shows the order-of-magnitude estimates of the PVTC interactions. These estimates do not take into account factors of  $s_w^2$  and  $N_c$  that could modify the expected scaling of the LECs.

The contact terms entering the Lagrangian  $\mathcal{L}_{PVTC,NN}$  are products of a pair of bilinears of nucleon fields that are odd under P and even under CP. The most general bilinear product reads

$$\tilde{O}_{AB} = \sum_{a,b=0}^3 F_{ab} (\bar{N} \tau_a \Gamma_A N) (\bar{N} \tau_b \Gamma_B N), \quad (22)$$

where  $\Gamma_A$  and  $\Gamma_B$  are elements of the Clifford algebra with the possible addition of 4-gradients and  $F_{ab}$  are unknown parameters. To violate P but conserve CP, at least one 4-gradient is required. We must build isoscalar, isovector and isotensor terms as discussed in Section 2. The operators moreover have to conserve the electric charge and thus commute with the third component of the isospin operator. The terms with

only one gradient operator are collected in  $\mathcal{L}_{PVTC,NN}^{(1)}$  (i.e. of chiral order 1). Only five independent terms can be written [44], corresponding to the five possible  $S \leftrightarrow P$  transitions in NN scattering [45]. It is more convenient to give the Lagrangian using the non-relativistic reduction of the nucleon fields  $N_r$ :

$$\begin{aligned} \mathcal{L}_{PVTC,NN}^{(1)} = & \frac{1}{\Lambda_\chi^2 f_\pi} \left[ \frac{C_1}{2} \nabla \times (N_r^\dagger \boldsymbol{\sigma} N_r) \cdot N_r^\dagger \boldsymbol{\sigma} N_r + \frac{C_2}{2} \nabla \times (N_r^\dagger \boldsymbol{\sigma} \tau_a N_r) \cdot N_r^\dagger \boldsymbol{\sigma} \tau_a N_r \right. \\ & + C_3 \epsilon_{ab3} \nabla \cdot (N_r^\dagger \boldsymbol{\sigma} \tau_a N_r) N_r^\dagger \tau_b N_r + C_4 \nabla \times (N_r^\dagger \boldsymbol{\sigma} \tau_3 N_r) \cdot N_r^\dagger \boldsymbol{\sigma} N_r \\ & \left. + \frac{C_5}{2} \mathcal{I}_{ab} \nabla \times (N_r^\dagger \boldsymbol{\sigma} \tau_a N_r) \cdot N_r^\dagger \boldsymbol{\sigma} \tau_b N_r \right]. \end{aligned} \quad (23)$$

The factor  $\frac{1}{\Lambda_\chi^2 f_\pi}$  has been chosen to ensure  $C_i$  are dimensionless and for convenience in the power counting. The construction of Eq. (23) and the elimination of redundancies will be discussed in more details in Section 4. The operators multiplying the LECs  $C_{1,2}$  are isoscalar, those multiplying  $C_{3,4}$  change isospin by one unit, while that multiplying  $C_5$  is an isotensor. The scaling of the LECs from naive dimensional analysis [120] is given by

$$C_i \sim G_F \Lambda_\chi f_\pi, \quad (24)$$

which once again does not take into account the suppression by  $s_w^2$  affecting, for example, the isovector operators. The operators in Eq. (23) contribute to the PVTC potential at NLO (suppressed by  $(Q/\Lambda_\chi)^2$  with respect to LO), and we will give the potential derived from them in Eq. (60). The terms appearing in  $\mathcal{L}_{PVTC,NN}^{(3)}$  contain two additional gradients and contribute to the PVTC potential at higher order. They have not been considered so far.

Finally, there are some terms with  $3\pi$  vertices appearing in  $\mathcal{L}_{PVTC,\pi\pi\pi}^{(2)}$  as discussed in Ref. [42]. These terms would contribute to the  $Q^2$  PVTC potential, but their contributions at the end vanishes as discussed in Subsect. 3.4.

### 3.1.1 Connection to the underlying PVTC sources

Attempts to estimate the values of the coupling constants were performed mainly in the framework of the meson exchange models (which will be discussed in Section 5). However, since in both  $\chi$ EFT and meson exchange frameworks the lowest order pion-nucleon Lagrangian term is the same as given in Eq. (18), we can report here the values for  $h_\pi^1$  estimated from the underlying fundamental theory also before the advent of  $\chi$ EFT [121, 122, 123, 124, 125, 126, 127]. One of the most comprehensive calculation including all previous results was performed in 1980 by Desplanques, Donoghue, and Holstein (DDH) [50] using the valence quark model. Additional calculations have been performed later [128, 129, 130], using similar or other methods and finding qualitatively similar results. These estimates, however, are based on a series of rather uncertain assumptions (see, for example, Ref. [131]). For example, DDH presented not a single value for  $h_\pi^1$  but rather a *range* inside of which it was extremely likely that this parameter would be found [50]. In addition they presented also a single number called the “best value” but this is described simply as an educated guess in view of all the uncertainties. The values of  $h_\pi^1$  were [50]

$$\text{DDH: } h_\pi^1 = 4.56 \times 10^{-7} \quad (\text{“best value”}), \quad h_\pi^1 = 0 - 11.4 \times 10^{-7} \quad (\text{“reasonable range”}). \quad (25)$$

Some years ago, a lattice QCD calculation of  $h_\pi^1$  has also been made [132], resulting in the following estimate

$$\text{Lattice: } h_\pi^1 = (1.1 \pm 0.5) \times 10^{-7}, \quad (26)$$

where the theoretical uncertainty is related to the statistical Monte Carlo error. While the systematic errors are expected to be within the quoted statistical error [132], we stress that the calculation was performed at a heavy pion mass and not extrapolated to the physical point, disconnected diagrams were not included, and operator renormalization was neglected.

Regarding the other LECs entering the contact Lagrangian given in Eq. (23), no direct estimates were reported in literature. These LECs were estimated by comparing the expression of contact potential with the potential developed using the exchanges of heavy mesons, as for example, in the DDH potential [46, 42] (this issue will be considered in more detail in Sect. 5). However, since also the DDH estimates are rather uncertain, here we will not discuss this issue.

### 3.2 The PVTV Lagrangian

The PVTV chiral Lagrangian taking into account the QCD  $\bar{\theta}$  term was first considered in the seminal paper by Crewther, di Vecchia, Veneziano and Witten [102], and consequently revisited in Refs. [133, 134, 135, 136, 137]. Subleading terms in the chiral expansion were systematically constructed in Refs. [65, 69]. The chiral Lagrangian induced by the dimension-six operators in Eq. (7) were derived in Refs. [68, 69].

As before, in  $SU(2)$   $\chi$ PT, the PVTV Lagrangian can be organized in sectors with different numbers of pions and nucleons

$$\mathcal{L}_{PVTV} = \mathcal{L}_{PVTV,\pi N} + \mathcal{L}_{PVTV,NN} + \mathcal{L}_{PVTV,\pi\pi\pi} + \dots, \quad (27)$$

$$\mathcal{L}_{PVTV,\pi N} = \mathcal{L}_{PVTV,\pi N}^{(0)} + \mathcal{L}_{PVTV,\pi N}^{(1)} + \dots, \quad (28)$$

$$\mathcal{L}_{PVTV,NN} = \mathcal{L}_{PVTV,NN}^{(1)} + \mathcal{L}_{PVTV,NN}^{(3)} + \dots, \quad (29)$$

$$\mathcal{L}_{PVTV,\pi\pi\pi} = \mathcal{L}_{PVTV,\pi\pi\pi}^{(0)} + \dots. \quad (30)$$

As in the previous subsection, we report here only the most important interactions for each sector, focusing on the terms with the minimum number of pion fields entering in the final expression of the potential. Terms with additional pions are not universal for the different PVTV sources at the quark level, but instead depend on their chiral-symmetry breaking pattern. These differences only enter at higher order in the potentials than we consider here.

In the PVTV case, the simultaneous violation of P, T, and isospin symmetry allows for a pion tadpole linear in the pion field  $\sim \pi_3$  with a corresponding LEC proportional to the symmetry-violating source terms at the quark level. Such tadpoles can always be removed by appropriate field redefinitions of the pion and nucleon fields [65, 68, 69]. At LO in the chiral expansion, the tadpole removal is the same as the vacuum alignment procedure at the quark level [101]. While tadpoles can be removed, the corresponding field redefinitions affect other couplings in the chiral Lagrangian. In particular, for chiral-symmetry-breaking CP sources that do not transform as a quark mass term, a PVTV three-pion vertex of chiral order  $Q^0$  is left behind [68, 69].

$$\mathcal{L}_{PVTV,\pi\pi\pi}^{(0)} = M\bar{\Delta}\pi_3\vec{\pi}^2, \quad (31)$$

where  $\bar{\Delta}$  is a LEC. Other three-pion vertices will appear at N<sup>2</sup>LO, but they will contribute to high orders of the PTVV potential.

Arguably the most important interactions appear in the pion-nucleon sector. Simultaneous violation of P, T, and chiral symmetry allows for non-derivative single-pion-nucleon interactions, something which is not possible in the PCTC Lagrangian. In principle, three different interactions can be written

$$\mathcal{L}_{PVTV,\pi N}^{(0)} = \bar{g}_0 \bar{N} \vec{\pi} \cdot \vec{\tau} N + \bar{g}_1 \bar{N} \pi_3 N + \bar{g}_2 \bar{N} \pi_3 \tau_3 N, \quad (32)$$

corresponding, respectively, to an isospin singlet, vector, and tensor interaction. As discussed below, the relative size of the LECs  $\bar{g}_{0,1,2}$  strongly depends on the quark-level PTVV source under consideration. In the case of CP-violation from chiral invariant operators, such as the gCEDM,  $\bar{g}_i$  are suppressed by powers of the pion masses, and the pion-nucleon Lagrangian contains chiral-invariant, derivative couplings as important as those in Eq. (32) [68]. These can however always be absorbed into a shift of  $\bar{g}_0$  and of the  $\Delta I = 0$  NN operators discussed below.

The NLO Lagrangian contains several two-pion two-nucleon PTVV interactions [65, 68, 69, 75], but, for all CP-violating sources, they contribute to the two- and three-body PTVV potentials at N<sup>3</sup>LO and N<sup>2</sup>LO, respectively. We therefore ignore these couplings. Isospin-breaking sources also generate a single-pion-nucleon NLO coupling. The coupling involves a time derivative of the pion field, thus inducing a relativistic correction in the  $\mathcal{O}(Q)$  PTVV potential. At N<sup>2</sup>LO the number of interactions proliferates significantly and there are also new pure pionic interactions. These contributions can either be absorbed into LO LECs or appear at high orders in the PTVV potential considered here.

Apart from pionic and pion-nucleon interactions, there appear PTVV NN contact interactions. As in the PVTC case, at least one gradient is required such that these operators start at order  $Q$ . Terms with three or more gradients have not been considered so far. At order  $Q$ , only five independent interactions of this kind can be written, corresponding to the five possible  $S \leftrightarrow P$  transitions (see Section 4 for a general discussion of this kind of interaction terms). Neglecting terms with multiple pions, the Lagrangian reads (again, it is convenient to write it in terms of the non-relativistic nucleon field  $N_r$ )

$$\begin{aligned} \mathcal{L}_{PVTV,NN}^{(1)} &= \frac{1}{\Lambda_\chi^2 f_\pi} \left[ \bar{C}_1 \nabla \cdot (N_r^\dagger \boldsymbol{\sigma} N_r) N_r^\dagger N_r + \bar{C}_2 \nabla \cdot (N_r^\dagger \boldsymbol{\sigma} \tau_a N_r) N_r^\dagger \tau_a N_r \right. \\ &+ \bar{C}_3 \nabla \cdot (N_r^\dagger \boldsymbol{\sigma} \tau_3 N_r) N_r^\dagger N_r + \bar{C}_4 \nabla \cdot (N_r^\dagger \boldsymbol{\sigma} N_r) N_r^\dagger \tau_3 N_r \\ &\left. + \bar{C}_5 \mathcal{I}_{ab} \nabla \cdot (N_r^\dagger \boldsymbol{\sigma} \tau_a N_r) N_r^\dagger \tau_b N_r \right]. \quad (33) \end{aligned}$$

As suggested by the factor of  $\Lambda_\chi^2$  which we pulled out of the definition of the LECs, in  $\chi$ EFT these operators contribute in general at N<sup>2</sup>LO and are suppressed with respect to the PTVV one-pion exchange (OPE) potential. The only exception, as discussed in Sec. 3.2.1, are quark-level operators that do not break chiral symmetry, for which  $\bar{C}_{1,2}$  are as important as the contributions from  $\bar{g}_{0,1}$ .

Finally, the calculation of EDMs or other PTVV electromagnetic moments requires the inclusion of electromagnetic currents. Nucleon EDMs are induced by pion loops involving the interactions in  $\mathcal{L}_{TV,\pi N}^{(0,1)}$ . The renormalization of these loops requires the inclusion of short-distance counter terms contributing to

|                      | $(4\pi\epsilon_{m_\pi})\bar{\theta}$ | $(4\pi\epsilon_{m_\pi})\epsilon_v\tilde{c}_g^{(u,d)}$ | $(4\pi\epsilon_{m_\pi})\epsilon_v\tilde{c}_\gamma^{(u,d)}$ | $4\pi\epsilon_v\tilde{C}_G$       | $\epsilon_v\Xi_{1,2}^{(ud)}/(4\pi)$ | $\epsilon_v\Sigma_{1,2}^{(ud)}/(4\pi)$ |
|----------------------|--------------------------------------|---|--|-----------------------------------|-------------------------------------|--|
| $\Delta$             | $\epsilon_{m_\pi}$                   | $\epsilon_{m_\pi}$                                    | —  | $\varepsilon\epsilon_{m_\pi}^2$   | 1                                   | $\epsilon_{m_\pi}$                     |
| $\bar{g}_0$          | 1                                    | 1   | —  | $\epsilon_{m_\pi}$                | $\varepsilon\epsilon_{m_\pi}$       | $\epsilon_{m_\pi}$                     |
| $\bar{g}_1$          | $\varepsilon\epsilon_{m_\pi}$        | 1   | —  | $\varepsilon\epsilon_{m_\pi}$     | 1                                   | $\varepsilon\epsilon_{m_\pi}$          |
| $\bar{g}_2$          | $\varepsilon^2\epsilon_{m_\pi}^2$    | $\varepsilon\epsilon_{m_\pi}$                         | —  | $\varepsilon^2\epsilon_{m_\pi}^2$ | $\varepsilon\epsilon_{m_\pi}$       | $\varepsilon^2\epsilon_{m_\pi}^2$      |
| $\bar{d}_{0,1}f_\pi$ | $e\epsilon_\chi$                     | $e\epsilon_\chi$                                      | $e\epsilon_\chi$   | $e\epsilon_\chi$                  | $e\epsilon_\chi$                    | $e\epsilon_\chi$                       |
| $\bar{C}_{1,2}$      | 1                                    | 1   | —  | 1                                 | $\varepsilon\epsilon_{m_\pi}$       | 1                                      |
| $\bar{C}_{3,4}$      | $\varepsilon\epsilon_{m_\pi}$        | 1   | —  | $\varepsilon\epsilon_{m_\pi}$     | 1                                   | $\varepsilon\epsilon_{m_\pi}$          |
| $\bar{C}_5$          | $\varepsilon^2\epsilon_{m_\pi}^2$    | $\varepsilon\epsilon_{m_\pi}$                         | —  | $\varepsilon^2\epsilon_{m_\pi}^2$ | $\varepsilon\epsilon_{m_\pi}$       | $\varepsilon^2\epsilon_{m_\pi}^2$      |

**Table 1.** Scaling of the LECs in the chiral Lagrangian in dependence of the microscopic CP violation sources. We introduced the counting parameters  $\epsilon_v \equiv \Lambda_\chi^2/v^2$ ,  $\epsilon_{m_\pi} \equiv m_\pi^2/\Lambda_\chi^2$ ,  $\epsilon_\chi \equiv f_\pi^2/\Lambda_\chi^2$ . With  $\epsilon_{m_\pi} \sim \epsilon_\chi$ , we introduced two different parameters to explicitly track insertions of the light quark masses from the QCD Lagrangian.  $\varepsilon$  is the isospin breaking parameter  $\varepsilon = (m_d - m_u)/(m_d + m_u) \simeq 1/3$ . The scaling of the LECs induced by dimension-six sources assume a Peccei-Quinn mechanism. A “—” implies the interaction is only induced at higher order than considered here. The parameters  $\bar{C}_{1,2}$ ,  $\bar{C}_{3,4}$ , and  $\bar{C}_5$  are the LECs entering the contact PVTV potential, respectively of isoscalar, isovector, and isotensor type.

the nucleon EDMs. Such counter terms indeed appear in the chiral Lagrangian

$$\mathcal{L}_{PVTV,N\gamma} = \frac{1}{4}\bar{N}(\bar{d}_0 + \bar{d}_1\tau_3)\epsilon^{\mu\nu\alpha\beta}\sigma_{\mu\nu}N F_{\alpha\beta}, \quad (34)$$

where  $F_{\alpha\beta}$  is the electromagnetic field strength and  $\bar{d}_0$  and  $\bar{d}_1$  are LECs related to the proton and neutron EDMs, respectively. The above interactions are sufficient for calculations of hadronic and nuclear PVTV scattering observables and EDMs up to NLO in the chiral expansion. Calculations of higher PVTV moments, such as magnetic quadrupole moments, can depend on additional LECs [138].

### 3.2.1 Connection to the underlying PVTV sources

In the previous section we listed the PVTV hadronic interactions relevant for observables of experimental interest. However, for a given PVTV source at the quark-gluon level, a specific hierarchy among the various interactions appear. The relative importance of the LECs in Eqs. (31), (32), (33) and (34) for the different microscopic sources of CP violation is summarized in Table 1. These estimates are based on NDA [120]. NDA is valid in the regime in which the strong coupling  $g_s$  is non-perturbative, and, as done for NDA estimates of the chiral-invariant PCTC interactions, we will take  $g_s \simeq 4\pi$ . In addition, for dimension-six sources, we assumed that a Peccei-Quinn mechanism [139] relaxes  $\bar{\theta}$  to an induced  $\bar{\theta}_{\text{ind}}$ , which depends on the coefficients and vacuum matrix elements of the operators in Eq. (7) [52, 140, 141]. The scaling of the couplings without this assumption can be found in Ref. [68]. To make the power counting explicit, we introduced three ratios of scales

$$\epsilon_v \equiv \frac{\Lambda_\chi^2}{v^2}, \quad \epsilon_{m_\pi} \equiv \frac{m_\pi^2}{\Lambda_\chi^2}, \quad \epsilon_\chi \equiv \frac{f_\pi^2}{\Lambda_\chi^2} = \frac{1}{(4\pi)^2}. \quad (35)$$

Numerically,  $\epsilon_\chi \sim \epsilon_{m_\pi}$ , but we define two different parameters to track the dependence of the LECs on the quark masses. To assess the size of the contribution of different CP violating sources to the nucleon and nuclear EDMs, the scaling of the LECs in Table 1 can be combined with a naive estimate of these observables. As we will discuss in detail in Sections 3.2.2 and 6.4, the nucleon EDM receives tree level

contributions from  $\bar{d}_{0,1}$  and loop contributions by  $\bar{g}_0$  and  $\bar{g}_1$ , leading to

$$d_{n,p} \sim \frac{\bar{d}_0 \mp \bar{d}_1}{2} + \frac{e}{f_\pi} \epsilon_\chi \left( \alpha_0 \bar{g}_0 + \alpha_1 \bar{g}_1 \epsilon_{m_\pi}^{1/2} + \dots \right), \quad (36)$$

where  $e$  is the electric charge and the coefficients of the loops  $\alpha_{0,1}$  will be given explicitly in Section 3.2.2. The additional suppression of  $\bar{g}_1$  is due to the fact that this coupling only involves neutral pions, which do not interact with a single photon at LO. Nuclear EDMs, on the other hand, receive tree level contributions from the single nucleon EDM, and from pion-nucleon and nucleon-nucleon couplings,

$$d_A = a_n d_n + a_p d_p + e \left( a_\Delta \bar{\Delta} + \sum_{i=0}^2 a_i \bar{g}_i + \epsilon_\chi \sum_{i=1}^5 A_i \bar{C}_i \right). \quad (37)$$

The coefficients  $a_{n,p}$ ,  $a_{\Delta,0,1,2}$  and  $A_{1,\dots,5}$  depend on the nucleus under consideration, and in Section 6.4 we will present results for their calculation in chiral EFT for the deuteron,  ${}^3\text{H}$  and  ${}^3\text{He}$ . By power counting, they are expected to be  $\mathcal{O}(1)$  (measured in units of fm in the case of the dimensionful  $a_{\Delta,0,1,2}$  and  $A_{1,\dots,5}$ ), barring isospin selection rules, which for example suppress the contributions of the isoscalar operators  $\bar{g}_0$  and  $\bar{C}_{1,2}$  in nuclei with  $N = Z$ , such as the deuteron [142, 143]<sup>6</sup>.

The reader should be aware that the dimensionless Wilson coefficients of the dimension-six operators,  $\tilde{c}_g^{(u,d)}$ ,  $\tilde{c}_\gamma^{(u,d)}$ ,  $\tilde{C}_G$ ,  $\Xi_{1,2}^{(ud)}$  and  $\Sigma_{1,2}^{(ud)}$  also come with intrinsic suppression factors. These arise from the typical loop and chiral factors that appear in BSM models. For example, quark and gluon dipole operators are typically induced at the one-loop level, and the quark EDM and chromo-EDM coefficients come with explicit factors of the quark mass (already included in Eq. (7)). This implies that one can expect  $\{\tilde{c}_g^{(u,d)}, \tilde{c}_\gamma^{(u,d)}, \tilde{C}_G\} = \mathcal{O}(\epsilon_\Lambda / (4\pi)^2)$ , where  $\epsilon_\Lambda = v^2 / \Lambda_X^2$ . Of course this is just an estimate and certainly models exist where these operators appear only at the two- or higher-loop level. On the other hand, the four-quark operators  $\Xi$  and  $\Sigma$  can be induced at tree level, so that  $\{\Xi, \Sigma\} = \mathcal{O}(\epsilon_\Lambda)$ . Once the matching coefficients are calculated in a given model, Table 1 and Eqs. (36)-(37) allow to identify the dominant low-energy operator and to get a rough idea of the EDM constraints.

Table 1 highlights that the chiral and isospin properties of the quark-level CP-violating sources induce very specific hierarchies between different low-energy couplings. These hierarchies in turn imply different relations between the EDMs of the nucleon, deuteron, and three-nucleon systems, which, if observed, would allow to disentangle the various CP-violating sources. From Table 1 we see that chiral-symmetry-breaking sources, such as  $\bar{\theta}$ ,  $\tilde{c}_g^{(u,d)}$  and  $\Xi_{1,2}^{(u,d)}$ , induce relatively large PVTV pion-nucleon couplings. These couplings appear in the table with entry 1, indicating no further suppression. In particular, the isoscalar  $\bar{\theta}$  term and isovector  $\Xi^{(u,d)}$  predominantly induce, respectively,  $\bar{g}_0$  and  $\bar{g}_1$ , while a qCEDM would yield both couplings with similar strengths. The consequence is that for these sources light nuclear EDMs are enhanced with respect to the nucleon EDM. For these chiral-symmetry-breaking sources, the contact nucleon interactions proportional to  $\bar{C}_i$  are suppressed in the chiral expansion because these operators involve an explicit derivative. The suppression can be explicitly seen combining the scaling in Table 1 with the explicit factor of  $\epsilon_\chi$  in Eqs. (33) and (37).

Chiral invariant sources such as the Weinberg operator  $\tilde{C}_G$  and the four-quark operators  $\Sigma_{1,2}^{(u,d)}$ , on the other hand, require additional chiral-symmetry breaking to generate  $\bar{g}_{0,1}$ , as indicated by extra powers

<sup>6</sup>  $\bar{g}_0$  and  $\bar{C}_{1,2}$  contribute to the deuteron EDM in conjunction with isospin breaking in the strong interaction, or via the spin-orbit coupling of the photon to the nucleons [143]. Both contributions are beyond the accuracy we work at in this paper.



of  $\epsilon_{m_\pi}$ . In this case, EDMs of light-nuclei are expected to be of similar size as the nucleon EDM. Furthermore, the contact nucleon operators proportional to  $\bar{C}_{1,2}$  now contribute to the PVTV potential at the same order as  $\bar{g}_{0,1}$ . Finally, the qEDM mostly induces  $\bar{d}_{0,1}$ , all other couplings being suppressed by  $\mathcal{O}(\alpha_{\text{em}})$ , where  $\alpha_{\text{em}}$  is the fine structure constant  $\sim 1/137$ . In this case one expects nuclear EDMs to be dominated by the constituent nucleon EDMs.

While most statements are source-dependent, there is an important general message hidden in Table 1. There is no PVTV source for which the couplings  $\bar{g}_2$  and  $\bar{C}_{3,4,5}$  appear at LO. For all sources they appear with a relative suppression of  $\epsilon\epsilon_{m_\pi}$  or  $\epsilon_\chi$  compared to other PVTV interactions. For most calculations one can simply neglect the associated interactions, reducing the number of LECs entering the expression of hadronic and nuclear observables. The suppression of the LECs  $\bar{g}_2$  and  $\bar{C}_{3,4,5}$  ultimately is a consequence of imposing gauge invariance on the dimension-six PVTV sources.

Table 1 relies on NDA estimates for hadronic matrix elements [120]. A more quantitative assessment of the discriminating power of EDM experiments necessitates to replace the NDA estimates in Table 1 with solid nonperturbative calculations of the LECs. At the moment, there exist controlled estimates only of a few LECs. The pion-nucleon couplings  $\bar{g}_0$  induced by the QCD  $\bar{\theta}$  term is related by chiral symmetry to modifications in the baryon spectrum [102]. In particular, in  $SU(2)$   $\chi$ PT  $\bar{g}_0$  is related to the quark mass contribution to the nucleon mass splitting [65, 144], up to N<sup>2</sup>LO corrections. Using Lattice QCD evaluations of the nucleon mass splitting [145, 146], one finds

$$\bar{g}_0(\bar{\theta}) = (15.5 \pm 2.6) \cdot 10^{-3} \bar{\theta}, \quad (38)$$

where the 15% error includes both the Lattice QCD error on  $m_n - m_p$ , and an estimate of the error from N<sup>2</sup>LO chiral corrections. Unfortunately, chiral-symmetry-based relations do not allow to extract  $\bar{g}_1$  and  $\bar{d}_{0,1}$ .  $\bar{g}_1$  has been estimated with resonance saturation leading to  $\bar{g}_1(\bar{\theta})/\bar{g}_0(\bar{\theta}) \simeq -0.2$ , somewhat larger than expected from NDA [73]. The LECs  $\bar{d}_{0,1}$  are usually estimated by naturalness arguments and considered to be of similar size to non-analytic contributions to the isoscalar and isovector nucleon EDM, see the Subsect. 3.2.2.

The relation between PVTV pion-nucleon couplings and corrections to the nucleon and pion masses is not specific to the QCD  $\bar{\theta}$  term, but can be generalized to all chiral-symmetry-breaking sources, such as for example the qCEDM [68, 147] and  $\Xi_{1,2}^{(ud)}$  [148, 141]. Since corrections to spectroscopic quantities should be easier to compute on the lattice, these chiral relations allow a calculation of  $\bar{g}_{0,1}$  in Lattice QCD. While promising, this strategy has yet to lead to controlled results. The best estimate of  $\bar{g}_{0,1}$  induced by the qCEDM comes from QCD sum rules [149, 52]

$$\bar{g}_0 = (0.1 \pm 0.2) \left( 0.7\tilde{c}_g^{(u)} - 1.5\tilde{c}_g^{(d)} \right) \cdot 10^{-6}, \quad \bar{g}_1 = (0.4_{-0.2}^{+0.8}) \left( 0.7\tilde{c}_g^{(u)} - 1.5\tilde{c}_g^{(d)} \right) \cdot 10^{-6}. \quad (39)$$

These estimates agree with NDA, especially for  $\bar{g}_1$ . However,  $\bar{g}_0$  seems to be slightly suppressed, in agreement with large- $N_c$  expectations [150].

Only for the four quark operators proportional to  $\Xi_{1,2}^{(ud)}$  of Eq. (7) does the three-pion vertex with LEC  $\bar{\Delta}$  appear at LO in the chiral Lagrangian. For this case, the LEC  $\bar{\Delta}$  is related by  $SU(3)$  symmetry to  $K \rightarrow \pi\pi$  matrix elements and  $K - \bar{K}$  matrix elements that have been calculated on the lattice. We obtain

$$\bar{\Delta} = \frac{f_\pi}{Mv^2} \left( \mathcal{A}_{1LR} \text{Im} \Xi_1^{(ud)} + \mathcal{A}_{2LR} \text{Im} \Xi_2^{(ud)} \right), \quad (40)$$

with

$$\mathcal{A}_{1LR}(\mu = 3 \text{ GeV}) = (2.2 \pm 0.13) \text{ GeV}^2, \quad \mathcal{A}_{2LR}(\mu = 3 \text{ GeV}) = (10.1 \pm 0.6) \text{ GeV}^2. \quad (41)$$

The matrix elements in Eq. (41) are in good agreement with NDA. The value of  $\bar{\Delta}$  also determines the tadpole component of  $\bar{g}_1$ , which again is in line with NDA.

Most of the remaining LECs are undetermined at present. The focus of the Lattice QCD community has been on the matrix elements connecting the nucleon EDMs to the  $\bar{\theta}$  term [151, 152, 103], the qEDMs [153, 154], the qCEDMs [152, 155], and the Weinberg operator [156]. Some results are given in next subsection.

### 3.2.2 The nucleon EDM in chiral perturbation theory

The PVTV LECs defined in the previous section can be used to calculate the nucleon PVTV electric dipole form factor (EDFF). At zero momentum transfer, the EDFFs are identified with the nucleon EDMs. In dimensional regularization with modified minimal subtraction up to NLO in the chiral expansion, the EDMs are given by [137, 157]

$$d_n = \bar{d}_0(\mu) - \bar{d}_1(\mu) + \frac{eg_A\bar{g}_0}{(4\pi)^2 f_\pi} \left( \log \frac{m_\pi^2}{\mu^2} - \frac{\pi m_\pi}{2M} \right), \quad (42)$$

$$d_p = \bar{d}_0(\mu) + \bar{d}_1(\mu) - \frac{eg_A\bar{g}_0}{(4\pi)^2 f_\pi} \left[ \left( \log \frac{m_\pi^2}{\mu^2} - \frac{2\pi m_\pi}{M} \right) - \frac{\bar{g}_1}{\bar{g}_0} \frac{\pi m_\pi}{2M} \right], \quad (43)$$

where  $\mu$  is the dimensional regularization scale. The leading loops proportional to  $\bar{g}_0$  are divergent and renormalized by the  $\mu$ -dependent LECs  $\bar{d}_{0,1}$ . The NLO corrections proportional to  $m_\pi/M$  are finite. The LEC  $\bar{\Delta}$  does not contribute at this order for any of the PVTV sources. As standard in  $\chi$ PT, the loops are associated to inverse powers of  $(4\pi f_\pi)^2 = \Lambda_\chi^2$ . Combined with the scaling of the LECs in Table 1, we conclude that for the  $\bar{\theta}$  term and the qCEDMs the leading loop proportional to  $\bar{g}_0$  and the counter terms  $\bar{d}_{0,1}$  appear at the same order. For all other PVTV sources, the short-range counter terms  $\bar{d}_{0,1}$  are expected to dominate the nucleon EDMs. In no scenario can the EDMs be calculated solely from the pion-nucleon LECs  $\bar{g}_{0,1}$  as is often assumed in the literature. Estimates for the nucleon EDMs are often obtained by setting  $\mu = M$  and  $\bar{d}_{0,1}(\mu = M) = 0$  such that EDMs depend on the value of  $\bar{g}_{0,1}$ , which for some PVTV sources is better known.

The separation between the short-range and loop contributions is scheme dependent and therefore not physical. Lattice QCD calculations can therefore only calculate the total nucleon EDMs  $d_n$  and  $d_p$ . In recent years, significant efforts have been made towards calculating the nucleon EDMs in terms of the underlying PVTV sources. Most efforts have focused on the QCD  $\bar{\theta}$  term and the qEDM. The most recent results for the  $\bar{\theta}$  term [103] give

$$d_n = -(1.5 \pm 0.7) \cdot 10^{-3} \bar{\theta} \text{ e fm}, \quad d_p = (1.1 \pm 1.0) \cdot 10^{-3} \bar{\theta} \text{ e fm}, \quad (44)$$

in good agreement, but with sizeable uncertainties, with expectations from the chiral logarithm in Eq. (42) using Eq. (38). In the case of the qEDM, the nucleon EDM is related to the tensor charges, which have

been computed with good accuracy [153, 154]. Using the FLAG average [154], we get

$$\begin{aligned} d_n &= g_T^d \frac{Q_u m_u}{v^2} \tilde{c}_\gamma^{(u)} + g_T^u \frac{Q_d m_d}{v^2} \tilde{c}_\gamma^{(d)} = \left( -(0.96 \pm 0.22) \tilde{c}_\gamma^{(u)} - (4.0 \pm 0.4) \tilde{c}_\gamma^{(d)} \right) \cdot 10^{-9} e \text{ fm}, \\ d_p &= g_T^u \frac{Q_u m_u}{v^2} \tilde{c}_\gamma^{(u)} + g_T^d \frac{Q_d m_d}{v^2} \tilde{c}_\gamma^{(d)} = \left( (3.7 \pm 0.8) \tilde{c}_\gamma^{(u)} + (1.0 \pm 0.1) \tilde{c}_\gamma^{(d)} \right) \cdot 10^{-9} e \text{ fm}, \end{aligned} \quad (45)$$

where  $Q_{u,d}$  are the  $u$  and  $d$ -quark charges in units of the electric charge, and  $g_T^{u,d}$  the  $u$  and  $d$ -quark tensor charges of the proton, and the error on the r.h.s. of Eq. (45) is dominated by the uncertainty on the light quark masses.

On a longer time-scale, calculations of the qCEDMs and the Weinberg operator are also targeted. For now, the best results come from calculations using QCD sum rules [52, 158].

### 3.3 From the Lagrangian to the potential

In this subsection, we briefly present two methods that have been used to derive nucleon-nucleon potentials starting from a Lagrangian. We first introduce the notation used here and in the next subsections.

The process under consideration is the scattering of two nucleons from an initial state  $|\mathbf{p}_1 \mathbf{p}_2\rangle$  to the final state  $|\mathbf{p}'_1 \mathbf{p}'_2\rangle$  (hereafter the dependence on the spin-isospin quantum numbers is understood). It is convenient to define the momenta

$$\mathbf{K}_j = \frac{\mathbf{p}'_j + \mathbf{p}_j}{2}, \quad \mathbf{k}_j = \mathbf{p}'_j - \mathbf{p}_j, \quad (46)$$

where  $\mathbf{p}_j$  and  $\mathbf{p}'_j$  are the initial and the final momenta of the nucleon  $j$ . Furthermore it is useful to define

$$\boldsymbol{\sigma}_j \equiv (\boldsymbol{\sigma})_{s'_j, s_j} \equiv \langle \frac{1}{2} s'_j | \boldsymbol{\sigma} | \frac{1}{2} s_j \rangle, \quad \vec{\tau}_j \equiv (\vec{\tau})_{t'_j, t_j} \equiv \langle \frac{1}{2} t'_j | \vec{\tau} | \frac{1}{2} t_j \rangle, \quad (47)$$

which are the spin (isospin) matrix element between the final state  $s'_j$  ( $t'_j$ ) and the initial state  $s_j$  ( $t_j$ ) of the nucleon  $j$ .

Because  $\mathbf{k}_1 = -\mathbf{k}_2 \equiv \mathbf{k}$  from the overall momentum conservation  $\mathbf{p}_1 + \mathbf{p}_2 = \mathbf{p}'_1 + \mathbf{p}'_2$ , the momentum-space potential  $V$  is a function of the momentum variables  $\mathbf{k}$ ,  $\mathbf{K}_1$  and  $\mathbf{K}_2$ , namely

$$\langle \mathbf{p}'_1 \mathbf{p}'_2 | V | \mathbf{p}_1 \mathbf{p}_2 \rangle = V(\mathbf{k}, \mathbf{K}_1, \mathbf{K}_2) (2\pi)^3 \delta(\mathbf{p}_1 + \mathbf{p}_2 - \mathbf{p}'_1 - \mathbf{p}'_2). \quad (48)$$

Moreover, we can write in general

$$V(\mathbf{k}, \mathbf{K}_1, \mathbf{K}_2) = V^{(\text{CM})}(\mathbf{k}, \mathbf{K}) + V^{(\mathbf{P})}(\mathbf{k}, \mathbf{K}), \quad (49)$$

where  $\mathbf{K} = (\mathbf{K}_1 - \mathbf{K}_2)/2$ ,  $\mathbf{P} = \mathbf{p}_1 + \mathbf{p}_2 = \mathbf{K}_1 + \mathbf{K}_2$ , and the term  $V^{(\mathbf{P})}(\mathbf{k}, \mathbf{K})$  represents a boost correction to  $V^{(\text{CM})}(\mathbf{k}, \mathbf{K})$ , the potential in the center-of-mass frame (CM). Below we will ignore the boost correction and provide expressions for  $V^{(\text{CM})}(\mathbf{k}, \mathbf{K})$  only. Note that in the CM we define also  $\mathbf{p}_1 = -\mathbf{p}_2 \equiv \mathbf{p}$  and  $\mathbf{p}'_1 = -\mathbf{p}'_2 \equiv \mathbf{p}'$ . So we have  $\mathbf{k} = \mathbf{p}' - \mathbf{p}$  and  $\mathbf{K} = (\mathbf{p}' + \mathbf{p})/2$ , so in the following we also write  $V^{(\text{CM})}$  as  $V^{(\text{CM})}(\mathbf{p}, \mathbf{p}')$ . From now on, we will suppress the superscript ‘‘(CM)’’ for simplicity.

In order to derive the potential, two methods have been frequently used, the method of unitarity transformation (UT), and the method of the time-ordered perturbation theory (TOPT). They are briefly introduced below.

*The time-ordered perturbation theory method.* Let us consider the matrix element of the  $T$ -matrix,  $T_{fi} = \langle \mathbf{p}'_1 \mathbf{p}'_2 | T | \mathbf{p}_1 \mathbf{p}_2 \rangle$ , the ‘‘amplitude’’ of a process of scattering of two nucleons. Its square modulus  $|T_{fi}|^2$  is directly related to the cross section of the process. The conventional perturbative expansion for this matrix element is given as

$$T_{fi} = \langle \mathbf{p}'_1 \mathbf{p}'_2 | H_I \sum_{n=1}^{\infty} \left( \frac{1}{E_i - H_0 + i\epsilon} H_I \right)^{n-1} | \mathbf{p}_1 \mathbf{p}_2 \rangle, \quad (50)$$

where  $E_i$  is the energy of the initial state,  $H_0$  is the Hamiltonian describing free pions and nucleons, and  $H_I$  is the Hamiltonian describing interactions among these particles. These operators are defined to be in the Schrödinger picture and they can be derived from the Lagrangian constructed in terms of pions and nucleons as described, for example, in Refs. [159, 118]. The evaluation of  $T_{fi}$  is carried out in practice by inserting complete sets of  $H_0$  eigenstates between successive  $H_I$  factors. Power counting is then used to organize the expansion in powers of  $Q/\Lambda_\chi \ll 1$ , where  $Q$  stands for either an external momenta or the pion mass. We will use the ‘‘naive’’ Weinberg counting rules [2], namely, we will count simply the powers of both the external momenta and pion mass insertions (we will consider low energy processes only). Each term will be of some order  $(Q/\Lambda_\chi)^\nu$ . The terms with the lowest power of  $\nu$  will be the LO, and so on.

In the perturbative series given in Eq. (50), a generic contribution will be characterized by a certain number of vertices coming from the interaction Hamiltonian  $H_I$  and energy denominators, and it can be visualized also as a diagram (hereafter referred to as a TOPT diagram). Each vertex will give a ‘‘vertex function’’ and a  $\delta$  conservation of the momenta of the particles involved in the vertex. The vertex functions are the results of the matrix elements of terms appearing in  $H_I$  and are given as products of Dirac four-spinors, momenta, etc. A sum over the momenta of the particles entering the intermediate states is also present. When a diagram includes one or more loops, the  $\delta$ 's are not sufficient to eliminate all the sums over the momenta of the intermediate states. The energy denominators come from the factors  $1/(E_i - E_\alpha + i\epsilon)$ , where  $E_\alpha$  is the (kinetic) energy of a specific intermediate state entering the calculation. The chiral order of each diagram can be calculated as follows. One needs to consider:

1. The chiral order of the vertex functions, which can be calculated from the non-relativistic (NR) expansion of the nucleon Dirac four-spinors ( $1/M$  expansion), and from various other factors. Typically, the powers of  $p/M$  coming from the NR expansion of the nucleon Dirac four-spinors are counted as  $\sim Q^2$  [2, 4, 160]. In other approaches however they are considered to be of order  $Q$  [20, 161, 162]. In this paper, we will follow the first prescription.
2. The energy denominators. We note that typical momenta  $\mathbf{p}$  of the nucleons are much smaller than the mass of the nucleons, so we can treat them non relativistically. Namely  $\sqrt{p^2 + M^2} \simeq M + \frac{p^2}{2M} \sim O(Q^0) + O(Q^2)$ . Regarding the pion energies,  $\omega_{\mathbf{k}} = \sqrt{m_\pi^2 + k^2} \sim O(Q)$ . Usually in the energy denominator all the nucleon masses  $M$  cancel out and therefore we have two cases:
  - if there are no pions in the intermediate state, the energy denominator has only nucleon energy terms so it results of order  $1/Q^2$ .

- if there are pions in the intermediate states, the energy denominator reads

$$\frac{1}{\Delta E - \omega_k} \sim -\frac{1}{\omega_k} \left( 1 + \frac{\Delta E}{\omega_k} + \dots \right), \quad (51)$$

where the term  $\Delta E = E_1 + E_2 + \dots - E_i$  where  $E_1, \dots$  are the energies of the nucleons in the intermediate state and  $E_i$  is the initial scattering energy. In the Taylor expansion the first term is of order  $Q^{-1}$ , while the other terms are usually called “recoil corrections”. For the sake of consistency with the choice discussed above regarding the NR expansion of the Dirac 4-spinors, here we will count the  $p/M$  terms coming from recoil corrections as  $Q^2$  as well.

3. The number of loops, or better the number of the sums over the intermediate state momenta that remain after using the conservation  $\delta$ 's. Each loop at the end will give a contribution of order  $Q^3$ .
4. The number of disconnected parts of the diagram. For each of these parts, a  $\delta$  factor expressing the momentum conservation of each part is present. Then, if there are  $N_D$  disconnected parts, one of the  $\delta$  simply gives the total momentum conservation, a factor common to all diagrams and therefore not relevant. Each of the remaining  $N_D - 1$   $\delta$ 's at the end will “block” a sum over an external three-momentum, each one therefore reducing the chiral order by 3 units.

Once the  $T$ -matrix has been calculated, one would obtain in general

$$T_{fi} = \sum_{n=n_{\min}} T_{fi}^{(n)}, \quad (52)$$

where  $T_{fi}^{(n)} \sim Q^n$ . In all cases the sum starts from a minimum value  $n_{\min}$ ,  $n_{\min} = 0$  for the PCTC and  $n_{\min} = -1$  for the PVTC and PVTV amplitudes. The idea now is to “define” the potential acting between the two nucleons so that it can reproduce the same amplitude  $T_{fi}$ , namely, so that (for more details, see Ref. [118])

$$T_V = V + V \frac{1}{E_i - H_0^{(NN)} + i\epsilon} T_V \equiv T_{fi}, \quad (53)$$

where  $H_0^{(NN)}$  is the non-interacting Hamiltonian of two nucleons. Clearly, this procedure is not unique, since usually one imposes the relation  $T_V = T_{fi}$  to hold “on shell”, namely by requiring the conservation of the energy between initial and final states. This induces an ambiguity, as discussed for example in Ref. [162]. However, the obtained potentials are expected to be equivalent by means of a unitary or at least a similarity transformation [163].

Finally, to invert Eq. (53), one assumes that  $V$  has the same  $Q$  expansion as the  $T$  matrix,

$$V = \sum_{n=n_{\min}} V^{(n)}, \quad V^{(n)} \sim Q^n, \quad (54)$$

and Eq. (53) can be solved for  $V^{(n)}$  order-by-order (see, for example, Ref. [118] for more details). This procedure can be generalized to the  $A = 3$  case to define a three-nucleon potential and so on.

*The method of unitarity transformation.* The method of unitary transformation (MUT) has been pioneered in the fifties of the last century to derive nuclear potentials in the framework of pion field theory [164, 165]. In the context of chiral EFT, this approach was formulated in Refs. [166, 167]. Similarly to

TOPT, the MUT is applied to the pion-nucleon Hamiltonian which can be obtained from the effective Lagrangian in a straightforward way using the standard canonical formalism. Let  $\eta$  and  $\lambda$  denote the projection operators on the purely nucleonic subspace and the rest of the Fock space involving pion states with the usual properties  $\eta^2 = \eta$ ,  $\lambda^2 = \lambda$ ,  $\eta\lambda = \lambda\eta = 0$  and  $\eta + \lambda = 1$ . To derive nuclear forces and/or current operators, the Hamiltonian needs to be brought into a block-diagonal form with no coupling between the  $\eta$ - and  $\lambda$ -subspaces, which can be achieved via a suitably chosen unitary transformation  $U$ . Following Okubo, a unitary operator can be conveniently parametrized in terms of the operator  $A = \lambda A \eta$  that mixes the two subspaces via

$$U = \begin{pmatrix} \eta(1 + A^\dagger A)^{-1/2} & -A^\dagger(1 + AA^\dagger)^{-1/2} \\ A(1 + A^\dagger A)^{-1/2} & \lambda(1 + AA^\dagger)^{-1/2} \end{pmatrix}. \quad (55)$$

One then obtains the nonlinear decoupling equation for the operator  $A$ :

$$\tilde{H} \equiv U^\dagger H U \stackrel{!}{=} \begin{pmatrix} \eta \tilde{H} \eta & 0 \\ 0 & \lambda \tilde{H} \lambda \end{pmatrix} \implies \lambda (H - [A, H] - AHA) \eta = 0. \quad (56)$$

The solution of the decoupling equation and the calculation of the unitary operator  $U$  and the nuclear potential  $\eta \tilde{H} \eta$  is carried out in perturbation theory by employing the standard chiral expansion. The resulting expressions for the operators  $A$ ,  $U$  and  $\eta \tilde{H} \eta$  have a form of a sequence of vertices from the pion-nucleon Hamiltonian  $H$  and energy denominators involving the kinetic energies of particles in the intermediate states with one or more virtual pions. They are thus similar to the expressions emerging in the context of TOPT, see e.g. the operator in Eq. (50), and the corresponding matrix elements can also be interpreted in terms of TOPT-like diagrams. Notice that contrary to Eq. (50), the expressions in the MUT do, per construction, not involve energy denominators that vanish in the static limit of infinitely heavy nucleons and correspond to iterative contributions to the scattering amplitude. As explained in [167], in order to implement the chiral power counting in the algebraic approach outlined above it is convenient to rewrite it in terms of different variables. Using the rules given in the description of the TOPT approach and counting the powers of the soft scale  $Q$  for a given irreducible (i.e. of non-iterative type) connected  $N$ -nucleon TOPT-like diagram without external sources, one obtains for the chiral order  $n$  [2, 167]

$$n = -4 + 2N + 2L + \sum_i V_i \Delta_i, \quad (57)$$

where  $L$  is the number of loops,  $V_i$  is the number of vertices of type  $i$ . Further, the vertex dimension  $\Delta_i$  is given by  $\Delta_i = d_i + 1/2 n_i - 2$  with  $d_i$  and  $n_i$  being the number of derivatives and/or  $m_\pi$ -insertions and the number of nucleon fields, respectively. The above expression is convenient to use for estimating the chiral dimension of TOPT-like diagrams. For the MUT, it is, however, advantageous to rewrite it in the equivalent form

$$n = -2 + \sum_i V_i \kappa_i, \quad \kappa_i = d_i + \frac{3}{2} n_i + p_i - 4, \quad (58)$$

where  $p_i$  is the number of pionic fields. The parameter  $\kappa_i$  obviously corresponds to the inverse overall mass dimension of the coupling constant(s) accompanying a vertex of type  $i$ . In this form, chiral expansion becomes formally equivalent to the expansion in powers of the coupling constants, and it is straightforward to employ perturbation theory for solving the decoupling equation (56) and deriving the nuclear potentials  $\eta \tilde{H} \eta$ .

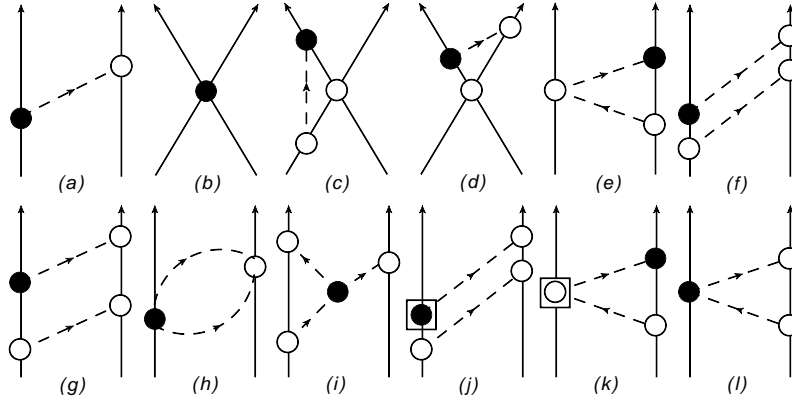


**Figure 1.** TOPT diagrams contributing up to  $N^2\text{LO}$  to the PVTC amplitude. Nucleons and pions are denoted by solid and dashed lines, respectively. The open (solid) circles represent LO PCTC (PVTC) vertices. The vertex depicted by a square surrounding an solid circle denotes the contribution of the subleading PVTC  $\pi NN$  terms coming from the Lagrangian given in Eq. (19). The vertex depicted by a square surrounding an open circle denotes the contribution of the subleading PCTC  $\pi\pi NN$  (PVTC  $\pi NN$ ) terms coming from the Lagrangian given in Eq. (13).

One nontrivial issue that emerges when applying chiral EFT to nuclear potentials concerns their renormalization. While on-shell scattering amplitudes, calculated in chiral EFT, can always be made finite by including the counterterms from the effective Lagrangian (provided one uses a chiral-symmetry preserving regularization scheme such as dimensional regularization), nuclear potentials represent scheme-dependent quantities, which correspond to non-iterative parts of the scattering amplitude. There is no a priori reason to expect all ultraviolet divergences emerging from TOPT-like diagrams, which give rise to nuclear forces, to be absorbable into a redefinition of the LECs. Indeed, it was found that the static PCTC three-nucleon force at order  $Q^4$  of the two-pion-one-pion exchange type cannot be renormalized if one uses the unitary transformation given in Eq. (55) [168]. On the other hand, the employed parametrization of the operator  $U$  is clearly not the most general one and represents just one possible choice. The freedom to change the off-shell behavior of the nuclear potentials, already mentioned in the context of TOPT, has been exploited in a systematic way in the PCTC sector in order to enforce renormalizability of nuclear forces (using dimensional regularization) [167, 169, 170, 171, 172]. The MUT has also been successfully applied to the effective Lagrangian in the presence of external classical sources in order to derive the corresponding nuclear current operators, see [160] and references therein.

### 3.4 The PVTC potential up to order $Q^2$

In this subsection we will discuss in detail the derivation of the PVTC potential up to  $N^2\text{LO}$  using the TOPT approach. We consider diagrams contributing to the  $T$ -matrix with one vertex coming from the PVTC Lagrangian, while all other vertices coming from the PCTC interaction. Diagrams with two or more PVTC vertices can be safely neglected.

The TOPT diagrams contributing to the PVTC  $T$ -matrix up to  $N^2\text{LO}$  are shown in Fig. 1 in panels (a)-(l). The one pion exchange diagram (a) gives a contribution to the  $T$ -matrix of order  $Q^{-1}$  (that will be our LO). The diagram (b) represents a PVTC contact interaction of order  $Q$ ; also the diagrams (c) and (d) with the PCTC contact vertex and one pion exchange are of order  $Q$ . The triangle diagram (e) with a PCTC  $\pi\pi NN$  vertex is of order  $Q$ , while if we consider the PVTC  $\pi\pi NN$  vertex as in panel (l) the diagram is of order  $Q^2$ . The box diagrams (f) and (g) includes contribution of order  $Q^0$  and  $Q$ ; the contribution of order  $Q^0$  is exactly canceled when inverting Eq. (53). Finally, the ‘‘bubble’’ diagram (h), the three-pion vertex

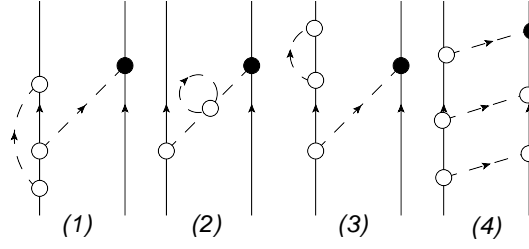


**Figure 2.** Other diagrams that would contribute at NLO. These diagrams contribute to the renormalization of the LECs (panels (1), (2) and (3)) or give a vanishing contribution to the potential (panel (4)) due to the inversion of Eq. (53). Notation as in Fig. 1.

diagram (i), the box diagram (j) with the  $\pi NN$  vertex coming from the subleading PVTC Lagrangian terms proportional to the LECs  $h_V^i$ , and also the diagram (k) with the  $\pi\pi NN$  vertex coming from the subleading PCTC Lagrangian terms proportional to the LECs  $c_i$ , are of order  $Q^2$ . These latter diagrams were considered for the first time in [173] using the MUT, and using TOPT in [174].

Contributions proportional to  $1/M$  coming from the NR expansion of the vertex functions or from recoil corrections in this work are considered to be at least of order  $N^3\text{LO}$ .

Other types of diagrams like those shown in panels (1), (2), (3) of Fig. 2 simply contribute to a renormalization of the coupling constants and masses, see Ref. [42] for more details. In the following, we will disregard these diagrams, but it should be taken into account that the formulas below are given in terms of the renormalized (physical) LECs and masses. The contribution of diagram (4) is cancelled when inverting Eq. (53).

Let us now consider each kind of diagram separately:

- *One pion exchange (OPE) diagram.* Diagram (a) of Fig. 1 gives the LO contribution ( $Q^{-1}$ ) to the potential

$$V_{PVTC}^{(-1)}(a) = \frac{g_A h_\pi^1}{2\sqrt{2}f_\pi} (\vec{\tau}_1 \times \vec{\tau}_2)_z \frac{i\mathbf{k} \cdot (\boldsymbol{\sigma}_1 + \boldsymbol{\sigma}_2)}{\omega_k^2}, \quad (59)$$

where  $\omega_k = \sqrt{k^2 + m_\pi^2}$ , and it comes directly from the LO expansion of the vertices and energy denominators. Derived from the same diagram, there are terms coming from the NR expansion of the vertices, the first correction being of order  $(p/M)^2$ . However, as discussed previously, they are counted to be of order  $Q^4$ , and thus the corresponding terms are considered to be suppressed by four orders with respect to  $V_{PVTC}^{(-1)}$ .

- *Contact terms (CT) diagrams.* The diagrams as that one depicted in panel (b) of Fig. 1 derive from the interaction terms appearing in  $\mathcal{L}_{PVTC,NN}^{(1)}$ . They give a contribution to the potential of order  $Q^1$ . As discussed in Chapter 4, this contribution can be written in various equivalent forms due to the Fierz identities [44]. We have chosen to write this part as follows [42]

$$\begin{aligned} V_{PVTC}^{(1)}(b) = & \frac{1}{\Lambda_\chi^2 f_\pi} [C_1 i(\boldsymbol{\sigma}_1 \times \boldsymbol{\sigma}_2) \cdot \mathbf{k} + C_2 (\vec{\tau}_1 \cdot \vec{\tau}_2) i(\boldsymbol{\sigma}_1 \times \boldsymbol{\sigma}_2) \cdot \mathbf{k} \\ & + C_3 (\vec{\tau}_1 \times \vec{\tau}_2)_z i(\boldsymbol{\sigma}_1 + \boldsymbol{\sigma}_2) \cdot \mathbf{k} + C_4 (\tau_{1z} + \tau_{2z}) i(\boldsymbol{\sigma}_1 \times \boldsymbol{\sigma}_2) \cdot \mathbf{k} \\ & + C_5 \mathcal{I}_{ab} \tau_{1a} \tau_{2b} i(\boldsymbol{\sigma}_1 \times \boldsymbol{\sigma}_2) \cdot \mathbf{k}]. \end{aligned} \quad (60)$$



where  $\Lambda_\chi = 4\pi f_\pi \approx 1.2$  GeV. The parameters  $C_i$ ,  $i = 1, \dots, 5$  are LECs. Different (but equivalent) forms of this part were used in Refs. [41, 173].

- *Contact plus OPE diagrams.* The diagrams (c) and (d) in Fig. 1 are representative of diagrams with a contact term and an OPE. However all these diagrams vanish after the integration over the loop variable.
- *NLO two pions exchange: triangle diagrams.* There are 6 different time-orderings of diagrams given in panel (e) in Fig. 1. After summing them, the total contribution from the triangle diagrams results to be [40, 175]

$$V_{PVTC}^{(1)}(e) = \frac{g_A h_\pi^1}{8\sqrt{2}f_\pi^3} (\vec{\tau}_1 \times \vec{\tau}_2)_z i\mathbf{k} \cdot (\boldsymbol{\sigma}_1 + \boldsymbol{\sigma}_2) \int \frac{d^3q}{(2\pi)^3} \frac{1}{\omega_+ \omega_- (\omega_+ + \omega_-)}, \quad (61)$$

where  $\omega_\pm = \sqrt{(\mathbf{q} \pm \mathbf{k})^2 + 4m_\pi^2}$ . The integral is singular and has to be regularized using some method. We will discuss this issue later.

- *NLO two pions exchange: box diagrams.* There are 48 diagrams represented by the diagrams of type (f) and (g) of Fig. 1 when we consider all possible time orderings. The final contribution is [40, 175]

$$\begin{aligned} V_{PVTC}^{(1)}(f, g) = & \frac{h_\pi^1 g_A^3}{8\sqrt{2}f_\pi^3} \int \frac{d^3q}{(2\pi)^3} \frac{\omega_+^2 + \omega_+ \omega_- + \omega_-^2}{\omega_+^3 \omega_-^3 (\omega_+ + \omega_-)} \\ & \{-2i(\tau_{1z} + \tau_{2z}) [\mathbf{q} \cdot \boldsymbol{\sigma}_1 (\mathbf{q} \times \mathbf{k}) \cdot \boldsymbol{\sigma}_2 - \mathbf{q} \cdot \boldsymbol{\sigma}_2 (\mathbf{q} \times \mathbf{k}) \cdot \boldsymbol{\sigma}_1] \\ & -2i(\tau_{1z} - \tau_{2z}) [\mathbf{q} \cdot \boldsymbol{\sigma}_2 (\mathbf{q} \times \mathbf{k}) \cdot \boldsymbol{\sigma}_1 + \mathbf{q} \cdot \boldsymbol{\sigma}_1 (\mathbf{q} \times \mathbf{k}) \cdot \boldsymbol{\sigma}_2] \\ & +i(\vec{\tau}_1 \times \vec{\tau}_2)_z (k^2 - q^2) \mathbf{k} \cdot (\boldsymbol{\sigma}_1 + \boldsymbol{\sigma}_2)\}, \end{aligned} \quad (62)$$

and it is of order  $Q^1$ . Again the integral is singular. In this case, in the amplitude  $T_{fi}$  there appears a term of order  $Q^0$  coming from diagram (g), but it cancels out when inverting Eq. (53).

- *Bubble diagrams.* We now turn to the diagrams contributing at order  $Q^2$ , that is at N<sup>2</sup>LO. The sum of “bubble” diagrams depicted in panel (h) of Fig. 1 mutually cancel and these diagrams do not give any contribution to the PVTC potential.
- *Diagrams with three pion vertices.* The expansion of the PVTC Lagrangian in terms of pions gives rise to two terms proportional to  $(\vec{\pi})^3$  which would contribute to  $T_{fi}$  via the diagram depicted in panel (i) of Fig. 1. However, after summing over all possible time orderings, the corresponding final contribution vanishes.
- *N<sup>2</sup>LO two pion exchanges: box diagrams.* The box diagrams contributes also at N<sup>2</sup>LO via diagrams of type (j) where the PVTC vertex comes from the subleading Lagrangian terms proportional to the LECs  $h_0^V$ ,  $h_1^V$ , and  $h_2^V$  in Eq. (19). We have [173, 75]

$$\begin{aligned} V_{PVTC}^{(2)}(j) = & \frac{g_A^3}{32f_\pi^4} \left[ \left( h_V^0 (3 + 2\vec{\tau}_2 \cdot \vec{\tau}_1) - \frac{4}{3} h_V^2 \mathcal{I}_{ab} \tau_{1b} \tau_{2b} \right) i \int \frac{d^3q}{(2\pi)^3} \frac{1}{\omega_+^2 \omega_-^2} [(\mathbf{q} \cdot \boldsymbol{\sigma}_1 (\mathbf{q} \times \mathbf{k}) \cdot \boldsymbol{\sigma}_2) \right. \\ & - (\mathbf{q} \cdot \boldsymbol{\sigma}_2 (\mathbf{q} \times \mathbf{k}) \cdot \boldsymbol{\sigma}_1)] - 2i h_V^1 \int \frac{d^3q}{(2\pi)^3} \frac{1}{\omega_+^2 \omega_-^2} [(\mathbf{q} \cdot \boldsymbol{\sigma}_1 (\mathbf{q} \times \mathbf{k}) \cdot \boldsymbol{\sigma}_2) \tau_{1z} \\ & \left. - (\mathbf{q} \cdot \boldsymbol{\sigma}_2 (\mathbf{q} \times \mathbf{k}) \cdot \boldsymbol{\sigma}_1) \tau_{2z}] + i h_V^1 (\vec{\tau}_1 \times \vec{\tau}_2)_z \mathbf{k} \cdot (\boldsymbol{\sigma}_1 + \boldsymbol{\sigma}_2) \int \frac{d^3q}{(2\pi)^3} \frac{q^2 - k^2}{\omega_+^2 \omega_-^2} \right]. \end{aligned} \quad (63)$$

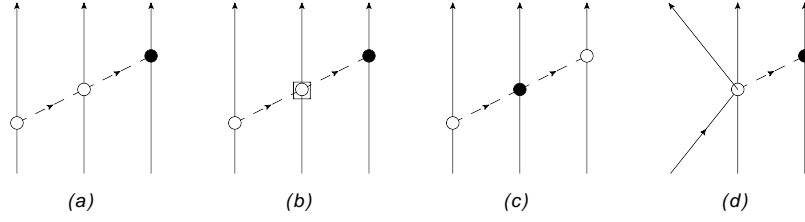


**Figure 3.** TOPT diagrams that would contribute to the PVTC 3N force For the notation see Fig. 1.

- $N^2LO$  two pion exchanges: triangle diagrams. The diagram depicted in panels (k) derives from a subleading  $\pi\pi NN$  vertices in the PCTC Lagrangians [173, 75], see Eq. (13),

$$V_{PVTC}^{(2)}(k) = -i \frac{c_4 h_\pi^1 g_A}{2\sqrt{2} f_\pi^3} \int \frac{d^3q}{(2\pi)^3} \frac{1}{\omega_+^2 \omega_-^2} \times [(\mathbf{q} \cdot \boldsymbol{\sigma}_1(\mathbf{q} \times \mathbf{k}) \cdot \boldsymbol{\sigma}_2)\tau_{2z} - (\mathbf{q} \cdot \boldsymbol{\sigma}_2(\mathbf{q} \times \mathbf{k}) \cdot \boldsymbol{\sigma}_1)\tau_{1z}]. \quad (64)$$

Note in Eq. (64) the presence of the LEC  $c_4$ , which belong to the PCTC sector [12].

The expression for the diagrams (l) comes from the LO PCTC and PVTC vertex functions. The final result is [173, 75]

$$V_{PVTC}^{(2)}(l) = -\frac{g_A^2}{8f_\pi^4} \int \frac{d^3q}{(2\pi)^3} \frac{1}{\omega_+^2 \omega_-^2} \times \{2h_A^1 [(\mathbf{q} \cdot \boldsymbol{\sigma}_1(\mathbf{q} \times \mathbf{k}) \cdot \boldsymbol{\sigma}_2)\tau_{2z} - (\mathbf{q} \cdot \boldsymbol{\sigma}_2(\mathbf{q} \times \mathbf{k}) \cdot \boldsymbol{\sigma}_1)\tau_{1z}] + h_A^2 \mathcal{I}_{ab} \tau_{1a} \tau_{2b} [(\mathbf{q} \cdot \boldsymbol{\sigma}_1(\mathbf{q} \times \mathbf{k}) \cdot \boldsymbol{\sigma}_2) - (\mathbf{q} \cdot \boldsymbol{\sigma}_2(\mathbf{q} \times \mathbf{k}) \cdot \boldsymbol{\sigma}_1)]\}, \quad (65)$$

where  $h_A^1$  and  $h_A^2$  are two of the LECs that appear in the Lagrangian terms given in Eq. (19).

Finally, we conclude this section by mentioning that at  $N^2LO$ , one should also include PVTC 3N forces. Examples of diagrams contributing to this 3N force are reported in Fig. 3. The chiral order of diagrams with more than two nucleons is discussed in detail in Ref. [167]. The diagram depicted in panel (a) with a LO PCTC  $\pi\pi NN$  vertex would contribute at NLO but summing over all the time-orderings it vanishes. The other three diagrams (the one in panel (b) has a subleading PCTC  $\pi\pi NN$  vertex proportional to  $c_i$ ,  $i = 1, \dots, 4$  [12]) are  $N^2LO$  and therefore they have to be considered in order to perform fully consistent calculations in  $A \geq 3$  systems. These kind of diagrams have not yet been considered in literature. Note that diagrams with a 3N PVTC contact vertex are highly suppressed, so no new LEC has to be introduced in this case.

### 3.4.1 Regularization of the PVTC potential

In this section we deal with the divergences in the loop diagrams. We will briefly present three methods frequently used in literature, namely the dimensional regularization (DR) method used e.g. in [161], the spectral function regularization (SFR) [176], and the novel (semi-)local momentum-space regularization approach of Ref. [19].

- *Dimensional regularization method.* This technique is well known for dealing with divergences of loop integrals present in Feynman diagrams, where the integration is performed over four-momenta. In case of time-ordering diagrams, the loops involve integrations over 3-dimensional momenta. To

deal with the singularities, the integrals are re-defined in  $d$  dimensions and successively one takes the limit  $d \rightarrow 3$ . The singular part is singled out by terms  $\sim 1/(3-d)$ , which then can be reabsorbed in some of the LECs. As usual, we define  $\epsilon = 3-d$ , and we assume that  $\epsilon \rightarrow 0$ . When we use the DR, it is better to “rescale” all the dimensional quantities with an energy scale  $\mu$ . Therefore we define  $q = \tilde{q}\mu$ ,  $m = \tilde{m}\mu$ , etc., where the “tilde” quantities are adimensional. We can now go to  $d$  dimension and manipulate the integrals as discussed in detail in Ref. [161], see also Ref. [177]. Here we limit ourselves to list the results needed to regularize the loop integrals we have encountered. Regarding the loop integrals appearing at NLO in Eqs. (61) and (62), we have

$$\int \frac{d^3q}{(2\pi)^3} \frac{1}{\omega_+ \omega_- (\omega_+ + \omega_-)} = -\frac{1}{4\pi^2} \left( L(k) - d_\epsilon + 2 \right), \quad (66)$$

$$\int \frac{d^3q}{(2\pi)^3} \frac{\omega_+^2 + \omega_+ \omega_- + \omega_-^2}{\omega_+^3 \omega_-^3 (\omega_+ + \omega_-)} = \frac{1}{16\pi^2} \frac{H(k)}{m_\pi^2}, \quad (67)$$

where

$$L(k) = \frac{1}{2k} \ln \frac{s+k}{s-k}, \quad H(k) = \frac{4m_\pi^2}{s^2} L(k), \quad s = \sqrt{4m_\pi^2 + k^2}, \quad (68)$$

and

$$d_\epsilon = \frac{2}{\epsilon} - \gamma + \ln \pi - \ln \frac{m_\pi^2}{\mu^2}, \quad (69)$$

which contains the divergent part (above  $\gamma$  is the Euler–Mascheroni constant).

The loop integrals appearing in the N<sup>2</sup>LO diagrams as in Eqs. (64) and (65) are of the form

$$\int \frac{d^3q}{(2\pi)^3} \frac{1}{\omega_+^2 \omega_-^2}, \quad (70)$$

$$\int \frac{d^3q}{(2\pi)^3} \frac{1}{\omega_+^2 \omega_-^2} q_i q_j, \quad (71)$$

The first integral is finite, but the second integrand diverges linearly for  $q \rightarrow \infty$ . The finite contribution to potential can be obtained using the DR method. Alternatively, one can impose an ultraviolet cut-off  $\Lambda_C$  on the integrals. The integrals then yield diverging parts as  $\Lambda_C \rightarrow \infty$ , which can be again reabsorbed by some LECs, finite parts independent on  $\Lambda_C$  that are exactly the same as obtained using the DR method, and a number of other terms which can be expressed in power series of  $Q/\Lambda_C$ , where  $Q$  is either  $k$  or  $m_\pi$ . Taking the limit  $\Lambda_C$  to infinity these latter parts would disappear. Since, in general we must fix  $\Lambda_C$  at a value greater than the typical energies of the  $\chi$ EFT, then these additional terms carry at least an additional power of  $Q$  which means they give contributions at N<sup>3</sup>LO (or beyond) to the potential. Therefore, for the integral in Eq. (71), we have followed the prescription to absorb the divergent parts in some LEC’s, disregard the parts depending on  $Q/\Lambda_C$ , and retaining the finite parts as those given by the DR method. Explicitly, the two integrals are given by

$$\int \frac{d^3q}{(2\pi)^3} \frac{1}{\omega_+^2 \omega_-^2} = \frac{A(k)}{4\pi}, \quad (72)$$

$$\int \frac{d^3q}{(2\pi)^3} \frac{1}{\omega_+^2 \omega_-^2} q_i q_j \Rightarrow \left( -\frac{s^2 A(k)}{8\pi} - \frac{m_\pi}{8\pi} \right) \delta_{ij} + \left( \frac{s^2 A(k)}{8\pi} - \frac{m_\pi}{8\pi} \right) \frac{k_i k_j}{k^2}, \quad (73)$$

where

$$A(k) = \frac{1}{2k} \arctan\left(\frac{k}{2m_\pi}\right). \quad (74)$$

- *Spectral function regularization method.* Pion loop integrals appearing in the two-pion exchange contributions discussed in the previous subsection can be generally expressed using a dispersive representation. Writing the momentum-space potentials in the general form  $V = \sum_i O_i W_i(k)$  with  $O_i$  being spin-isospin-momentum operators and  $W_i$  the corresponding structure functions that depend only on the momentum transfer  $k \equiv |\mathbf{k}|$ , the unsubtracted dispersion relations for the functions  $W_i(k)$  have the form [178]

$$W_i(k) = \frac{2}{\pi} \int_{2m_\pi}^{\infty} d\mu \mu \frac{\rho_i(\mu)}{\mu^2 + k^2}, \quad (75)$$

where the spectral functions  $\rho_i(\mu)$  are given by  $\rho_i = \Im(W_i(0^+ - i\mu))$ . Notice that the spectral integrals in Eq. (75) do not converge for potentials derived in chiral EFT since  $\rho_i(\mu)$  generally grow with  $\mu$ , and must be subtracted the appropriate number of times. The subtractions introduce terms which are polynomial in  $k^2$  and can be absorbed into the corresponding contact interactions. It was shown in Ref. [176] that even at fairly large internucleon distances, the potentials receive significant contributions from the spectral function in the region of  $\mu \gtrsim \Lambda_\chi$ , where the chiral expansion cannot be trusted. It was, therefore, proposed in that paper to employ an ultraviolet cutoff  $\Lambda$  in the spectral integrals. This can be shown to be equivalent to introducing a particular ultraviolet cutoff in the loop integrals over the momentum  $q$ . Using a sharp cutoff  $\Lambda$  in the spectral integrals over  $\mu$  leads to the following modification of the loop functions  $L(k)$  and  $A(k)$ :

$$\begin{aligned} L^\Lambda(k) &= \theta(\Lambda - 2m_\pi) \frac{s}{2k} \ln \frac{\Lambda^2 s^2 + k^2 l^2 + 2\Lambda k s l}{4m_\pi^2(\Lambda^2 + k^2)}, \\ A^\Lambda(k) &= \theta(\Lambda - 2m_\pi) \frac{1}{2k} \arctan \frac{k(\Lambda - 2m_\pi)}{k^2 + 2\Lambda m_\pi}, \end{aligned} \quad (76)$$

where we have introduced  $l = \sqrt{\Lambda^2 - 4m_\pi^2}$ . The resulting approach is referred to as the spectral function regularization. The limit of an infinitely large cutoff  $\Lambda$  corresponds to the previously considered case of dimensional regularization with  $L^\infty(k) = L(k)$  and  $A^\infty(k) = A(k)$ . The spectral function regularization approach with a finite value of  $\Lambda$  was employed in the PCTC potentials of Ref. [74] and the more recent work [18], and in the derivation of the N<sup>2</sup>LO PVTC potential in Ref. [46].

- *Local regularization in momentum space.* The previously introduced spectral function regularization approach has an unpleasant feature of inducing *long-range* finite- $\Lambda$  artifacts as can be seen by expanding the functions  $L^\Lambda(k)$  and  $A^\Lambda(k)$  in inverse powers of  $\Lambda$ . This feature may affect the applicability of chiral EFT for softer cutoff choices. Recently, local regulators in coordinate [179, 17] and momentum space [19] were introduced, which do not affect the analytic structure of the pion-exchange interactions and thus maintain the long-range part of the nuclear force. The approach of Ref. [19] amounts to replacing the static propagators of pions exchanged between different nucleons via

$$\frac{1}{q^2 + m_\pi^2} \longrightarrow \frac{1}{q^2 + m_\pi^2} \exp\left(-\frac{q^2 + m_\pi^2}{\Lambda^2}\right), \quad (77)$$

with  $q \equiv |\mathbf{q}|$ . Such a regulator obviously does not induce any long-range artifacts at any order in the  $1/\Lambda$ -expansion. This regularization approach can be easily implemented for two-pion exchange NN

potentials with no need to recalculate the various loop integrals. Using the feature that the regulator does not affect long-range interactions, it is easy to show that the regularization of a generic two-pion exchange contribution simply amounts to introducing a specific cutoff in the dispersive representation (modulo short-range interactions), namely [19]

$$\frac{2}{\pi} \int_{2m_\pi}^{\infty} d\mu \mu \frac{\rho_i(\mu)}{\mu^2 + k^2} \longrightarrow \frac{2}{\pi} \int_{2m_\pi}^{\infty} d\mu \mu \frac{\rho_i(\mu)}{\mu^2 + k^2} \exp\left(-\frac{\mu^2 + k^2}{2\Lambda^2}\right). \quad (78)$$

In Ref. [19], the regularized two-pion exchange contributions were defined using the requirement (i.e. a convention) that the corresponding potentials in coordinate space and derivatives thereof vanish at the origin. This is achieved by adding to the right-hand side of Eq. (78) a specific combination of (locally regularized) contact interactions allowed by the power counting. For more details and explicit expressions see Ref. [19]. This local regularization scheme has not been used for PVTC or PVTV nuclear potentials.

### 3.4.2 The regularized PVTC potential

Once the loop integrals have been manipulated as discussed previously, we can now write the PVTC potential up to N<sup>2</sup>LO derived from  $\chi$ EFT. In the following, some of the LEC's have been further redefined to absorb the singular parts coming from the loop integrals. If one has chosen to regularize the loop integral using the SFR method, then the functions  $L(k)$  and  $A(k)$  below have to be substituted with  $L^\Lambda(k)$  and  $A^\Lambda(k)$ , the spectral regularized functions, see Eq. (76). In summary,

$$V_{PVTC} = V_{PVTC}^{(-1)}(\text{OPE}) + V_{PVTC}^{(1)}(\text{CT}) + V_{PVTC}^{(1)}(\text{TPE}) + V_{PVTC}^{(2)}(\text{TPE}), \quad (79)$$

where

$$V_{PVTC}^{(-1)}(\text{OPE}) = \frac{g_A h_\pi^1}{2\sqrt{2}f_\pi} (\vec{\tau}_1 \times \vec{\tau}_2)_z \frac{i\mathbf{k} \cdot (\boldsymbol{\sigma}_1 + \boldsymbol{\sigma}_2)}{\omega_k^2}, \quad (80)$$

$$\begin{aligned} V_{PVTC}^{(1)}(\text{CT}) = & \frac{1}{\Lambda_\chi^2 f_\pi} [C_1 i(\boldsymbol{\sigma}_1 \times \boldsymbol{\sigma}_2) \cdot \mathbf{k} + C_2 (\vec{\tau}_1 \cdot \vec{\tau}_2) i(\boldsymbol{\sigma}_1 \times \boldsymbol{\sigma}_2) \cdot \mathbf{k} \\ & + C_3 (\vec{\tau}_1 \times \vec{\tau}_2)_z i(\boldsymbol{\sigma}_1 + \boldsymbol{\sigma}_2) \cdot \mathbf{k} + C_4 (\tau_{1z} + \tau_{2z}) i(\boldsymbol{\sigma}_1 \times \boldsymbol{\sigma}_2) \cdot \mathbf{k} \\ & + C_5 \mathcal{I}_{ab} \tau_{1a} \tau_{2b} i(\boldsymbol{\sigma}_1 \times \boldsymbol{\sigma}_2) \cdot \mathbf{k}], \end{aligned} \quad (81)$$

$$\begin{aligned} V_{PVTC}^{(1)}(\text{TPE}) = & -\frac{g_A h_\pi^1}{2\sqrt{2}f_\pi} \frac{1}{\Lambda_\chi^2} (\vec{\tau}_1 \times \vec{\tau}_2)_z i\mathbf{k} \cdot (\boldsymbol{\sigma}_1 + \boldsymbol{\sigma}_2) L(k) \\ & -\frac{g_A^3 h_\pi^1}{2\sqrt{2}f_\pi} \frac{1}{\Lambda_\chi^2} \left[ 4(\tau_{1z} + \tau_{2z}) i\mathbf{k} \cdot (\boldsymbol{\sigma}_1 \times \boldsymbol{\sigma}_2) L(k) \right. \\ & \left. + (\vec{\tau}_1 \times \vec{\tau}_2)_z i\mathbf{k} \cdot (\boldsymbol{\sigma}_1 + \boldsymbol{\sigma}_2) (H(k) - 3L(k)) \right], \end{aligned} \quad (82)$$

$$\begin{aligned} V_{PVTC}^{(2)}(\text{TPE}) = & -\frac{c_4 h_\pi^1 g_A}{\sqrt{2}f_\pi} \frac{\pi}{\Lambda_\chi^2} i\mathbf{k} \cdot (\boldsymbol{\sigma}_1 \times \boldsymbol{\sigma}_2) (\tau_{1z} + \tau_{2z}) s^2 A(k) \\ & + \frac{g_A^2}{2f_\pi^2} \frac{\pi}{\Lambda_\chi^2} \left\{ \left[ \frac{3g_A h_V^0}{4} + \frac{g_A h_V^0}{2} \vec{\tau}_1 \cdot \vec{\tau}_2 + \left( \frac{g_A h_V^1}{4} - h_A^1 \right) (\tau_{1z} + \tau_{2z}) \right. \right. \\ & \left. \left. - \left( h_A^2 + \frac{g_A h_V^2}{3} \right) \mathcal{I}_{ab} \tau_{1b} \tau_{2b} \right] i\mathbf{k} \cdot (\boldsymbol{\sigma}_1 \times \boldsymbol{\sigma}_2) \right. \\ & \left. - \frac{g_A h_V^1}{2} (\vec{\tau}_1 \times \vec{\tau}_2)_z i\mathbf{k} \cdot (\boldsymbol{\sigma}_1 + \boldsymbol{\sigma}_2) \left( 1 - \frac{2m_\pi^2}{s^2} \right) \right\} s^2 A(k). \end{aligned} \quad (83)$$

The NLO term  $V_{PVTC}^{(1)}(\text{TPE})$  derives from the regularized parts of  $V_{PVTC}^{(1)}(e)$  and  $V_{PVTC}^{(1)}(f, g)$ , while the N<sup>2</sup>LO term  $V_{PVTC}^{(2)}(\text{TPE})$  from  $V_{PVTC}^{(1)}(j)$ ,  $V_{PVTC}^{(1)}(k)$ , and  $V_{PVTC}^{(1)}(l)$ . Let us note that we have in total 11 LECs that must be determined from the experimental data: one in the LO term, five in the subleading order and five at N<sup>2</sup>LO. This potential is the same as the one derived using the MUT in Ref. [173].

Finally, the potential to be used in calculation of PVTC observables has to be regularized for large values of  $\mathbf{p}, \mathbf{p}'$ . The frequently used procedure is to multiply by a cutoff function containing a parameter  $\Lambda_C$

$$V_{PVTC}(\mathbf{p}, \mathbf{p}') \rightarrow f_{\Lambda_C}(\mathbf{p}, \mathbf{p}') V_{PVTC}(\mathbf{p}, \mathbf{p}'). \quad (84)$$

Usual choices for  $f_{\Lambda_C}$  are [74]

$$f_{\Lambda_C}(\mathbf{p}, \mathbf{p}') = \exp \left[ -\left( \frac{p}{\Lambda_C} \right)^n - \left( \frac{p'}{\Lambda_C} \right)^n \right], \quad (85)$$

where usually  $n = 6$ , adopted for example in Ref. [173], or

$$f_{\Lambda_C}(\mathbf{p}, \mathbf{p}') = \exp \left[ -\left( \frac{|\mathbf{p} - \mathbf{p}'|}{\Lambda_C} \right)^4 \right], \quad (86)$$

adopted in Ref. [42]. The value of the cutoff  $\Lambda_C$  is chosen to be around 400–600 MeV, and consistent with the analogous parameter used to regularize the PCTC potential.

The currently most accurate and precise PCTC NN potentials of Ref. [19] employ the local momentum-space regularization approach for pion-exchange contributions as described in section 3.4.1 in combination with a nonlocal Gaussian regulator given in Eq. (85) with  $n = 2$  and  $\Lambda_C = \Lambda$  for contact interactions ( $\Lambda$  is the cutoff used in the local regulator in Eqs. (77), (78)). The superior performance of the momentum-space regulator in Eq. (78) as compared with both the spectral-function regularization and a local multiplicative regularization as defined in Eq. (86) manifests itself in exponentially small distortions at large distances as visualized in Fig. 5 of [19].

Last but not least, we emphasize that using *different* regulators when calculating loop integrals in the nuclear potentials/currents and solving the Schrödinger equation to compute observables is generally incorrect. This issue becomes relevant at the chiral order, at which one encounters the first loop contributions to the 3N potentials and to the NN exchange current operators (i.e. at order  $Q^4$  or N<sup>3</sup>LO in the PCTC sector) [180, 181], which is beyond the accuracy of the calculations described in this review article. For more details and a discussion of a possible solution to this problem see Ref. [182].

### 3.4.3 Relevant PCTC and PVTC electromagnetic currents

Electromagnetic currents can be calculated in the  $\chi$ EFT expansion. For our purposes we require currents for the longitudinal asymmetry in radiative neutron capture on a proton target at thermal energies. As we deal with a real outgoing photon, the LO PCTC current is induced by the nucleon magnetic moment. At NLO there are contributions from the convection currents and one-pion-exchange currents proportional to  $g_A^2$ . At NLO the relevant currents become

$$\begin{aligned} \mathbf{J}_{PCTC} = & \sum_{j=1}^A \frac{e}{4M} \left\{ -[(1 + \kappa_0) + (1 + \kappa_1)\tau_{jz}] i(\boldsymbol{\sigma}_j \times \mathbf{q}) + (1 + \tau_{jz})(\mathbf{p}_j + \mathbf{p}'_j) \right\} \delta_{\mathbf{p}_j - \mathbf{p}'_j, \mathbf{q}} \\ & + \frac{eg_A^2}{4f_\pi^2} \sum_{j < k}^A i(\vec{\tau}_j \times \vec{\tau}_k)_z \left\{ 2\mathbf{k} \frac{\boldsymbol{\sigma}_j \cdot (\mathbf{k} + \mathbf{q}/2)}{(\mathbf{k} + \mathbf{q}/2)^2 + m_\pi^2} \frac{\boldsymbol{\sigma}_k \cdot (\mathbf{k} - \mathbf{q}/2)}{(\mathbf{k} - \mathbf{q}/2)^2 + m_\pi^2} \right. \\ & \left. - \boldsymbol{\sigma}_j \frac{\boldsymbol{\sigma}_k \cdot (\mathbf{k} - \mathbf{q}/2)}{(\mathbf{k} - \mathbf{q}/2)^2 + m_\pi^2} - \boldsymbol{\sigma}_k \frac{\boldsymbol{\sigma}_j \cdot (\mathbf{k} + \mathbf{q}/2)}{(\mathbf{k} + \mathbf{q}/2)^2 + m_\pi^2} \right\}, \end{aligned} \quad (87)$$

where  $\kappa_0 = -0.12$  and  $\mu_v = 3.71$  are the isoscalar and isovector anomalous nucleon magnetic moments.  $\mathbf{p}_j$  and  $\mathbf{p}'_j$  denote the incoming and outgoing momenta of nucleon  $j$  interacting with a photon of outgoing momentum  $\mathbf{q}$ . The intermediate pions carry momenta  $\mathbf{k} + \mathbf{q}/2 = \mathbf{p}_j - \mathbf{p}'_j$  or  $\mathbf{k} - \mathbf{q}/2 = \mathbf{p}'_k - \mathbf{p}_k$ . Ref. [173] used these currents in combination with N<sup>3</sup>LO  $\chi$ EFT potentials from Ref. [17] to calculate the total  $np \rightarrow d\gamma$  capture cross section. Using just the LO currents gives a cross section of  $305 \pm 4$  mb, which grows to  $319 \pm 5$  at NLO. The remaining 4% discrepancy to the experimental cross section  $334.2 \pm 0.5$ , indicates that N<sup>2</sup>LO currents should probably be included.

A consistent calculation of PVTC observables as the photon asymmetry in the  $\vec{n}p \rightarrow d\gamma$  radiative capture also requires the inclusion of PVTC currents. There is no one-body current in this case, as the anapole moment vanishes for on-shell photons [183]. As such, the leading PVTC currents arises from

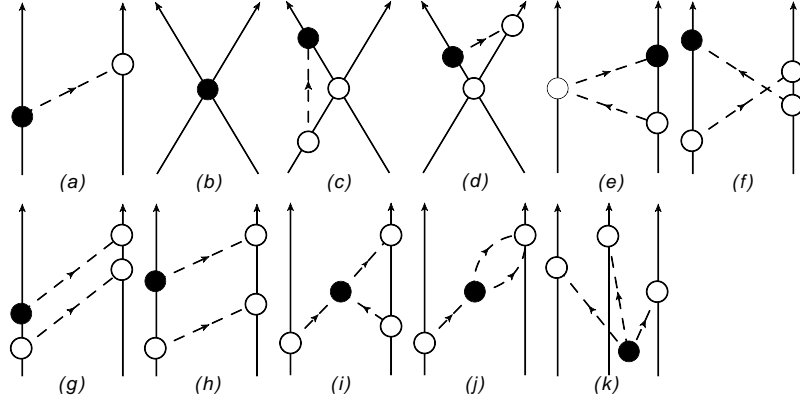


**Figure 4.** Time-ordered diagrams contributing to the PVTV potential (only a single time ordering is shown). Nucleons and pions are denoted by solid and dashed lines, respectively. The open (solid) circle represents a PCTC (PVTV) vertex.

one-pion-exchange currents

$$\begin{aligned}
 \mathbf{J}_{PVTC} = & \frac{eg_A h_\pi^1}{2\sqrt{2}f_\pi} \sum_{j < k}^A (\vec{\tau}_j \cdot \vec{\tau}_k - \tau_{jz} \tau_{kz}) \left\{ 2\mathbf{k} \frac{\boldsymbol{\sigma}_j \cdot (\mathbf{k} + \mathbf{q}/2) + \boldsymbol{\sigma}_k \cdot (\mathbf{k} - \mathbf{q}/2)}{[(\mathbf{k} + \mathbf{q}/2)^2 + m_\pi^2][(\mathbf{k} - \mathbf{q}/2)^2 + m_\pi^2]} \right. \\
 & \left. - \frac{\boldsymbol{\sigma}_j}{(\mathbf{k} - \mathbf{q}/2)^2 + m_\pi^2} - \frac{\boldsymbol{\sigma}_k}{(\mathbf{k} + \mathbf{q}/2)^2 + m_\pi^2} \right\}, \quad (88)
 \end{aligned}$$

where we stress the dependence on the PVTC pion-nucleon LEC  $h_\pi^1$ . Higher-order PVTC currents have not been developed.

### 3.5 The PVTV potential up to order $Q$

In this section, we discuss the derivation of the PVTV NN and 3N potentials at N<sup>2</sup>LO. The final expressions are given in terms of a sum of diagrams, which can be obtained either using the MUT [166, 184, 4], standard dimensional regularization [72] or the TOPT method [75]. In the following, we briefly report the derivation of the PVTV potential in the framework of TOPT approach.

The TOPT diagrams that give contribution to the NN PVTV potential up to N<sup>2</sup>LO (order  $Q^1$ ) are shown in Fig. 4. We do not consider diagrams which give contributions only to the renormalization of the LECs. In this section we write the final expression of the NN PVTV potential  $V_{PVTV}$  by having already taken into account the singular parts coming from loops. Note that for the PVTV potential the LO term is of order  $Q^{-1}$  as for the PVTC case. However, now there will be terms of order  $Q^0$ , which will be denoted as NLO terms, etc. We have

$$\begin{aligned}
 V_{PVTV}(\mathbf{p}, \mathbf{p}') = & V_{PVTV}^{(-1)}(\text{OPE}) + V_{PVTV}^{(1)}(\text{CT}) + V_{PVTV}^{(1)}(\text{TPE}) \\
 & + V_{PVTV}^{(0)}(3\pi) + V_{PVTV}^{(1)}(3\pi), \quad (89)
 \end{aligned}$$

namely coming from OPE diagrams at LO, TPE at N<sup>2</sup>LO, three-pion vertices ( $3\pi$ ) at NLO and at N<sup>2</sup>LO, and contact contributions (CT). From now on we define  $\bar{g}_0^* = \bar{g}_0 + \bar{g}_2/3$ . In this case, we report here the final form of the potential, namely, the LECs appearing in the expressions below are the physical



ones, having reabsorbed the various infinities generated by loops and diagrams like those shown in panels (1)–(3) of Fig.2.

- *One pion exchange diagram.* The OPE term, depicted in diagram (a) of Fig. 4, gives a contribution at LO, namely of order  $Q^{-1}$ , coming from the NR expansion of the vertices

$$V_{PVTV}^{(-1)}(\text{OPE}) = \frac{g_A \bar{g}_0^*}{2f_\pi} (\vec{\tau}_1 \cdot \vec{\tau}_2) \frac{i\mathbf{k} \cdot (\boldsymbol{\sigma}_1 - \boldsymbol{\sigma}_2)}{\omega_k^2} + \frac{g_A \bar{g}_2}{6f_\pi} (3\tau_{1z}\tau_{2z} - \vec{\tau}_1 \cdot \vec{\tau}_2) \frac{i\mathbf{k} \cdot (\boldsymbol{\sigma}_1 - \boldsymbol{\sigma}_2)}{\omega_k^2} \\ + \frac{g_A \bar{g}_1}{4f_\pi} \left[ (\tau_{1z} + \tau_{2z}) \frac{i\mathbf{k} \cdot (\boldsymbol{\sigma}_1 - \boldsymbol{\sigma}_2)}{\omega_k^2} + (\tau_{1z} - \tau_{2z}) \frac{i\mathbf{k} \cdot (\boldsymbol{\sigma}_1 + \boldsymbol{\sigma}_2)}{\omega_k^2} \right], \quad (90)$$

where there are an isoscalar, an isovector and an isotensor components. Contributions coming from the  $1/M$  expansion are considered to be suppressed at least by four orders with respect to  $V_{PVTV}^{(-1)}(\text{OPE})$ .

- *Contact term diagrams.* The potential  $V_{PVTV}^{(1)}(\text{CT})$ , derived from the NN contact diagrams (b) of Fig. 4, reads

$$V_{PVTV}^{(1)}(\text{CT}) = \frac{1}{\Lambda_\chi^2 f_\pi} \left\{ \bar{C}_1 i\mathbf{k} \cdot (\boldsymbol{\sigma}_1 - \boldsymbol{\sigma}_2) + \bar{C}_2 i\mathbf{k} \cdot (\boldsymbol{\sigma}_1 - \boldsymbol{\sigma}_2) \vec{\tau}_1 \cdot \vec{\tau}_2 \right. \\ + \frac{\bar{C}_3}{2} \left[ i\mathbf{k} \cdot (\boldsymbol{\sigma}_1 - \boldsymbol{\sigma}_2) (\tau_{1z} + \tau_{2z}) + i\mathbf{k} \cdot (\boldsymbol{\sigma}_1 + \boldsymbol{\sigma}_2) (\tau_{1z} - \tau_{2z}) \right] \\ + \frac{\bar{C}_4}{2} \left[ i\mathbf{k} \cdot (\boldsymbol{\sigma}_1 - \boldsymbol{\sigma}_2) (\tau_{1z} + \tau_{2z}) - i\mathbf{k} \cdot (\boldsymbol{\sigma}_1 + \boldsymbol{\sigma}_2) (\tau_{1z} - \tau_{2z}) \right] \\ \left. + \bar{C}_5 i\mathbf{k} \cdot (\boldsymbol{\sigma}_1 - \boldsymbol{\sigma}_2) (3\tau_{1z}\tau_{2z} - \vec{\tau}_1 \cdot \vec{\tau}_2) \right\}. \quad (91)$$

Notice that the above LECs  $\bar{C}_1$ ,  $\bar{C}_2$ ,  $\bar{C}_3$ ,  $\bar{C}_4$  and  $\bar{C}_5$  have been redefined to absorb various singular terms coming from the TPE and  $3\pi$  diagrams. It is possible to write ten operators which can enter  $V_{PVTV}^{(1)}(\text{CT})$  at order  $Q$  but only five of them are independent as discussed in Chapter 4. In this work we have chosen to write the operators in terms of  $\mathbf{k}$ , so that the  $r$ -space version of  $V_{PVTV}^{(1)}(\text{CT})$  will assume a simple local form with no gradients.

- *Contact terms with an OPE.* Diagrams like (c) and (d) of Fig. 4 vanish directly due to the integration over the loop momentum.
- *Two pions exchange diagrams.* The TPE term comes from the not singular contributions of panels (e)–(h) of Fig. 4. This term has no isovector component, as shown for the first time in [73]. It reads

$$V_{PVTV}^{(1)}(\text{TPE}) = \frac{g_A \bar{g}_0^*}{f_\pi \Lambda_\chi^2} \vec{\tau}_1 \cdot \vec{\tau}_2 i\mathbf{k} \cdot (\boldsymbol{\sigma}_1 - \boldsymbol{\sigma}_2) L(k) + \frac{g_A^3 \bar{g}_0^*}{f_\pi \Lambda_\chi^2} \vec{\tau}_1 \cdot \vec{\tau}_2 i\mathbf{k} \cdot (\boldsymbol{\sigma}_1 - \boldsymbol{\sigma}_2) (H(k) - 3L(k)) \\ - \frac{g_A \bar{g}_2}{3f_\pi \Lambda_\chi^2} (3\tau_{1z}\tau_{2z} - \vec{\tau}_1 \cdot \vec{\tau}_2) i\mathbf{k} \cdot (\boldsymbol{\sigma}_1 - \boldsymbol{\sigma}_2) L(k) \\ - \frac{g_A^3 \bar{g}_2}{3f_\pi \Lambda_\chi^2} (3\tau_{1z}\tau_{2z} - \vec{\tau}_1 \cdot \vec{\tau}_2) i\mathbf{k} \cdot (\boldsymbol{\sigma}_1 - \boldsymbol{\sigma}_2) (H(k) - 3L(k)), \quad (92)$$

where the loop functions  $L(k)$  and  $H(k)$  are defined in Eq. (68).

- *Diagrams with three pion vertices* The  $3\pi$ -exchange term gives a NLO contribution through the diagram (i) of Fig. 4,

$$V_{PVTV}^{(0)}(3\pi) = -\frac{5g_A^3 \bar{\Delta} M}{4f_\pi \Lambda_\chi^2} \pi \left[ (\tau_{1z} + \tau_{2z}) \frac{i\mathbf{k} \cdot (\boldsymbol{\sigma}_1 - \boldsymbol{\sigma}_2)}{\omega_k^2} + (\tau_{1z} - \tau_{2z}) \frac{i\mathbf{k} \cdot (\boldsymbol{\sigma}_1 + \boldsymbol{\sigma}_2)}{\omega_k^2} \right] \times \left( \left(1 - \frac{2m_\pi^2}{s^2}\right) s^2 A(k) + m_\pi \right), \quad (93)$$

where  $A(k)$  is given in Eq. (74). Additional contributions coming from diagram (i) deriving from the  $1/M$  expansion of the energy denominators and vertex functions are here neglected since we count them as  $N^3\text{LO}$ .

The diagram in panel (j) of Fig. 4 contributes to  $V_{PVTV}^{(3\pi)}$  at  $N^2\text{LO}$ ,

$$\begin{aligned} V_{PVTV}^{(1)}(3\pi) = & \frac{5g_A \bar{\Delta} M c_1}{2f_\pi \Lambda_\chi^2} \left[ (\tau_{1z} + \tau_{2z}) i\mathbf{k} \cdot (\boldsymbol{\sigma}_1 - \boldsymbol{\sigma}_2) \right. \\ & \left. + (\tau_{1z} - \tau_{2z}) i\mathbf{k} \cdot (\boldsymbol{\sigma}_1 + \boldsymbol{\sigma}_2) \right] 4 \frac{m_\pi^2}{\omega_k^2} L(k) \\ & - \frac{5g_A \bar{\Delta} M c_2}{6f_\pi \Lambda_\chi^2} \left[ (\tau_{1z} + \tau_{2z}) i\mathbf{k} \cdot (\boldsymbol{\sigma}_1 - \boldsymbol{\sigma}_2) \right. \\ & \left. + (\tau_{1z} - \tau_{2z}) i\mathbf{k} \cdot (\boldsymbol{\sigma}_1 + \boldsymbol{\sigma}_2) \right] \left( 2L(k) + 6 \frac{m_\pi^2}{\omega_k^2} L(k) \right) \\ & - \frac{5g_A \bar{\Delta} M c_3}{4f_\pi \Lambda_\chi^2} \left[ (\tau_{1z} + \tau_{2z}) i\mathbf{k} \cdot (\boldsymbol{\sigma}_1 - \boldsymbol{\sigma}_2) \right. \\ & \left. + (\tau_{1z} - \tau_{2z}) i\mathbf{k} \cdot (\boldsymbol{\sigma}_1 + \boldsymbol{\sigma}_2) \right] \left( 3L(k) + 5 \frac{m_\pi^2}{\omega_k^2} L(k) \right). \end{aligned} \quad (94)$$

Note in Eq. (94) the presence of the  $c_1$ ,  $c_2$  and  $c_3$  LECs, which belong to the PCTC Lagrangian given in Eq. (13). In Eqs. (93) and (94),  $\bar{\Delta}$  is a renormalized LEC.

The  $3\pi$  PVTV vertex gives rise to a three body interaction through the diagram (k) in Fig. 4. The lowest contribution appears at NLO while at  $N^2\text{LO}$  the various time orderings cancel out [75]. The final expression for the NLO of the  $3N$  PVTV potential is,

$$\begin{aligned} V_{PVTV}^{(0)}(3N) = & \frac{\bar{\Delta} g_A^3 M}{4f_\pi^3} (\vec{\tau}_1 \cdot \vec{\tau}_2 \tau_{3z} + \vec{\tau}_1 \cdot \vec{\tau}_3 \tau_{2z} + \vec{\tau}_2 \cdot \vec{\tau}_3 \tau_{1z}) \\ & \times \frac{(i\mathbf{k}_1 \cdot \boldsymbol{\sigma}_1) (i\mathbf{k}_2 \cdot \boldsymbol{\sigma}_2) (i\mathbf{k}_3 \cdot \boldsymbol{\sigma}_3)}{\omega_{k_1}^2 \omega_{k_2}^2 \omega_{k_3}^2}, \end{aligned} \quad (95)$$

where  $\mathbf{k}_i = \mathbf{p}'_i - \mathbf{p}$ . This expression is in agreement with that reported in Ref. [68, 69].

### 3.5.1 The PVTV current

The PVTV current up to now has been considered coming from the LO one-body contribution

$$\mathbf{J}_{PVTV} = - \sum_{j=1}^A \left[ d_p \frac{1 + \tau_{jz}}{2} + d_n \frac{1 - \tau_{jz}}{2} \right] i(\boldsymbol{\sigma}_j \cdot \mathbf{q}), \quad (96)$$

where  $d_p$  ( $d_n$ ) is the proton (neutron) EDM. In the nuclear physics applications, it is customary to consider  $d_p$  and  $d_n$  as unknown parameters, although they in principle can be estimated in terms of the LECs entering the  $\chi$ EFT, as we have seen in Sect. 3.2.2. The complete derivation of PVTV two-body currents has not been completed. Partial results have been given in Refs. [143, 73].

## 4 PVTC AND PVTV POTENTIALS IN PIONLESS EFT

In this section, we specifically focus on the contact few-nucleon interactions which enter the potentials in both chiral and pionless EFT formulations. We also discuss the expected hierarchy of the corresponding LECs as suggested by the large- $N_c$  analysis.

### 4.1 Effective Lagrangians

At distances much larger than the range of the interactions mediated by pions, the latter degrees of freedom can be integrated out of the effective theory, and the relevant effective Lagrangian can be written in terms of nucleon fields only, that interact through contact vertices.

At leading order these vertices involve one spatial derivative of fields, responsible for parity violation. Time derivatives can be eliminated by recursively using the equations of motion order by order in the low-energy expansion. This reflects our freedom in choosing the nucleon interpolating field, and amounts to a definite choice of the off-shell behavior of amplitudes. The theory can be formulated in terms of non-relativistic nucleon fields represented by two-component Pauli spinors  $N_r(x)$ . The relativistic  $1/M$  corrections, which can in principle be worked out (see e.g. [185]) will be of no interest here. Relativistic covariance requires that the interactions depend on the relative momenta only (momentum-dependent ‘‘drift’’ corrections, which vanish in the center-of-mass frame of two nucleon systems, are part of the above mentioned relativistic corrections). Thus, gradients of nucleon fields in two-nucleon contact operators may only enter in the combinations

$$\nabla(N_r^\dagger O_1 N_r) N_r^\dagger O_2 N_r, \quad [(N_r^\dagger i \overleftrightarrow{\nabla} O_1 N_r) N_r^\dagger O_2 N_r - N_r^\dagger O_1 N_r (N_r^\dagger i \overleftrightarrow{\nabla} O_2 N_r)], \quad (97)$$

where  $(ai \overleftrightarrow{\nabla} b) \equiv a(i \nabla b) - (i \nabla a)b$  and the factor  $i$ , meant to ensure the hermiticity, makes it odd under time-reversal.

Since the underlying mechanism of parity violation in the SM may induce  $\Delta I = 0, 1, 2$  transitions (at least to order  $G_F^2$ ), the effective Lagrangian will contain contact operators which transform as isoscalars or the neutral components of isovector and isotensors. In the two-nucleon case all these flavor structures are real, and therefore unaffected by the time-reversal operation, except for  $(\vec{\tau}_1 \times \vec{\tau}_2)_z$ , which changes sign.

## 4.2 PVTC Lagrangian

Following the general considerations outlined above, there are ten possible structures entering the two-nucleon contact Lagrangian in the PVTC case,

$$\Delta I = 0 \quad \left\{ \begin{array}{l} O_1^{PVTC} = \nabla \times (N_r^\dagger \boldsymbol{\sigma} N_r) \cdot N_r^\dagger \boldsymbol{\sigma} N_r, \\ O_2^{PVTC} = \nabla \times (N_r^\dagger \boldsymbol{\sigma} \tau^a N_r) \cdot N_r^\dagger \boldsymbol{\sigma} \tau^a N_r, \\ O_{1'}^{PVTC} = (N_r^\dagger i \overleftrightarrow{\nabla} \cdot \boldsymbol{\sigma} N_r) N_r^\dagger N_r - N_r^\dagger \boldsymbol{\sigma} N_r \cdot (N_r^\dagger i \overleftrightarrow{\nabla} N_r), \\ O_{2'}^{PVTC} = (N_r^\dagger i \overleftrightarrow{\nabla} \cdot \boldsymbol{\sigma} \tau^a N_r) N_r^\dagger \tau^a N_r - N_r^\dagger \boldsymbol{\sigma} \tau^a N_r \cdot (N_r^\dagger i \overleftrightarrow{\nabla} \tau^a N_r), \end{array} \right. \quad (98)$$

$$\Delta I = 1 \quad \left\{ \begin{array}{l} O_3^{PVTC} = \epsilon^{ab3} \nabla \cdot (N_r^\dagger \boldsymbol{\sigma} \tau^a N_r) N_r^\dagger \tau^b N_r, \\ O_4^{PVTC} = \nabla \times (N_r^\dagger \boldsymbol{\sigma} \tau^3 N_r) \cdot N_r^\dagger \boldsymbol{\sigma} N_r, \\ O_{3'}^{PVTC} = (N_r^\dagger i \overleftrightarrow{\nabla} \cdot \boldsymbol{\sigma} \tau^3 N_r) N_r^\dagger N_r - N_r^\dagger \boldsymbol{\sigma} \tau^3 N_r \cdot (N_r^\dagger i \overleftrightarrow{\nabla} N_r), \\ O_{4'}^{PVTC} = (N_r^\dagger i \overleftrightarrow{\nabla} \cdot \boldsymbol{\sigma} N_r) N_r^\dagger \tau^3 N_r - N_r^\dagger \boldsymbol{\sigma} N_r \cdot (N_r^\dagger i \overleftrightarrow{\nabla} \tau^3 N_r), \end{array} \right.$$

$$\Delta I = 2 \quad \left\{ \begin{array}{l} O_5^{PVTC} = \mathcal{I}_{ab} \nabla \times (N_r^\dagger \boldsymbol{\sigma} \tau^a N_r) \cdot N_r^\dagger \boldsymbol{\sigma} \tau^b N_r, \\ O_{5'}^{PVTC} = \mathcal{I}_{ab} \left[ (N_r^\dagger i \overleftrightarrow{\nabla} \cdot \boldsymbol{\sigma} \tau^a N_r) N_r^\dagger \tau^b N_r - N_r^\dagger \boldsymbol{\sigma} \tau^a N_r \cdot (N_r^\dagger i \overleftrightarrow{\nabla} \tau^b N_r) \right]. \end{array} \right.$$

The Fermi statistics of nucleon fields, together with Fierz's reshuffling of spin-isospin indices allow to establish linear relations between primed and unprimed operators,

$$\begin{aligned} O_{1'}^{PVTC} &= \frac{1}{2} (O_1^{PVTC} + O_2^{PVTC}), \\ O_{2'}^{PVTC} &= \frac{1}{2} (3O_1^{PVTC} - O_2^{PVTC}), \\ O_{3'}^{PVTC} &= O_3^{PVTC} + O_4^{PVTC}, \\ O_{4'}^{PVTC} &= -O_3^{PVTC} + O_4^{PVTC}, \\ O_{5'}^{PVTC} &= O_5^{PVTC}, \end{aligned} \quad (99)$$

thus reducing the number of independent operators to five, so that the effective Lagrangian can be written as

$$\mathcal{L}_{PVTC,NN}^{(1)} = \frac{1}{\Lambda_\chi^2 f_\pi} \left[ \frac{1}{2} C_1 O_1^{PVTC} + \frac{1}{2} C_2 O_2^{PVTC} + C_3 O_3^{PVTC} + C_4 O_4^{PVTC} + \frac{1}{2} C_5 O_5^{PVTC} \right], \quad (100)$$

where  $C_i$  are LECs. This Lagrangian is identical to that reported in Eq. (23). From this Lagrangian, one can derive the potential given in Eq. (60).

The five LECs are in a one-to-one correspondence with the possible S-P transitions in two-nucleon systems [45], namely  $^1S_0$ - $^3P_0$  ( $\Delta I = 0, 1, 2$ ),  $^3S_1$ - $^1P_1$  ( $\Delta I = 0$ ) and  $^3S_1$ - $^3P_1$  ( $\Delta I = 1$ ). This may be shown explicitly by using the spin-isospin projection operators [45, 186, 187, 188]

$$P_{0,0} = \frac{1}{\sqrt{8}} \sigma_2 \tau_2, \quad P_{0,a} = \frac{1}{\sqrt{8}} \sigma_2 \tau_2 \tau_a, \quad P_{i,0} = \frac{1}{\sqrt{8}} \sigma_2 \sigma_i \tau_2, \quad P_{i,a} = \frac{1}{\sqrt{8}} \sigma_2 \sigma_i \tau_2 \tau_a, \quad (101)$$

normalized according to

$$\text{Tr} P_{\mu,\alpha} P_{\nu,\beta}^\dagger = \frac{1}{2} \delta_{\mu\nu} \delta_{\alpha\beta}, \quad \mu(\nu) = 0, i(j), \quad \alpha(\beta) = 0, a(b), \quad (102)$$

such that the operator  $(N_r^T P_{\mu,\alpha} N_r)^\dagger$  creates a correctly normalized two-nucleon state with the appropriate spin-isospin quantum numbers. The relevant operators [188]

$$\begin{aligned}
 O_{\Delta I=0}^{(1S_0-3P_0)} &= (N_r^T \sigma^2 \tau^2 \tau^a N_r)^\dagger (N_r^T i \overleftrightarrow{\nabla} \cdot \sigma^2 \sigma \tau^2 \tau^a N_r) + \text{h.c.}, \\
 O_{\Delta I=1}^{(1S_0-3P_0)} &= -ie^{ab3} (N_r^T \sigma^2 \tau^2 \tau^a N_r)^\dagger (N_r^T i \overleftrightarrow{\nabla} \cdot \sigma^2 \sigma \tau^2 \tau^b N_r) + \text{h.c.}, \\
 O_{\Delta I=2}^{(1S_0-3P_0)} &= \mathcal{I}_{ab} (N_r^T \sigma^2 \tau^2 \tau^a N_r)^\dagger (N_r^T i \overleftrightarrow{\nabla} \cdot \sigma^2 \sigma \tau^2 \tau^b N_r) + \text{h.c.}, \\
 O_{\Delta I=0}^{(3S_1-1P_1)} &= (N_r^T \sigma^2 \sigma \tau^2 N_r)^\dagger \cdot (N_r^T i \overleftrightarrow{\nabla} \sigma^2 \tau^2 N_r) + \text{h.c.}, \\
 O_{\Delta I=1}^{(3S_1-3P_1)} &= (N_r^T \sigma^2 \sigma \tau^2 N_r)^\dagger \cdot (N_r^T \overleftrightarrow{\nabla} \times \sigma^2 \sigma \tau^2 \tau^3 N_r) + \text{h.c.},
 \end{aligned} \tag{103}$$

are related to the original basis via Fierz's transformations as follows,

$$\begin{aligned}
 O_{\Delta I=0}^{(1S_0-3P_0)} &= 3O_1^{PVTC} + O_2^{PVTC}, \\
 O_{\Delta I=1}^{(1S_0-3P_0)} &= 4O_4^{PVTC}, \\
 O_{\Delta I=2}^{(1S_0-3P_0)} &= -2O_5^{PVTC}, \\
 O_{\Delta I=0}^{(3S_1-1P_1)} &= -O_1^{PVTC} + O_2^{PVTC}, \\
 O_{\Delta I=1}^{(3S_1-3P_1)} &= -4O_3^{PVTC},
 \end{aligned} \tag{104}$$

whence one can read the relation between the partial-waves projected LECs and the  $C_i$ . The potential derived from the operators given in Eq. (103) has been often used in studies of PVTC observables. It is given explicitly as [37, 39]

$$\begin{aligned}
 V_{PVTC}^{(1)}(GHH) &= \frac{1}{2Mm_\rho^2} \left\{ \Lambda_{\Delta I=0}^{(1S_0-3P_0)} \left[ 2(\boldsymbol{\sigma}_1 - \boldsymbol{\sigma}_2) \cdot \mathbf{K} + i(\boldsymbol{\sigma}_1 \times \boldsymbol{\sigma}_2) \cdot \mathbf{k} \right] \right. \\
 &+ \Lambda_{\Delta I=0}^{(3S_1-1P_1)} \left[ 2(\boldsymbol{\sigma}_1 - \boldsymbol{\sigma}_2) \cdot \mathbf{K} - i(\boldsymbol{\sigma}_1 \times \boldsymbol{\sigma}_2) \cdot \mathbf{k} \right] \\
 &+ \Lambda_{\Delta I=1}^{(1S_0-3P_0)} (\tau_{1z} + \tau_{2z}) 2(\boldsymbol{\sigma}_1 - \boldsymbol{\sigma}_2) \cdot \mathbf{K} \\
 &+ \Lambda_{\Delta I=1}^{(3S_1-3P_1)} (\tau_{1z} - \tau_{2z}) 2(\boldsymbol{\sigma}_1 + \boldsymbol{\sigma}_2) \cdot \mathbf{K} \\
 &\left. + \Lambda_{\Delta I=2}^{(1S_0-3P_0)} I^{ab} \tau_{1a} \tau_{2b} \frac{2}{\sqrt{6}} (\boldsymbol{\sigma}_1 - \boldsymbol{\sigma}_2) \cdot \mathbf{K} \right\},
 \end{aligned} \tag{105}$$

where the five LECs  $\Lambda_{\Delta T}^{(\dots)}$  are in one-to-one correspondence with  $C_{1-5}$ . Explicitly

$$\begin{aligned}
 \Lambda_{\Delta I=0}^{(1S_0-3P_0)} &= \frac{\kappa}{2} (C_1 + C_2), \\
 \Lambda_{\Delta I=0}^{(3S_1-1P_1)} &= \frac{\kappa}{2} (3C_2 - C_1), \\
 \Lambda_{\Delta I=1}^{(1S_0-3P_0)} &= \kappa C_4, \\
 \Lambda_{\Delta I=1}^{(3S_1-3P_1)} &= \kappa C_3, \\
 \Lambda_{\Delta I=2}^{(1S_0-3P_0)} &= \sqrt{6} \kappa C_5,
 \end{aligned} \tag{106}$$

where  $\kappa = 2Mm_\rho^2/f_\pi \Lambda_\chi^2$ .

### 4.3 PVTV Lagrangian

The  $T$ -odd sector is very similar (see also Ref. [189]): one starts with a list of ten redundant operators,

$$\Delta I = 0 \quad \left\{ \begin{array}{l} O_1^{PVTV} = \nabla \cdot (N_r^\dagger \boldsymbol{\sigma} N_r) N_r^\dagger N_r, \\ O_2^{PVTV} = \nabla \cdot (N_r^\dagger \boldsymbol{\sigma} \tau^a N_r) N_r^\dagger \tau^a N_r, \\ O_{1'}^{PVTV} = (N_r^\dagger i \overleftrightarrow{\nabla} \times \boldsymbol{\sigma} N_r) \cdot N_r^\dagger \boldsymbol{\sigma} N_r, \\ O_{2'}^{PVTV} = (N_r^\dagger i \overleftrightarrow{\nabla} \times \boldsymbol{\sigma} \tau^a N_r) \cdot N_r^\dagger \boldsymbol{\sigma} \tau^a N_r, \end{array} \right.$$

$$\Delta I = 1 \quad \left\{ \begin{array}{l} O_3^{PVTV} = \nabla \cdot (N_r^\dagger \boldsymbol{\sigma} \tau^3 N_r) N_r^\dagger N_r, \\ O_4^{PVTV} = \nabla \cdot (N_r^\dagger \boldsymbol{\sigma} N_r) N_r^\dagger \tau^3 N_r, \\ O_{3'}^{PVTV} = (N_r^\dagger i \overleftrightarrow{\nabla} \times \boldsymbol{\sigma} \tau^3 N_r) \cdot N_r^\dagger \boldsymbol{\sigma} N_r + (N_r^\dagger i \overleftrightarrow{\nabla} \times \boldsymbol{\sigma} N_r) \cdot N_r^\dagger \boldsymbol{\sigma} \tau^3 N_r, \\ O_{4'}^{PVTV} = \epsilon^{ab3} \left[ (N_r^\dagger i \overleftrightarrow{\nabla} \cdot \boldsymbol{\sigma} \tau^a N_r) N_r^\dagger \tau^b N_r + (N_r^\dagger i \overleftrightarrow{\nabla} \tau^a N_r) \cdot N_r^\dagger \boldsymbol{\sigma} \tau^b N_r \right], \end{array} \right. \quad (107)$$

$$\Delta I = 2 \quad \left\{ \begin{array}{l} O_5^{PVTV} = \mathcal{I}_{ab} \nabla \cdot (N_r^\dagger \boldsymbol{\sigma} \tau^a N_r) N_r^\dagger \tau^b N_r, \\ O_{5'}^{PVTV} = \mathcal{I}_{ab} (N_r^\dagger i \overleftrightarrow{\nabla} \times \boldsymbol{\sigma} \tau^a N_r) \cdot N_r^\dagger \boldsymbol{\sigma} \tau^b N_r, \end{array} \right.$$

and uses Fierz's identities to establish the linear relations,

$$\begin{aligned} O_{1'}^{PVTV} &= -O_1^{PVTV} - O_2^{PVTV}, \\ O_{2'}^{PVTV} &= -3O_1^{PVTV} + O_2^{PVTV}, \\ O_{3'}^{PVTV} &= -2O_3^{PVTV} - 2O_4^{PVTV}, \\ O_{4'}^{PVTV} &= -2O_3^{PVTV} + 2O_4^{PVTV}, \\ O_{5'}^{PVTV} &= -2O_5^{PVTV}, \end{aligned} \quad (108)$$

so that the Lagrangian only depends on five LECs,

$$\mathcal{L}_{PVTV,NN}^{(1)} = \frac{1}{\Lambda_\chi^2 f_\pi} \sum_{i=1}^5 \bar{C}_i O_i^{PVTV}, \quad (109)$$

from which one can derive the potential given in Eq. (91).

The five S-P transition operators only differ from the  $T$ -even case by a factor of  $i$ ,

$$\begin{aligned} \bar{O}_{\Delta I=0}^{(1S_0^{-3}P_0)} &= (N_r^T \sigma^2 \tau^2 \tau^a N_r)^\dagger (N_r^T \overleftrightarrow{\nabla} \cdot \sigma^2 \boldsymbol{\sigma} \tau^2 \tau^a N_r) + \text{h.c.}, \\ \bar{O}_{\Delta I=1}^{(1S_0^{-3}P_0)} &= \epsilon^{ab3} (N_r^T \sigma^2 \tau^2 \tau^a N_r)^\dagger (N_r^T i \overleftrightarrow{\nabla} \cdot \sigma^2 \boldsymbol{\sigma} \tau^2 \tau^b N_r) + \text{h.c.}, \\ \bar{O}_{\Delta I=2}^{(1S_0^{-3}P_0)} &= \mathcal{I}_{ab} (N_r^T \sigma^2 \tau^2 \tau^a N_r)^\dagger (N_r^T \overleftrightarrow{\nabla} \cdot \sigma^2 \boldsymbol{\sigma} \tau^2 \tau^b N_r) + \text{h.c.}, \\ \bar{O}_{\Delta I=0}^{(3S_1^{-1}P_1)} &= (N_r^T \sigma^2 \boldsymbol{\sigma} \tau^2 N_r)^\dagger \cdot (N_r^T \overleftrightarrow{\nabla} \sigma^2 \tau^2 N_r) + \text{h.c.}, \\ \bar{O}_{\Delta I=1}^{(3S_1^{-3}P_1)} &= (N_r^T \sigma^2 \boldsymbol{\sigma} \tau^2 N_r)^\dagger \cdot (N_r^T i \overleftrightarrow{\nabla} \times \sigma^2 \boldsymbol{\sigma} \tau^2 \tau^3 N_r) + \text{h.c.}, \end{aligned} \quad (110)$$

related to the original basis as follows,

$$\bar{O}_{\Delta I=0}^{(1S_0-3P_0)} = 6O_1^{PVTV} + 2O_2^{PVTV}, \quad (111)$$

$$\bar{O}_{\Delta I=1}^{(1S_0-3P_0)} = -4O_3^{PVTV} - 4O_4^{PVTV}, \quad (112)$$

$$\bar{O}_{\Delta I=2}^{(1S_0-3P_0)} = -4O_5^{PVTV}, \quad (113)$$

$$\bar{O}_{\Delta I=0}^{(3S_1-1P_1)} = 2O_1^{PVTV} - 2O_2^{PVTV}, \quad (114)$$

$$\bar{O}_{\Delta I=1}^{(3S_1-3P_1)} = 4O_3^{PVTV} - 4O_4^{PVTV}. \quad (115)$$

#### 4.4 Constraints from the large- $N_c$ limit

In 't Hooft combined large- $N_c$  and small coupling limit, with  $g_s^2 N_c$  fixed [190], QCD considerably simplifies, while maintaining many of the features of the actual theory, becoming a theory of stable hadrons. The baryons emerge as dense systems of many quarks, subjected to a mean field potential [191]. Nucleon-nucleon interactions exhibit in this limit a spin-flavor symmetry [192, 193, 194]. Indeed, due to the fact that nucleons carry definite spin and isospin of  $O(1)$ , interactions inducing a change in either spin or isospin are suppressed relative to the dominant  $O(N_c)$  ones, that are either spin-isospin independent ( $\sim 1$ ) or dependent on both ( $\sim \sigma\tau$ ). The large- $N_c$  counting of momenta follows from the observation that the nucleon-nucleon scattering amplitude is in this limit a sum of meson exchange poles, each one depending only on the relative momentum transfer. The average relative momenta can only appear as relativistic corrections, which are suppressed by inverse powers of  $M \sim O(N_c)$ .

Apparently the resulting scaling laws do not conform with the operator identities (99) and (108) and seem to imply a dependence on the choice of operator basis. However, one can start with the redundant set of operators, pertinent to a theory of distinguishable nucleons, since the large- $N_c$  arguments outlined above are completely general and do not rely on the statistics of the interacting baryons (the only assumption is that they both carry spin and isospin of  $O(1)$ ). As a result one obtains the large- $N_c$  scaling of the LECs in the PVTV contact potential,

$$\begin{aligned} C_2 &\sim C_5 \sim O(1), \\ C_3 &\sim C_4 \sim C_{3'} \sim O(1/N_c), \\ C_1 &\sim C_{1'} \sim C_{2'} \sim C_{5'} \sim O(1/N_c^2), \\ C_{4'} &\sim O(1/N_c^3), \end{aligned} \quad (116)$$

and in the PVTV one,

$$\begin{aligned} \bar{C}_3 &\sim O(1), \\ \bar{C}_1 &\sim \bar{C}_2 \sim \bar{C}_{2'} \sim \bar{C}_5 \sim \bar{C}_{5'} \sim O(1/N_c), \\ \bar{C}_4 &\sim \bar{C}_{3'} \sim \bar{C}_{4'} \sim O(1/N_c^2), \\ \bar{C}_{1'} &\sim O(1/N_c^3). \end{aligned} \quad (117)$$

Therefore we have only two leading LECs in the PVTC potential ( $C_2$  and  $C_5$  corresponding to  $\Delta I = 0, 2$  respectively) and only one in the PVTV potential ( $\bar{C}_3$  with  $\Delta I = 1$ ) [47, 150]. This largely increases the predictive power for low-energy hadronic parity violation, and allows to put more severe constraints on the forthcoming experimental results. Notice however that the above results are obtained by simply projecting the Hartree Hamiltonian in the nucleon-nucleon sector. A consistent treatment would require to consider the induced effect on NN contact vertices of  $\Delta$  exchanges, since the latter are enhanced, in

the large- $N_c$  limit, due to the degeneracy between nucleon and delta masses implied by the spin-flavor symmetry.

Moreover, for the PVTV case, this picture is obscured by the fact that the magnitude of the five contact LECs depends strongly on the particular type of the CP-violating source at the quark level. For example, the QCD  $\bar{\theta}$  term conserves isospin symmetry such that  $\bar{C}_{3,4,5}$  are suppressed by powers of  $\varepsilon\epsilon_{m_\pi}$  compared to  $\bar{C}_{1,2}$  (see Table 1). Despite the possible  $1/N_c$  suppression of  $\bar{C}_{1,2}$  compared to  $\bar{C}_3$  the former are still expected to dominate.

## 5 ONE-MESON EXCHANGE MODELS

In the past, a simple and rather efficient description of the strong PCTC NN interaction was obtained in terms of a sum of single meson exchanges [195, 196]. These models started to be popular since the discovery of various meson resonances during the sixties. The potentials were generally constructed taking into account the exchanges of pions ( $J^P = 0^-, m_\pi = 138$  MeV),  $\eta$ -mesons ( $J^P = 0^-, m_\eta = 550$  MeV), and  $\rho$ - and  $\omega$ -mesons ( $J^P = 1^-, m_{\rho,\omega} = 770, 780$  MeV), but clearly, the number of mesons to be included is somewhat arbitrary. This picture has been extended also to describe PVTC and PVTV interactions, simply considering single meson exchanges where one of the vertex is strong and PCTC, while the other violates P and conserves T or violates both P and T. Then, all the dynamics of such interactions is contained in a number of PVTC and PVTV nucleon-nucleon-meson (NNM) coupling constants.

|   | $\bar{N}N$ | $\bar{N}i\gamma_5N$ | $\bar{N}\gamma_\mu N$ | $\bar{N}\gamma_\mu\gamma_5N$ | $\bar{N}\sigma_{\mu\nu}N$ | $\pi_a$     | $\rho_a$     | $\eta$ | $\omega$ |
|---|------------|---------------------|-----------------------|------------------------------|---------------------------|-------------|--------------|--------|----------|
| H | +          | +                   | +                     | +                            | +                         | +           | +            | +      | +        |
| P | +          | -                   | +                     | -                            | +                         | -           | +            | -      | +        |
| C | +          | +                   | -                     | +                            | -                         | $(-)^{a+1}$ | $-(-)^{a+1}$ | +      | -        |

**Table 2.** Transformation properties of fermion bilinears with different elements of the Clifford algebra and various meson fields under hermitian conjugation (H), parity (P), and charge conjugation (C). Note that the pion and rho-meson fields are isospin triplets,  $a = 1, 2, 3$ .

One starts by writing the Lagrangian consistent of Yukawa-like NNM vertices, invariant under the proper Lorentz transformations, and either conserving or violating the discrete P, C, T symmetries. The building blocks of the Lagrangian are therefore nucleon bilinears multiplied by a meson field arranged so that Lorentz symmetry is satisfied. For the construction of the PCTC Lagrangian, one usually includes only isospin-conserving terms, however, for the PVTC and PVTV Lagrangians also isospin-violating terms have to be included as the underlying operators at the quark level are not necessarily isospin symmetric. A summary of the transformation properties of nucleon bilinears with different elements of the Clifford algebra and the various meson fields under hermitian conjugation (H), parity P, and charge conjugation C are reported in Table 2.

Using these properties it is not difficult to write the Lagrangians. For example, the strong  $\mathcal{L}_{\text{PCTC}}$  Lagrangian constructed with these mesons is given by (here we list only isospin -conserving terms)

$$\begin{aligned}
 \mathcal{L}_{\text{PCTC}} &= g_\pi \bar{N} i \gamma_5 \vec{\tau} \cdot \vec{\pi} N + g_\eta \bar{N} i \gamma_5 \eta N \\
 &- g_\rho \bar{N} \left( \gamma^\mu - i \frac{\chi_V}{2M} \sigma^{\mu\nu} q_\nu \right) \vec{\tau} \cdot \vec{\rho}_\mu N \\
 &- g_\omega \bar{N} \left( \gamma^\mu - i \frac{\chi_S}{2M} \sigma^{\mu\nu} q_\nu \right) \omega_\mu N,
 \end{aligned} \tag{118}$$



| Coupling       | DDH [50]<br>Reasonable Range | DDH [50]<br>“Best” Value |
|----------------|------------------------------|--------------------------|
| $h_{\pi}^1$    | 0 → 30                       | 12                       |
| $h_{\rho}^0$   | 30 → -81                     | -30                      |
| $h_{\rho}^1$   | -1 → 0                       | -0.5                     |
| $h_{\rho}^2$   | -20 → -29                    | -25                      |
| $h_{\omega}^0$ | 15 → -27                     | -5                       |
| $h_{\omega}^1$ | -5 → -2                      | -3                       |

**Table 3.** Weak NNM couplings as estimated in Ref. [50]. All numbers are quoted in units of the value  $3.8 \times 10^{-8}$ .

where  $q^\mu$  is the meson momentum <sup>7</sup>,  $\pi_a$ ,  $\rho_a^\mu$ ,  $\eta$  and  $\omega^\mu$  are meson fields and  $g_\pi, \dots$  PCTC coupling constants. Above,  $\chi_V$  and  $\chi_S$  are the ratios of the tensor to vector coupling constant for  $\rho$  and  $\omega$ , respectively. Assuming vector-meson dominance [197], they can be related to the iso-vector and iso-scalar magnetic moments of a nucleon ( $\chi_V = 3.70$  and  $\chi_S = -0.12$ ). Note that the pion and rho-meson are isospin triplets, therefore the fields have the isospin index  $a = 1, \dots, 3$ . Moreover, the rho- and omega-mesons have spin 1, and their fields correspondingly are vector fields with index  $\mu = 0, \dots, 3$ .

Let us now consider the PVTC Lagrangian constructed in terms of the same mesons. In this case one has to take into account Barton’s theorem [198], which asserts that exchange of neutral and spinless mesons between on-shell nucleons is forbidden by CP invariance, and therefore they cannot enter in a PVTC Lagrangian. Therefore only  $\pi^\pm, \rho$  and  $\omega$  vertices need to be considered and the form of the PVTC effective Lagrangian is [131]

$$\begin{aligned}
 \mathcal{L}_{\text{PVTC}} &= \frac{h_{\pi}^1}{\sqrt{2}} \bar{N} (\vec{\pi} \times \vec{\tau})_3 N \\
 &+ \bar{N} \left( h_{\rho}^0 \vec{\tau} \cdot (\vec{\rho})^\mu + h_{\rho}^1 \rho_3^\mu + \frac{h_{\rho}^2}{2\sqrt{6}} (3\tau_3 \rho_3^\mu - \vec{\tau} \cdot (\vec{\rho})^\mu) \right) \gamma_\mu \gamma_5 N \\
 &+ \bar{N} (h_{\omega}^0 \omega^\mu + h_{\omega}^1 \tau_3 \omega^\mu) \gamma_\mu \gamma_5 N - h_{\rho}^{\prime 1} \bar{N} (\vec{\tau} \times (\vec{\rho})^\mu)_3 \frac{\sigma_{\mu\nu} q^\nu}{2M} \gamma_5 N, \tag{119}
 \end{aligned}$$

where  $h_{\pi}^1, \dots$  are PVTC coupling constants to be determined. As discussed also in Section 3, where we focused in particular on the pion-nucleon PVTC constant  $h_{\pi}^1$ , attempts to estimate the magnitude of these couplings from the fundamental theory were reported in several papers [121, 122, 123, 124, 125, 126, 127]. In particular, in the DDH paper [50], the authors presented *reasonable ranges* inside of which these parameters were extremely likely to be found, together with a set of “best values” (see Table 3). Clearly, these values have to be considered as educated guesses in view of all the uncertainties of their evaluation. Of the seven unknown weak couplings  $h_{\pi}^1, h_{\rho}^0, \dots$ , there are estimates that indicate that  $h_{\rho}^{\prime 1}$  is quite small [199] and this term was generally omitted, leaving PVTC observables to be described in terms of six constants.

<sup>7</sup> More appropriately, these Lagrangian terms should be written in terms of four-gradients. For example

$$\bar{N} i \frac{\chi_V}{2M} \sigma^{\mu\nu} q_\nu \vec{\tau} \cdot \vec{\rho}_\mu N \rightarrow -\bar{N} \frac{\chi_V}{2M} [\partial_\nu, \sigma^{\mu\nu} \vec{\tau} \cdot \vec{\rho}_\mu] N.$$

where  $[\cdot, \cdot]$  denotes the commutator.

In the same manner, we can write the PVTV Lagrangian composed of NNM vertices [200, 142]

$$\mathcal{L}_{\text{PVTV}} = \bar{N}[\bar{g}_\pi^0 \vec{\tau} \cdot \vec{\pi} + \bar{g}_\pi^1 \pi_3 + \bar{g}_\pi^2 (3\tau_3 \pi_3 - \vec{\tau} \cdot \vec{\pi})]N \quad (120)$$

$$+ \bar{N}[\bar{g}_\eta^0 \eta + \bar{g}_\eta^1 \tau_3 \eta]N \quad (121)$$

$$+ \bar{N} \frac{1}{2M} [\bar{g}_\rho^0 \vec{\tau} \cdot (\vec{\rho})^\mu + \bar{g}_\rho^1 \rho_3^\mu + \bar{g}_\rho^2 (3\tau_z \rho_3^\mu - \vec{\tau} \cdot (\vec{\rho})^\mu)] \sigma_{\mu\nu} q^\nu \gamma_5 N \quad (122)$$

$$+ \bar{N} \frac{1}{2M} [\bar{g}_\omega^0 \omega_\mu + \bar{g}_\omega^1 \tau_z \omega_\mu] \sigma^{\mu\nu} q_\nu \gamma_5 N, \quad (123)$$

where  $\bar{g}_\alpha^i$ ,  $i = 0, 1, 2$ , are PVTV meson-nucleon coupling constants. In this case, there were no attempts to obtain the values of these coupling constants from the fundamental theory, as also the magnitude of the parameters entering the underlying theory is unknown.

From these Lagrangians, the PVTC and PVTV interactions are obtained as a sum of single-meson exchange diagrams. Regarding PVTC, below we report the potential in the form obtained by DDH [50]

$$\begin{aligned} V_{\text{PVTC}} = & -\frac{g_\pi h_\pi^1}{2\sqrt{2}M} i(\vec{\tau}_1 \times \vec{\tau}_2)_z \frac{(\boldsymbol{\sigma}_1 + \boldsymbol{\sigma}_2) \cdot \mathbf{k}}{k^2 + m_\pi^2} \\ & -\frac{g_\rho}{M} \left[ \vec{\tau}_1 \cdot \vec{\tau}_2 h_\rho^0 + \frac{(\tau_{1z} + \tau_{2z})}{2} h_\rho^1 + \frac{3\tau_{1z}\tau_{2z} - \vec{\tau}_1 \cdot \vec{\tau}_2}{2\sqrt{6}} h_\rho^2 \right] \\ & \times \left[ \frac{2(\boldsymbol{\sigma}_1 - \boldsymbol{\sigma}_2) \cdot \mathbf{K} + (1 + \chi_V) i(\boldsymbol{\sigma}_1 \times \boldsymbol{\sigma}_2) \cdot \mathbf{k}}{k^2 + m_\rho^2} \right] \\ & -\frac{g_\omega}{M} \left[ h_\omega^0 + \frac{(\tau_{1z} + \tau_{2z})}{2} h_\omega^1 \right] \left[ \frac{2(\boldsymbol{\sigma}_1 - \boldsymbol{\sigma}_2) \cdot \mathbf{K} + (1 + \chi_S) i(\boldsymbol{\sigma}_1 \times \boldsymbol{\sigma}_2) \cdot \mathbf{k}}{k^2 + m_\omega^2} \right] \\ & + \left[ \frac{g_\rho h_\rho^1}{M} \frac{(\tau_{1z} - \tau_{2z})(\boldsymbol{\sigma}_1 + \boldsymbol{\sigma}_2) \cdot \mathbf{K}}{k^2 + m_\rho^2} \right] - \left[ \frac{g_\omega h_\omega^1}{M} \frac{(\tau_{1z} - \tau_{2z})(\boldsymbol{\sigma}_1 + \boldsymbol{\sigma}_2) \cdot \mathbf{K}}{k^2 + m_\omega^2} \right] \\ & - \left[ \frac{g_\rho h_\rho^{1'}}{2M} \frac{i(\vec{\tau}_1 \times \vec{\tau}_2)_z (\boldsymbol{\sigma}_1 + \boldsymbol{\sigma}_2) \cdot \mathbf{k}}{k^2 + m_\rho^2} \right], \end{aligned} \quad (124)$$

where  $\mathbf{k}$  and  $\mathbf{K}$  are defined in Eq. (46). Often the potential is regularized for large values of  $k$ , modifying the meson propagators so that  $1/(k^2 + m_x^2) \rightarrow f_{\Lambda_x}(k^2)/(k^2 + m_x^2)$ , where  $x = \pi, \rho$ , and  $\omega$ . For example, in Ref. [201] the following regularization was chosen

$$\frac{1}{k^2 + m_x^2} \rightarrow \frac{1}{k^2 + m_x^2} \left( \frac{\Lambda_x^2 - m_x^2}{\Lambda_x^2 + k^2} \right)^2, \quad (125)$$

The parameters  $\Lambda_\pi$ ,  $\Lambda_\rho$ , and  $\Lambda_\omega$  were chosen to have values 1.72 GeV, 1.31 GeV, and 1.50 GeV, respectively [201]. However, the cutoff functions  $f_{\Lambda_x}(k^2)$  were not always applied and also their form can vary.

Several PVTC observables have been studied using the DDH potential, with the aim to identify the values of the six or seven coupling constants, see for example Refs. [34, 36, 37]. Up to now the lack of accurate experimental values has prevented the completion of this task.

The PVTV potential was derived in Ref. [202, 203, 204, 142]. The momentum space version reads

$$\begin{aligned}
 V_{\text{PVTV}} = & +\frac{g_\pi}{2M} \left[ \bar{g}_\pi^0 \vec{\tau}_1 \cdot \vec{\tau}_2 + \bar{g}_\pi^1 \frac{(\tau_{1z} + \tau_{2z})}{2} + \bar{g}_\pi^2 (3\tau_{1z}\tau_{2z} - \vec{\tau}_1 \cdot \vec{\tau}_2) \right] \frac{i(\boldsymbol{\sigma}_1 - \boldsymbol{\sigma}_2) \cdot \mathbf{k}}{m_\pi^2 + k^2} \\
 & -\frac{g_\rho}{2M} \left[ \bar{g}_\rho^0 \vec{\tau}_1 \cdot \vec{\tau}_2 + \bar{g}_\rho^1 \frac{(\tau_{1z} + \tau_{2z})}{2} + \bar{g}_\rho^2 (3\tau_{1z}\tau_{2z} - \vec{\tau}_1 \cdot \vec{\tau}_2) \right] \frac{i(\boldsymbol{\sigma}_1 - \boldsymbol{\sigma}_2) \cdot \mathbf{k}}{m_\rho^2 + k^2} \\
 & +\frac{g_\eta}{2M} \left[ \bar{g}_\eta^0 + \bar{g}_\eta^1 \frac{(\tau_{1z} + \tau_{2z})}{2} \right] \frac{i(\boldsymbol{\sigma}_1 - \boldsymbol{\sigma}_2) \cdot \mathbf{k}}{m_\eta^2 + k^2} \\
 & -\frac{g_\omega}{2M} \left[ \bar{g}_\omega^0 + \bar{g}_\omega^1 \frac{(\tau_{1z} + \tau_{2z})}{2} \right] \frac{i(\boldsymbol{\sigma}_1 - \boldsymbol{\sigma}_2) \cdot \mathbf{k}}{m_\omega^2 + k^2} \\
 & + \left[ \frac{g_\pi \bar{g}_\pi^1 (\tau_{1z} - \tau_{2z}) i(\boldsymbol{\sigma}_1 + \boldsymbol{\sigma}_2) \cdot \mathbf{k}}{4M (k^2 + m_\pi^2)} \right] + \left[ \frac{g_\rho \bar{g}_\rho^1 (\tau_{1z} - \tau_{2z}) i(\boldsymbol{\sigma}_1 + \boldsymbol{\sigma}_2) \cdot \mathbf{k}}{4M (k^2 + m_\rho^2)} \right] \\
 & - \left[ \frac{g_\eta \bar{g}_\eta^1 (\tau_{1z} - \tau_{2z}) i(\boldsymbol{\sigma}_1 + \boldsymbol{\sigma}_2) \cdot \mathbf{k}}{4M (k^2 + m_\eta^2)} \right] - \left[ \frac{g_\omega \bar{g}_\omega^1 (\tau_{1z} - \tau_{2z}) i(\boldsymbol{\sigma}_1 + \boldsymbol{\sigma}_2) \cdot \mathbf{k}}{4M (k^2 + m_\omega^2)} \right]. \quad (126)
 \end{aligned}$$

Also in this case, cut off functions can be applied in order to regularize the large  $k$  behavior of  $V_{\text{PVTV}}$ . It is worthwhile to stress that the PVTV meson-exchange potential involves significantly more parameters than the LO PVTV chiral potential which depends in principle only on 4 LECs  $\bar{g}_{0,1}$  and  $\bar{C}_{1,2}$ , with  $\bar{g}_2$ ,  $\bar{\Delta}$ , and  $\bar{C}_{3,4,5}$  appearing at subleading orders. While the meson-exchange potential can be mapped onto the short-distance  $\bar{C}_i$  operators, the dynamics from the 3-pion  $\bar{\Delta}$  interaction is not captured in this way.

## 6 SELECTED RESULTS FOR VARIOUS PVTC AND PVTV OBSERVABLES

In this section we present a selection of results obtained with the chiral EFT potentials and currents described in Sect. 3 for various PVTC and PVTV observables. We will discuss first in the next three subsections the parity violation in the radiative neutron capture on the proton, then the longitudinal asymmetry in  $\vec{p}p$  scattering, and subsequently the  $\vec{n}$ - $p$  and  $\vec{n}$ - $d$  spin rotations. Finally, in the last subsection, we present some results for the EDM of light nuclei. Our motivation to include these results in the review is mainly to establish benchmarks to help future applications. We include also a ‘‘minimum’’ analysis how the current experimental data constrain some of the values of the LECs entering the  $\chi\text{EFT}$  interactions.

Results obtained using the pionless EFT can be found, for example, in Refs. [36, 37, 39]. The meson-exchange potentials (in particular the DDH model) were used to analyze the results of several experiments of PVTC observables also in medium and heavy nuclei. For a summary of the obtained results, see, for example, Refs. [131, 34, 39]. Calculations of the EDM of light nuclei using the meson exchange potential were performed in Refs. [142, 205, 206].

### 6.1 Parity violation in radiative neutron capture on the proton

The radiative neutron capture on the proton  $\vec{n}p \rightarrow d\gamma$ , where  $d$  denotes the deuteron and  $\vec{n}$  a longitudinally polarized neutron, represents a very interesting process to study PVTC effects in nuclear physics. The longitudinal analyzing power for this process is defined as

$$A_\gamma(\theta) = \frac{d\sigma_+(\theta) - d\sigma_-(\theta)}{d\sigma_+(\theta) + d\sigma_-(\theta)} = a_\gamma \cos \theta, \quad (127)$$

where  $d\sigma_{\pm}(\theta)$  is the differential cross section for positive/negative helicity neutrons, and  $\theta$  is defined as the angle between the neutron spin and the outgoing photon momentum.  $a_{\gamma}$  has been targeted by several experiments in the last decades. A first nonzero signal was reported last year for incoming neutrons of thermal energies [207],

$$a_{\gamma} = (-3.0 \pm 1.4 \pm 0.2) \cdot 10^{-8}. \quad (128)$$

albeit only two standard deviations away from a null measurement.

The theoretical asymmetry is given by

$$a_{\gamma} = \frac{-\sqrt{2} \operatorname{Re} \left[ M_1^*(^1S_0) E_1(^3S_1) + E_1^*(^1S_0) M_1(^3S_1) \right] + \operatorname{Re} \left[ E_1^*(^3S_1) M_1(^3S_1) \right]}{|M_1(^1S_0)|^2 + |E_1(^1S_0)|^2 + |M_1(^3S_1)|^2 + |E_1(^3S_1)|^2}, \quad (129)$$

where  $X_{\ell}(^{2S+1}S_J)$  are reduced matrix elements (RMEs) either of electric ( $X = E$ ) or magnetic ( $X = M$ ) type, of multipolarity  $\ell$ , and describing the EM transition from the  $n - p$  system in the scattering state  $^{2S+1}S_J$  [208].

Compared to the PVTC longitudinal analyzing power in proton-proton scattering discussed later,  $a_{\gamma}$  comes with a big advantage. The initial neutron-proton state can be in a  $^3S_1$  state, such that the process is sensitive to  $^3S_1 \leftrightarrow ^3P_1$  transitions and thus depends on the LO PVTC NN potential. In chiral EFT the LO potential only depends on the LEC  $h_{\pi}^1$ , such that measurements of  $a_{\gamma}$  provide a unique chance to pin down the value of this LEC, something which is much more difficult in proton-proton scattering, where the contribution of the LO potential vanishes. The disadvantage is that  $\vec{n}p \rightarrow d\gamma$  is an electromagnetic process and therefore depends on P-conserving and P-violating electromagnetic currents.

As can be seen from Eq. (129), nonzero  $a_{\gamma}$  requires an interference between electric and magnetic dipole currents. As such, just including the leading magnetic moment current in the presence of the LO PVTC NN potential leads to a vanishing result and NLO currents are necessary. There are then three relevant contributions that consist of interference between the isovector nucleon magnetic moment and

1. the one-body convection current in combination with the PVTC NN potential,
2. the two-body PCTC currents in combination with the PVTC NN potential,
3. the two-body PVTC currents.

Each of these contributions is sizeable:  $a_{\gamma}^1 = (-0.27 \pm 0.03)h_{\pi}^1$ ,  $a_{\gamma}^2 = (-0.53 \pm 0.02)h_{\pi}^1$ , and  $a_{\gamma}^3 = (0.72 \pm 0.03)h_{\pi}^1$  where the theoretical error bands are obtained from cut-off variations in the strong NN potential and do not reflect uncertainties from higher-order contributions [173]. While these uncertainties are small on the individual contributions, they lead to a sizeable uncertainty on the total analyzing power [173]

$$a_{\gamma} = a_{\gamma}^1 + a_{\gamma}^2 + a_{\gamma}^3 = (-0.11 \pm 0.05)h_{\pi}^1. \quad (130)$$

The cancellations between the different contributions are related to gauge invariance [209, 208, 173] and this explains the relatively large total theoretical uncertainty. While the electromagnetic currents given above are explicitly gauge invariant as they result from the gauge-invariant  $\chi$ EFT Lagrangian, explicit gauge invariance is lost due to applied regulator when solving the NN scattering and bound-state equations. Future calculations can probably reduce the uncertainty by using regulators that do not violate explicit gauge invariance, but such schemes have not been applied to PVTC processes. Alternatively, it is possible to apply the Siegert theorem to relate part of the electric dipole currents to the one-body

charge density. Ref. [210] applied the Siegert theorem in combination with phenomenological strong potentials to calculate  $a_\gamma$  finding a result in good agreement with the central value in Eq. (130). Such calculations however do not include an uncertainty estimate, for instance from missing transverse currents that are not included when applying the Siegert theorem. In this light, Eq. (130) can be interpreted as a conservative result. It would be interesting to redo the calculation of  $a_\gamma$  in an updated framework to reduce the theoretical uncertainty.

The contribution to  $a_\gamma$  of the short range components of the potential is considered to be negligible. For example, using the meson-exchange model, the calculations have shown that  $a_\gamma$  is essentially unaffected by short-range contributions [211, 212, 213, 208], represented in this case by  $\rho$  and  $\omega$  exchanges. Within  $\chi$ EFT, a resonance saturation estimate of the short-distance LECs contributing to the asymmetry led to short-distance contributions to  $a_\gamma$  of roughly  $5 \cdot 10^{-9}$  and thus very small [173]. Therefore, considering the theoretical expression given in Eq. (129) and the experimental value given in Eq. (128), we obtain an estimate for the LEC  $h_\pi^1$

$$h_\pi^1 = (2.7 \pm 1.8) \times 10^{-7}. \quad (131)$$

Note that the large experimental error and the large theoretical uncertainty only allow to establish the positive sign and that the magnitude of this LEC is consistent with the Lattice QCD preliminary evaluation reported in Eq. (26) [132].

## 6.2 Parity violation in $\vec{p}p$ scattering

PVTC effects in proton-proton scattering can be studied by looking at the longitudinal analyzing power  $A_z(E, \theta)$  defined as,

$$A_z(E, \theta) = \frac{\sigma_+(\theta, E) - \sigma_-(\theta, E)}{\sigma_+(\theta, E) + \sigma_-(\theta, E)}, \quad (132)$$

where  $\theta$  is the scattering angle and  $E$  the energy of the protons in the laboratory frame, and  $\sigma_+(\theta, E)$  ( $\sigma_-(\theta, E)$ ) the cross section when the polarization of the incoming proton is parallel (anti-parallel) to the beam direction. Actually the experiments detect the particles scattered in angular range  $[\theta_1, \theta_2]$  and the measured quantity is an ‘‘average’’ of the asymmetry over the total cross-section in this range, explicitly

$$\bar{A}_z(E) = \frac{\int_{\theta_1 \leq \theta \leq \theta_2} d \cos \theta A_z(\theta, E) \sigma(\theta, E)}{\int_{\theta_1 \leq \theta \leq \theta_2} d \cos \theta \sigma(\theta, E)}, \quad (133)$$

where

$$\sigma(\theta, E) = \frac{1}{2} (\sigma_+(\theta, E) + \sigma_-(\theta, E)) \quad (134)$$

is the unpolarized differential cross-section for the process. There exist three measurements of the angle-averaged  $\vec{p}p$  longitudinal asymmetry  $\bar{A}_z(E)$ , see Eq. (133), obtained at different laboratory energies  $E$  [214, 215, 216]. The measurements and the angle ranges are reported in Table 4.

The isospin state of two proton system is  $|pp\rangle \equiv |T = 1, T_z = 1\rangle$ , therefore the LO contribution that comes from the OPE vanishes and the LEC  $h_\pi^1$  will contribute to the observable only via the TPE box diagrams that appear at NLO and N<sup>2</sup>LO. Taking into account the isospin selection rules, the longitudinal asymmetry can be written as

$$\bar{A}_z = h_\pi^1 a_0^{(pp)} + C a_1^{(pp)} + \tilde{h} a_2^{(pp)}, \quad (135)$$

| $E$ (MeV) | $\overline{A}_z$ ( $10^{-7}$ ) | $(\theta_1, \theta_2)$ |
|-----------|--------------------------------|------------------------|
| 13.6      | $-0.97 \pm 0.20$               | $(20^\circ, 78^\circ)$ |
| 45        | $-1.53 \pm 0.21$               | $(23^\circ, 52^\circ)$ |
| 221       | $+0.84 \pm 0.34$               | $(5^\circ, 90^\circ)$  |

**Table 4.** Values of  $\overline{A}_z$  and angle ranges for the three measurements of the  $\vec{p}p$  longitudinal analyzing power [214, 215, 216].

| $E$ [MeV] | $a_0^{(pp)}$ (NLO) | $a_0^{(pp)}$ (N <sup>2</sup> LO) | $a_0^{(pp)}$ (TOT) | $a_1^{(pp)}$ | $a_2^{(pp)}$ |
|-----------|--------------------|----------------------------------|--------------------|--------------|--------------|
| 13.6      | 0.289              | 0.160                            | 0.449              | -0.044       | -0.215       |
| 45        | 0.595              | 0.355                            | 0.950              | -0.084       | -0.475       |
| 221       | -0.281             | -0.187                           | -0.468             | 0.036        | 0.251        |

**Table 5.** Values of the coefficients  $a_i^{(pp)}$  calculated with the  $\chi$ EFT N<sup>2</sup>LO PVTC potential described in Sect. 3.4 and the N<sup>4</sup>LO PCTC potential derived in Ref. [18] at the three energies corresponding to the experimental data points. The PVTC potential has been regularized as in Eq. (86) adopting the value  $\Lambda_C = 500$  MeV for the cutoff parameter. The PCTC potential has been regularized with the same value of the cutoff parameter. For the coefficient  $a_0^{(pp)}$  we give separately the contributions of the NLO and N<sup>2</sup>LO terms only and then their sum, see Eq. (138).

where the first two terms are NLO contributions and the third term enters at N<sup>2</sup>LO. We defined

$$C = C_1 + C_2 + 2(C_4 + C_5), \quad (136)$$

$$\tilde{h} = \frac{5g_A}{4}h_V^0 + 2\left(\frac{g_A}{4}h_V^1 - h_A^1\right) - 2\left(\frac{g_A}{3}h_V^2 + h_A^2\right), \quad (137)$$

and  $a_0^{(pp)}$ ,  $a_1^{(pp)}$ ,  $a_2^{(pp)}$  are numerical coefficients independent on the LEC values (but they depend on the energy). The values of the coefficients  $a_0^{(pp)}$ ,  $a_1^{(pp)}$ , and  $a_2^{(pp)}$  calculated with the  $\chi$ EFT N<sup>2</sup>LO PVTC potential described in Sect. 3.4 and the N<sup>4</sup>LO PCTC potential derived in Ref. [18] are reported in Table 5. The only coefficient which receives contributions from both the NLO and N<sup>2</sup>LO potentials is  $a_0^{(pp)}$ . In the table, we report separately the two contributions and also the total contribution, given simply as

$$a_0^{(pp)}(\text{TOT}) = a_0^{(pp)}(\text{NLO}) + a_0^{(pp)}(\text{N}^2\text{LO}), \quad a_0^{(pp)}(\text{N}^2\text{LO}) = c_4 a_0^{(pp)}(4). \quad (138)$$

The value of  $a_0^{(pp)}(\text{N}^2\text{LO})$  has been obtained assuming a value  $c_4 = 3.56 \text{ GeV}^{-1}$  [217]. This correction to  $a_0^{(pp)}$  is of the order of  $\sim 50\%$  with respect to the NLO value, somewhat larger than expected. This is related by the unnaturally large value of the  $\pi NN$  LEC  $c_4$  appearing in the PCTC Lagrangian (13). This value has been obtained from the Roy-Steiner analysis of  $\pi N$  scattering data at N<sup>2</sup>LO performed in Ref. [217].

Unfortunately, of the performed measurements, the two at the lowest energy do not give independent information. In fact, the observable  $\overline{A}_z$  at low energy scales as  $\sqrt{E}$ , since its energy dependence in this energy range is driven solely by that of the S-wave (strong interaction) phase shift [218]. Because of this scaling, it is not possible to fit from these data all three LECs  $h_\pi^1$ ,  $C$ , and  $\tilde{h}$  at the same time. If we fix the value  $h_\pi^1 = 2.7 \times 10^{-7}$  from the central value as extracted from the  $\vec{n}p \rightarrow d\gamma$  observable, see Eq. (131), then we can perform a  $\chi^2$  analysis of the three data points listed in Table 4 in order to fix the values of  $C$  and  $\tilde{h}$ . Note that this value of  $h_\pi^1$  was obtained from the  $\vec{n}p \rightarrow d\gamma$  calculation performed in Ref. [173]

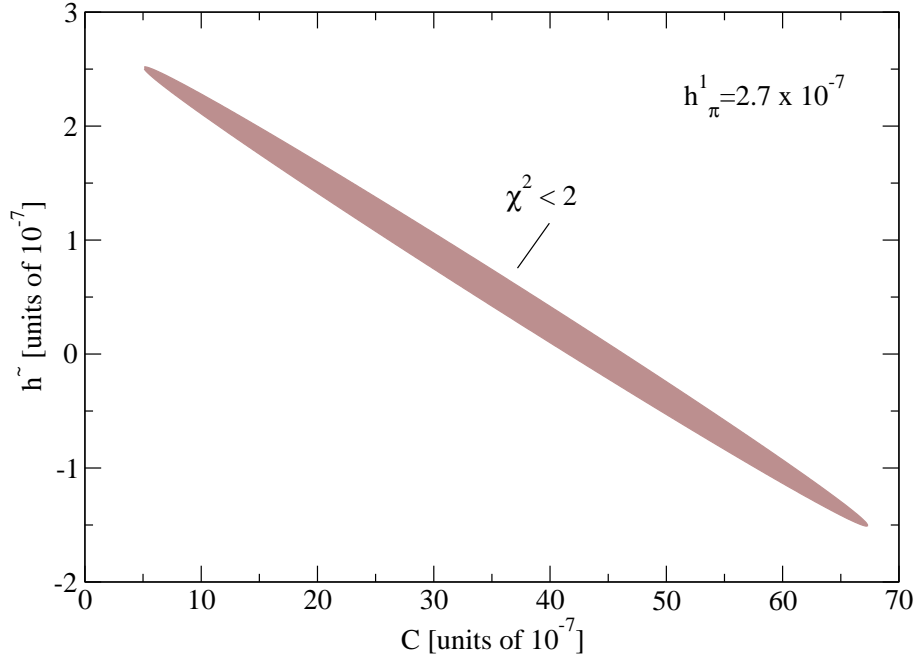


**Figure 5.** Region of  $C$  and  $\tilde{h}$  values for which  $\chi^2 \leq 2$  for the  $\vec{p}$ - $p$  longitudinal asymmetry. The calculation is based on the coefficients  $a_0^{(pp)}$ ,  $a_1^{(pp)}$ , and  $a_2^{(pp)}$  reported in Table 5 assuming the value  $h_\pi^1 = 2.7 \times 10^{-7}$ .

using a different PCTC potential than that one used to compute the  $a_i^{(pp)}$  coefficients. However, since the  $\vec{n}p \rightarrow d\gamma$  experiment depends mainly on the peripheral regions of the process, the value of  $a_\gamma$  is not very sensitive to the PCTC interaction (see also the calculations reported in Ref. [219]).

First of all, if we restrict ourselves to an NLO analysis, using  $h_\pi^1 = 2.7 \times 10^{-7}$  we would obtain  $C = (49 \pm 2) \cdot 10^{-7}$ . If we take into account also the N<sup>2</sup>LO LEC, we report in Fig. 5 the  $C$  and  $\tilde{h}$  values for which  $\chi^2 \leq 2$ , which form an elliptical region. As can be seen, there appears to be a strong correlation between  $C$  and  $\tilde{h}$  and the range of allowed values of the LECs is rather large  $5 \times 10^{-7} < C < 67 \times 10^{-7}$  and  $-1.5 \times 10^{-7} < \tilde{h} < 2.5 \times 10^{-7}$ . Note that the ellipse is rather narrow and almost coincides with a straight line. See also Refs. [46, 42] for a similar analysis performed at NLO for the LECs  $h_\pi^1$  and  $C$  only.

The previous discussion did not take into account the large uncertainty of the  $h_\pi^1$  coupling constant after the fit of the  $\vec{n}$ - $p$  radiative capture asymmetry. In Table 6, we report representative values of  $C$  and  $\tilde{h}$  giving the minimum value of  $\chi^2$  corresponding to range of values for  $h_\pi^1$  as given in Eq. (131). In the fourth column we report values for  $C$  if we neglect the N<sup>2</sup>LO contributions (setting  $\tilde{h} = 0$ ). We conclude that the combination of the  $\vec{p}p$  and  $\vec{n}p \rightarrow d\gamma$  asymmetries allows for a rough extraction of the LO and NLO LECs  $h_\pi^1$  and  $C$ , but is insufficient to also pinpoint the N<sup>2</sup>LO LEC  $\tilde{h}$ . The uncertainty of the extractions of  $h_\pi^1$  and  $C$  is dominated by theoretical and experimental uncertainties related to the PVTC asymmetry in the radiative neutron capture process.

| $h_\pi^1$ | $C$  | $\tilde{h}$ | $C(\tilde{h} = 0)$ |
|-----------|------|-------------|--------------------|
| 0.9       | 27.7 | 0.11        | $28 \pm 2$         |
| 2.7       | 34.5 | 0.97        | $49 \pm 2$         |
| 4.5       | 41.2 | 1.84        | $69 \pm 3$         |

**Table 6.** Values for  $C$  and  $\tilde{h}$  corresponding to different values of  $h_\pi^1$  (all LECs are given in units of  $10^{-7}$ ) giving the minimum value of the  $\chi^2$  in the fit of the three experimental  $\vec{p}$ - $p$  data points. For example, for  $h_\pi^1 = 2.7 \times 10^{-7}$ , the  $C$ ,  $\tilde{h}$  values are those lying in the center of the elliptical contour shown in Fig. 5. The fourth column corresponds to an analysis where we ignore the N<sup>2</sup>LO contributions and thus set  $\tilde{h} = 0$ .

### 6.3 The $\vec{n}$ - $p$ and $\vec{n}$ - $d$ spin rotation

The spin rotation of neutron traversing a slab of matter in a plane transverse to the beam direction induced by the PVTC potential is given by

$$\frac{d\phi^{(nX)}}{dz} = \frac{2\pi\rho}{(2S_X + 1)v_{\text{rel}}} \text{Re} \sum_{m_n m_X} \epsilon_{m_n}^{(-)} \langle p\hat{\mathbf{z}}; m_n, m_X | V_{PVTC} | p\hat{\mathbf{z}}; m_n, m_X \rangle^{(+)}, \quad (139)$$

where  $\rho$  is the density of hydrogen or deuterium nuclei for  $X = p$  or  $d$ ,  $|p\hat{\mathbf{z}}; m_n, m_X\rangle^{(\pm)}$  are the  $n$ - $X$  scattering states with outgoing-wave (+) and incoming-wave (−) boundary conditions and relative momentum  $\mathbf{p} = p\hat{\mathbf{z}}$  taken along the spin-quantization axis (the  $\hat{\mathbf{z}}$ -axis),  $S_X$  is the  $X$  spin, and  $v_{\text{rel}} = p/\mu$  is the magnitude of the relative velocity,  $\mu$  being the  $n$ - $X$  reduced mass. The expression above is averaged over the spin projections  $m_X$ ; however, the phase factor  $\epsilon_{m_n} = (-)^{1/2-m_n}$  is  $\pm 1$  depending on whether the neutron has  $m_n = \pm 1/2$ . We consider the  $n$ - $p$  and  $n$ - $d$  spin rotations for vanishing incident neutron energy (measurements of this observable are performed using ultracold neutron beams). In the following, we assume  $\rho = 0.4 \times 10^{23} \text{ cm}^{-3}$ . The rotation angle depends linearly on the PVTC LECs, as higher-order weak corrections are negligible. We write

$$\begin{aligned} \frac{d\phi^{(nX)}}{dz} = & h_\pi^1 a_0^{(nX)} + C_1 a_1^{(nX)} + C_2 a_2^{(nX)} + C_3 a_3^{(nX)} + C_4 a_4^{(nX)} + C_5 a_5^{(nX)} \\ & + h_V^0 b_1^{(nX)} + h_V^1 b_2^{(nX)} + h_V^2 b_3^{(nX)} + h_A^1 b_4^{(nX)} + h_A^2 b_5^{(nX)}, \end{aligned} \quad (140)$$

where the  $a_i^{(nX)}$  for  $i = 0, \dots, 5$  and  $b_i^{(nX)}$  for  $i = 1, \dots, 5$  are numerical coefficients. The coefficient  $a_0^{(nX)}$  receives contributions from different chiral orders, in particular

$$a_0^{(nX)} = a_0^{(nX)}(\text{LO}) + a_0^{(nX)}(\text{NLO}) + a_0^{(nX)}(\text{N}^2\text{LO}). \quad (141)$$

The values of these coefficients for the  $n$ - $p$  case and the cut-off value  $\Lambda = 500 \text{ MeV}$  are listed in Table 7. From that Table, it is possible to appreciate the chiral convergence for the coefficients  $a_0^{(np)}$ . The NLO correction is  $\sim 10\%$  of the LO result. In this case, the N<sup>2</sup>LO contribution vanishes since the LEC  $h_\pi^1$  in  $V_{PVTC}^{(2)}$ (TPE) multiplies the operator  $(\tau_{1z} + \tau_{2z})$ . The  $\vec{n}$ - $p$  spin rotation is sensitive to all the LECs except for the LECs  $C_4$  and  $h_A^1$  multiplying again the isospin term  $(\tau_{1z} + \tau_{2z})$ ; in particular, there is a large sensitivity to  $C_5$  and  $h_A^2$ , which multiply the isotensor terms of the PVTC potential.



|                                  |       |              |        |              |        |
|----------------------------------|-------|--------------|--------|--------------|--------|
| $a_0^{(np)}$ (LO)                | 1.227 | $a_1^{(np)}$ | 0.257  | $b_1^{(np)}$ | 1.653  |
| $a_0^{(np)}$ (NLO)               | 0.137 | $a_2^{(np)}$ | 0.178  | $b_2^{(np)}$ | -0.181 |
| $a_0^{(np)}$ (N <sup>2</sup> LO) | 0.000 | $a_3^{(np)}$ | 0.106  | $b_3^{(np)}$ | 1.882  |
| $a_0^{(np)}$ (TOT)               | 1.364 | $a_4^{(np)}$ | 0.000  | $b_4^{(np)}$ | 0.000  |
|                                  |       | $a_5^{(np)}$ | -0.949 | $b_5^{(np)}$ | 4.456  |

**Table 7.** Values of the coefficients entering the expression of the  $\vec{n}$  - $p$  spin rotation in units of Rad m<sup>-1</sup> calculated for the  $\chi$ EFT N<sup>2</sup>LO PVTC potential described in Sect. 3.4 and the N<sup>4</sup>LO PCTC potential derived in Ref. [18] at vanishing neutron beam energy. The PVTC potential has been regularized as in Eq. (86) adopting the value  $\Lambda_C = 500$  MeV for the cutoff parameter. The PCTC potential has been regularized with the same value of the cutoff parameter. For  $a_0^{(np)}$  we give explicitly the contribution of the different orders, the sum of the three contributions is given in fourth row.

|              |        |
|--------------|--------|
| $a_0^{(nd)}$ | 2.179  |
| $a_1^{(nd)}$ | -0.010 |
| $a_2^{(nd)}$ | -0.160 |
| $a_3^{(nd)}$ | 0.191  |
| $a_4^{(nd)}$ | 0.064  |
| $a_5^{(nd)}$ | 0.000  |

**Table 8.** The same as in Table 7 but for the  $\vec{n}$  - $d$  spin rotation and using the  $\chi$ EFT NLO PVTC potential and the N<sup>3</sup>LO PCTC potential derived in Ref. [5].

Regarding the  $\vec{n}$ - $d$  spin rotation, the coefficients, as reported in Table 8, are calculated by using only the NLO PVTC potential. We note the large sensitivity to  $h_\pi^1$  (this fact is well known [201, 220]), and to the LEC's  $C_2$  and  $C_3$ .

At present there are no measurements of these quantities, however their experimental knowledge could be very useful in isolating certain combinations of LECs.

## 6.4 EDM of light nuclei

The EDM operator  $\hat{D}$  is composed by two parts,

$$\hat{D} = \hat{D}_{\text{PCTC}} + \hat{D}_{\text{PVTV}}. \quad (142)$$

$\hat{D}_{\text{PCTC}}$  is the electric dipole operator derived from the current  $\mathbf{J}_{\text{PCTC}}$  given in Eq. (87), after using the long wavelength approximation and the continuity equation [221], explicitly

$$\hat{D}_{\text{PCTC}} = e \sum_i \frac{1 + \tau_z(i)}{2} \mathbf{r}_i, \quad (143)$$

where  $e > 0$  is the electric unit charge,  $\tau_z(i)$  and  $\mathbf{r}_i$  are the  $z$  component of the isospin and the position of the  $i$ -th particle. This operator implicitly takes into account also the main part of the two-body PCTC

currents. The  $\hat{D}_{\text{PVTV}}$  contribution comes from the PVTV current at LO given in Eq. (96) and it reads

$$\hat{D}_{\text{PVTV}} = \frac{1}{2} \sum_i [(d_p + d_n) + (d_p - d_n)\tau_z(i)] \sigma_i, \quad (144)$$

where  $d_p$  and  $d_n$  are the EDM of proton and neutron, respectively and  $\sigma_i$  is the spin operator which act on the  $i$ -th particle. As discussed in Sect. 3.5.1 and in Refs. [143, 73] the  $\hat{D}_{\text{PVTV}}$  should also include contributions from transition currents at N<sup>2</sup>LO. These are not considered in this review.

The EDM of an  $A$  nucleus can be expressed as

$$\begin{aligned} d^A &= \langle \psi_+^A | \hat{D}_{\text{PVTV}} | \psi_+^A \rangle + 2 \langle \psi_+^A | \hat{D}_{\text{PCTC}} | \psi_-^A \rangle \\ &\equiv d_{\text{PVTV}}^A + e d_{\text{PCTC}}^A, \end{aligned} \quad (145)$$

where  $|\psi_+^A\rangle$  ( $|\psi_-^A\rangle$ ) is defined to be the even-parity (odd-parity) component of the wave function. In general, due to the smallness of the LECs, the EDM depends linearly on the PVTV LECs

$$d_{\text{PVTV}}^A = d_p a_p + d_n a_n \quad (146)$$

$$\begin{aligned} d_{\text{PCTC}}^A &= \bar{g}_0 a_0 + \bar{g}_1 a_1 + \bar{g}_2 a_2 \\ &+ \bar{C}_1 A_1 + \bar{C}_2 A_2 + \bar{C}_3 A_3 + \bar{C}_4 A_4 + \bar{C}_5 A_5 + \bar{\Delta} a_\Delta, \end{aligned} \quad (147)$$

where the  $a_i$  for  $i = 0, 1, 2$ ,  $A_i$  for  $i = 1, \dots, 5$ ,  $a_\Delta$ , and  $a_p$ ,  $a_n$  are coefficients independent on the LEC values (all coefficients except  $a_p$  and  $a_n$  have the unit of a length). For the deuteron,  $d_{\text{PVTV}}^2$  is dominated by one-body components, proportional to the neutron and proton EDM. The coefficients  $a_p$  and  $a_n$  multiplying the intrinsic neutron and proton EDM, as already pointed out first in Ref. [222] and then in Ref. [66], are given by,

$$a_n = a_p = \left(1 - \frac{3}{2} P_D\right), \quad (148)$$

where  $P_D$  is the percentage of D-wave present in the deuteron wave function.  $d_{\text{PCTC}}^2$ , in the case of the deuteron, receives contribution only from the LECs  $\bar{g}_1$ ,  $\bar{\Delta}$ ,  $\bar{C}_3$  and  $\bar{C}_4$ . The coefficients calculated with the  $\chi$ EFT N<sup>2</sup>LO PVTV potential described in Sect. 3.5 and the N<sup>4</sup>LO PCTC potential derived in Ref. [18] are reported in Table 9. The cutoff for both the PCTC and PVTV potentials has been chosen to be  $\Lambda_C = 500$  MeV. The coefficients  $a_1$ ,  $A_3$  and  $A_4$  agree well with the power counting expectation in Eq. (37). The slight suppression of  $a_1$  compared with the naive estimate  $a_1 \sim 1$  is in very good agreement with the perturbative pion power counting [70]. The LO perturbative pion calculation of  $a_1$  agrees with the value in Table 9 at the 20% level [70]. Results obtained in chiral EFT with N<sup>2</sup>LO PCTC potentials [66], and with ‘‘hybrid’’ approaches [143, 222] based on chiral PVTV and phenomenological PCTC potentials, also agree well with the results reported in Table 9. The contribution of the three-pion coupling  $a_\Delta$  is a bit more problematic. We find in this case that the contribution of the N<sup>2</sup>LO term is of the order of  $\sim 60\%$  of the NLO term. We will discuss the issue of these large N<sup>2</sup>LO corrections more in detail below.

Depending on the source of CP violation at the quark level, the deuteron EDM can be dominated by different LECs. For sources such as quark chromo-EDMs and four-quark operators  $\Xi$ , for which  $\bar{g}_1$  is induced without any chiral suppression, the pion-exchange contribution proportional to  $\bar{g}_1$  is expected to dominate the deuteron EDM. For sources such as quark EDMs or the Weinberg operator, however, the deuteron EDM is well approximated by the sum of the nucleon EDMs. For the  $\theta$ -term, the pion-exchange

|                                     |        |
|-------------------------------------|--------|
| $a_n(a_p)$                          | 0.939  |
| $a_1$ [fm]                          | 0.200  |
| $A_3$ [fm]                          | 0.013  |
| $A_4$ [fm]                          | -0.013 |
| $a_\Delta$ (NLO) [fm]               | -0.894 |
| $a_\Delta$ (N <sup>2</sup> LO) [fm] | +0.590 |
| $a_\Delta$ (TOT) [fm]               | -0.304 |

**Table 9.** Values of the coefficients entering the expression of the deuteron EDM calculated for the  $\chi$ EFT N<sup>2</sup>LO PVTV potential described in Sect. 3.5 and the N<sup>4</sup>LO PCTC potential derived in Ref. [18]. The PVTC potential has been regularized as in Eq. (86) adopting the value  $\Lambda_C = 500$  MeV for the cutoff parameter. The PCTC potential has been regularized with the same value of the cutoff parameter. For  $a_\Delta$  we give explicitly the contribution of the different orders, the sum of the two contributions is given in the last row.

|                                     | <sup>3</sup> H | <sup>3</sup> He |
|-------------------------------------|----------------|-----------------|
| $a_n$                               | -0.033         | 0.908           |
| $a_p$                               | 0.909          | -0.033          |
| $a_0$ [fm]                          | -0.053         | 0.054           |
| $a_1$ [fm]                          | 0.158          | 0.158           |
| $a_2$ [fm]                          | -0.119         | 0.119           |
| $A_1$ [fm]                          | 0.006          | -0.006          |
| $A_2$ [fm]                          | -0.010         | 0.010           |
| $A_3$ [fm]                          | -0.008         | -0.008          |
| $A_4$ [fm]                          | 0.013          | 0.013           |
| $A_5$ [fm]                          | -0.022         | 0.022           |
| $a_\Delta$ (NLO) [fm]               | -0.941         | -0.929          |
| $a_\Delta$ (N <sup>2</sup> LO) [fm] | +0.598         | +0.591          |
| $a_\Delta$ (TOT) [fm]               | -0.343         | -0.339          |

**Table 10.** The same as in Table 9 but for the <sup>3</sup>H and <sup>3</sup>He EDM.

contributions are expected to be minor as well. Given measurements of the deuteron and nucleon EDMs, one can, therefore, identify the underlying source of CP violation [223, 70].

As regarding the <sup>3</sup>H and <sup>3</sup>He EDMs, the results are summarized in Table 10. The coefficients  $a_0$  and  $a_1$  are again a bit smaller than the  $\mathcal{O}(1)$  expectation. Note that the value for  $a_0$  reported in Table 9 is approximately 50% smaller than that reported in Ref. [66]. This difference can be traced back to the contribution of the TPE, which was not included in that work. Performing the calculations at LO, namely including only the OPE term, the  $a_0$  coefficient results to agree with that reported in Ref. [66]. The values of the numerical coefficients are mostly equal in modulus between <sup>3</sup>H and <sup>3</sup>He except  $a_p$  and  $a_n$ . The coefficients associated to isovector terms have the same sign while all the others are opposite. Again the contribution of the N<sup>2</sup>LO potential term to  $a_\Delta$  is significant, about 60%. This issue is discussed below.

Let us now consider in more detail the issue of the NLO and N<sup>2</sup>LO contributions to  $a_\Delta$ . We have seen that in all cases the N<sup>2</sup>LO correction to  $a_\Delta$  is of the order of 60%, a bit larger than expected. Explicitly, the coefficient  $a_\Delta$  can be written as [75]

$$a_\Delta = a_\Delta(\text{NLO}) + a_\Delta(\text{N}^2\text{LO}), \quad (149)$$

$$a_\Delta(\text{NLO}) = a_\Delta(0) + a_\Delta(3N), \quad (150)$$

$$a_\Delta(\text{N}^2\text{LO}) = c_1 a_\Delta(1) + c_2 a_\Delta(2) + c_3 a_\Delta(3), \quad (151)$$

|                          | ${}^2\text{H}$ | ${}^3\text{H}$ | ${}^3\text{He}$ |
|--------------------------|----------------|----------------|-----------------|
| $a_{\Delta}(0)$ [fm]     | -0.894         | -0.751         | -0.749          |
| $a_{\Delta}(3N)$ [fm]    | -              | -0.190         | -0.180          |
| $a_{\Delta}(1)$ [fm GeV] | 0.120          | 0.098          | 0.098           |
| $a_{\Delta}(2)$ [fm GeV] | -0.119         | -0.110         | -0.109          |
| $a_{\Delta}(3)$ [fm GeV] | -0.207         | -0.198         | -0.196          |

**Table 11.** Values of the various components coefficients  $a_{\Delta}$  as given in Eq. (149) in units of  $e$  fm for the different nuclei. The coefficients have been evaluated using the  $\text{N}^4\text{LO}$  PC potential derived in Ref. [18] and using a cutoff parameter of value  $\Lambda_C = 500$  MeV.

where  $a_{\Delta}(0)$  comes from the NLO potential  $V_{PVTV}^{(0)}(3\pi)$  given in Eq. (93) and  $a_{\Delta}(3N)$  from the 3N potential given in Eq. (95). The  $\text{N}^2\text{LO}$  terms come from  $V_{PVTV}^{(1)}(3\pi)$ , where the LECs  $c_1$ ,  $c_2$  and  $c_3$  appear. To calculate the values reported in Tables 9 and 10, the following values were adopted:  $c_1 = -1.10$   $\text{GeV}^{-1}$ ,  $c_2 = +3.57$   $\text{GeV}^{-1}$ , and  $c_3 = -5.54$   $\text{GeV}^{-1}$  as reported in Refs. [217, 224]. The large  $\text{N}^2\text{LO}$  corrections are caused by the large values of these LECs.<sup>8</sup> For more detail, see Ref. [75]. For the trinucleon systems, the values of  $a_{\Delta}(3N)$  give a correction to  $a_{\Delta}(\text{NLO})$  of the order of  $\sim 25\%$ , which is in line with the chiral perturbation theory prediction because these contributions appear at the same order.

Similarly to the deuteron EDM, the trinucleon EDMs can be dominated by different terms. As the isoscalar interaction proportional to  $\bar{g}_0$  and  $\bar{C}_{1,2}$  now gives a sizable contribution, the trinucleon EDMs are noticeably different from the nucleon EDMs for the QCD  $\theta$ -term, the quark chromo-EDMs, the four-quark operators  $\Xi$ , and potentially the Weinberg operator and the four-quark operators  $\Sigma$ . These EDMs therefore provide complementary information to the deuteron and nucleon EDMs. Combined measurements of all these EDMs would allow one to unravel various BSM models of new CP violation [71].

## 7 CONCLUSIONS AND PERSPECTIVES

In this paper we have discussed the current status of the PVTC and PVTV nuclear interactions using the traditional approach based on phenomenological boson exchange models and utilizing the modern frameworks of pionless and chiral EFT. The study of PVTC signals in nuclei is interesting since it derives from the nonleptonic weak interactions between quarks. Furthermore, a solid understanding of the manifestation of PVTC interactions at the nuclear level would give us confidence in the analysis of the more exotic PVTV case and other BSM nuclear observables. In fact, PVTV observables provide very valuable information since they are sensitive to interactions originating from the  $\theta$ -term in the SM and even to more exotic mechanisms appearing in BSM theories.

As discussed in this review, the theoretical understanding of the PVTC and PVTV interactions is already rather advanced. Interactions in  $\chi\text{EFT}$  have been developed up to  $\text{N}^2\text{LO}$ . The convergence of the  $\chi\text{EFT}$  appears to be problematic only for the contributions proportional to the  $\pi\pi NN$  LECs  $c_i$ , due to the large values of those coefficients as it results from  $\pi N$  scattering data [217]. Given that the LECs  $c_{2,3,4}$  are largely driven by the  $\Delta(1232)$  [225], one may expect a better convergence in the formulation of chiral EFT that includes the  $\Delta$  as an explicit degree of freedom. Furthermore, large  $N_c$  analysis may help in reducing the number of contact LECs. Also Lattice QCD calculations start to give valuable information [132, 226].

<sup>8</sup> Notice that the values of the LECs  $c_i$  obtained from the pion-nucleon amplitude at NLO, which would be appropriate for  $V_{PVTV}^{(1)}$ , are considerably smaller in magnitude. We, however, decided to adopt the larger values to be consistent with the employed PCTC potential.

We have also reported the results of the theoretical calculations of several observables performed using the potentials derived within the  $\chi$ EFT framework. The PVTC observables considered include *i*) the longitudinal asymmetry in  $\vec{n}$ - $p$  radiative capture, *ii*) the longitudinal asymmetry in proton-proton elastic scattering, and *iii*) the spin rotation of a neutron beam passing through a hydrogen and deuterium gas. As an example of PVTV observable, we have studied the EDMs of some light nuclei. The main motivation to study these observables is that for such light systems, the theoretical analysis can be carried out without invoking any uncontrolled approximations. Thus, the comparison with the experimental data can be performed unambiguously. The analyses of PVTC and PVTV observables using meson exchange models can be found in other review articles [131, 34, 39] and are not reported here.

As discussed previously, there exists a first measurement of the parameter  $a_\gamma$  of the radiative neutron capture on the proton  $\vec{n}p \rightarrow d\gamma$ . The large error derives from the smallness of this parameter which makes this measurement very awkward [207]. This observable is directly connected to the LO pion-nucleon PVTC coupling constant  $a_\gamma \sim h_\pi^1$ . However, as we have seen, the theoretical estimate of the proportionality coefficient has been obtained with a relatively large theoretical uncertainty due to sizeable cancellations between different contributions. Therefore, to infer information from this observable, it will be necessary to make progress in both the experimental and theoretical analyses.

Other important information is brought forth by the three measurements at different energies of the  $\vec{p}$ - $p$  longitudinal asymmetry. This observable is sensitive to  $h_\pi^1$  via the TPE component of the PVTC potential and also to other LECs. In fact, owing to the isospin quantum numbers  $T = 1$ ,  $T_z = 1$  of the  $p$ - $p$  system, the LO contribution vanishes. Moreover, at NLO (N<sup>2</sup>LO), this observable depends on two (three) combinations of the LECs. Unfortunately, only two of the performed measurements give independent information. These two data have not been obtained with enough accuracy, so the constraints to the (combinations of) LECs which can be obtained are not so stringent [46, 42], as discussed in Subsect. 6.2. For this observable the wave functions are easily obtained, however the vanishing of the LO contribution makes the  $\chi$ PT convergence more uncertain. On the other hand, it would be very useful to have more accurate experimental measurements.

Regarding the spin rotation observables, no experiments to measure the  $\vec{n}$ - $p$  and  $\vec{n}$ - $d$  spin rotation angles, which could provide useful information on some of the contact term LECs, are planned at present. The experimental detection of a non-vanishing  $\vec{n}$ - $p$  spin rotation would be rather important for two reasons: *i*) the theoretical treatment of the two-nucleon system does not present any difficulty numerically, while *ii*) this observable is sensitive to the LO term and therefore the chiral expansion of the potential is well under control, as discussed in Subsect. 6.3. Regarding the  $\vec{n}$ - $d$  spin rotation, the same is not completely true since, as discussed in Sect. 3.4 one has to include also the PVTC 3N interaction terms which start to appear at N<sup>2</sup>LO. This is an interesting extension of  $\chi$ EFT which will be considered in future. From the experimental point of view, we note that there is an experiment in progress trying to measure the  $\vec{n}$ -<sup>4</sup>He spin rotation at NIST [227]. Some years ago there was a measure of the longitudinal asymmetry in  $\vec{p}$ -<sup>4</sup>He scattering, but this experiment has been performed at a rather high energy of the proton beam (46 MeV) [228] and this makes the theoretical treatment very difficult and impossible without some approximations.

Also a measurement of the  $\vec{n}$ -<sup>3</sup>He longitudinal asymmetry at the SNS facility is in progress, and the experimental value should be published soon. For this  $A = 4$  system it is possible to perform accurate calculations of the wave functions [42], and therefore this observable may give valuable information in the near future.

To have the possibility to pin down all the LECs (6 LECs at NLO and 5 more at N<sup>2</sup>LO) more experimental information will be necessary in any case. In particular, an interesting possibility would be to measure PVTC observables in the  $A = 3$  system, such as the longitudinal asymmetry of  $\vec{p}$ - $d$  elastic scattering and the photon asymmetry in  $\vec{n}$ - $d$  radiative capture. For both reactions, the theoretical treatment would be straightforward, once the PVTC 3N force has been taken into account.

Regarding the PVTV observables, the measurement of EDMs of particles is the most promising observable for studying CP violation beyond CKM mixing matrix effects. Currently, there are proposals for the direct measurement of EDMs of electrons, single nucleons and light nuclei in dedicated storage rings [77, 78, 81, 229, 82]. This new approach plans to reach an accuracy of  $\sim 10^{-16} e \text{ fm}$ , improving the sensitivity in particular in the hadronic sector. Any measurement of a non-vanishing EDM of this magnitude would provide evidence of PVTV beyond CKM effects [52, 55, 56, 57]. However, a single measurement will be insufficient to identify the source of PVTV, only the availability of the measurement of EDM of various light nuclei such as  $^2\text{H}$ ,  $^3\text{H}$ , and  $^3\text{He}$  can impose constraints on all the LECs. Other light nuclear EDMs have been discussed in Refs. [206, 230]. EDMs of heavy diamagnetic systems provide very important information as well, but the systems are too large for chiral EFT calculations.

Other observables sensitive to PVTV effects are the transmission of polarized neutrons through a polarized target [231, 232], in particular for heavy nuclei the PVTV effects can be enhanced by factors as large as  $10^6$  [233, 234], see also Ref. [235]. In order to exploit this enhancement, some experiments are being planned, such as the NOPTREX experiment at RIKEN [236, 237]. Also polarized nucleon – polarized deuteron scattering has been proposed as a way to detect PVTV signals [220, 238]. Finally, searching for a large PVTV violations in polarized  $\beta$ -decay of  $^8\text{Li}$  via measurements of the triple vector correlation is under consideration [239]. Clearly, it would be important to be able to detect a nonzero PVTV signal in all these experiments to be able to pin down the values of all the LECs.

From the theoretical point of view, calculations of the EDM of  $^2\text{H}$ ,  $^3\text{H}$  and  $^3\text{He}$  can be performed very accurately, also taking into account the contributions of the PVTV 3N force. The robustness of the calculation has been checked by evaluating the EDMs of the nuclei using different chiral orders in the PCTC potential. The discrepancy between the use of the N<sup>2</sup>LO and the N<sup>4</sup>LO PCTC potential has been found to be approximately 5% [75].

Currently, the only missing ingredient is the two-body PVTV N<sup>2</sup>LO currents [143, 73]. Once this problem will be solved, one will achieve a fully consistent calculation of the EDM of light nuclei up to N<sup>2</sup>LO. There are also plans to perform theoretical studies of PVTV observables in  $\vec{n}$ - $\vec{p}$  and  $\vec{n}$ - $\vec{d}$  scattering in order to have independent and complementary information of PVTV effects.

The PVTV  $\chi\text{EFT}$  interaction developed in the previous sections depends on 11 coupling constants that should be determined by comparing with experimental data. As already pointed out by many authors [65, 68, 69] and discussed in Subsect. 3.2.1, the LECs  $\bar{g}_2$ ,  $\bar{C}_3$ ,  $\bar{C}_4$  and  $\bar{C}_5$  are suppressed for all CP-violation sources. However, for certain sources, the suppression is not too severe. For example, in Ref. [66], an analysis of the nuclear EDM in the minimal left-right scenario is presented in which the Lagrangian terms with LECs  $\bar{C}_3$  and  $\bar{C}_4$  appear at N<sup>2</sup>LO. In any case, since the CP-violation sources are not known, the only way to determine them is to fit all possible LECs and then compare the results with predictions for various scenarios.

Most of the observables discussed so far were obtained (or they are planned to be studied) at low energies, where also the pionless EFT framework is valid. The advantage of this framework is related to the fact that the resulting potentials depends on five LECs. Then, assuming the validity of the large

$N_c$  analysis [47, 49], the number of dominant LECs could be further reduced. This new paradigm is advocated for the PVTC case in Ref. [39]. For this case, only two LECs are expected to be dominant, the other three demoted to be subleading. Unfortunately, the photon asymmetry of  $\vec{n}p \rightarrow d\gamma$  depends on the subleading LECs (this could explain its relative smallness) and therefore cannot be used to give information on the two leading LECs. Moreover, only one of the measured  $\vec{p}-p$  longitudinal asymmetry at low energy may be used to test if this hierarchy is realized in Nature (the other measurement is taken at too high energy to be used in the pionless EFT framework). The other observable which could give valuable information could be  $\vec{n}-^3\text{He}$  longitudinal asymmetry, for which experimental data should appear soon. However, no theoretical calculations of this observable performed in the framework of pionless EFT are available at present. Additional information could be obtained by calculations of these LECs using Lattice QCD, presently in progress. Regarding the PVTV observables in pionless EFT, here the large  $N_c$  analysis predicts that only one of the LECs should be dominant, while the other four being suppressed. However, this picture is partially obscured by the fact that the magnitude of the five contact LECs would depend very much on the particular type of the CP-violating source.

In conclusions, the study of PVTC and PVTV observables is an active area of research that provide important tests of the SM and hopefully future evidence for BSM physics.

## CONFLICT OF INTEREST STATEMENT

The Authors declare that the research was conducted in the absence of any commercial or financial relationships that could be construed as a potential conflict of interest.

## AUTHOR CONTRIBUTIONS

All Authors contributed to this article at about the same level.

## FUNDING

JdV was supported by the RHIC Physics Fellow Program of the RIKEN BNL Research Center.

EE was supported by BMBF (Grant No. 05P18PCFP1) and by DFG through funds provided to the Sino-German CRC 110 “Symmetries and the Emergence of Structure in QCD” (Grant No. TRR110).

EM was supported in part by the LDRD program at Los Alamos National Laboratory, the DOE topical collaboration on “Nuclear Theory for Double-Beta Decay and Fundamental Symmetries”, the US DOE, Office of Science, Office of Nuclear Physics, under award numbers DE-AC52-06NA25396.

LG, AG, and MV were supported by INFN through the National Initiative “FBS”.

## REFERENCES

- [1] Machleidt, R. (2017). Historical perspective and future prospects for nuclear interactions. *Int. J. Mod. Phys. E*26, 1730005. doi:10.1142/S0218301317300053
- [2] Weinberg, S. (1990). Nuclear forces from chiral Lagrangians. *Phys. Lett. B*251, 288–292. doi:10.1016/0370-2693(90)90938-3
- [3] Ordóñez, C., Ray, L., and van Kolck, U. (1996). The Two nucleon potential from chiral Lagrangians. *Phys. Rev. C*53, 2086–2105. doi:10.1103/PhysRevC.53.2086

- [4] Epelbaum, E., Hammer, H.-W., and Meißner, U.-G. (2009). Modern Theory of Nuclear Forces. *Rev. Mod. Phys.* 81, 1773–1825. doi:10.1103/RevModPhys.81.1773
- [5] Machleidt, R. and Entem, D. R. (2011). Chiral effective field theory and nuclear forces. *Phys. Rept.* 503, 1–75. doi:10.1016/j.physrep.2011.02.001
- [6] Weinberg, S. (1966). Pion scattering lengths. *Phys. Rev. Lett.* 17, 616–621. doi:10.1103/PhysRevLett.17.616
- [7] Weinberg, S. (1968). Nonlinear realizations of chiral symmetry. *Phys. Rev.* 166, 1568–1577. doi:10.1103/PhysRev.166.1568
- [8] Weinberg, S. (1979). Phenomenological Lagrangians. *Physica A96*, 327–340. doi:10.1016/0378-4371(79)90223-1
- [9] Coleman, S. R., Wess, J., and Zumino, B. (1969). Structure of phenomenological Lagrangians. 1. *Phys. Rev.* 177, 2239–2247. doi:10.1103/PhysRev.177.2239
- [10] Callan, C. G., Jr., Coleman, S. R., Wess, J., and Zumino, B. (1969). Structure of phenomenological Lagrangians. 2. *Phys. Rev.* 177, 2247–2250. doi:10.1103/PhysRev.177.2247
- [11] Gasser, J. and Leutwyler, H. (1984). Chiral Perturbation Theory to One Loop. *Annals Phys.* 158, 142. doi:10.1016/0003-4916(84)90242-2
- [12] Bernard, V., Kaiser, N., and Meißner, U.-G. (1995). Chiral dynamics in nucleons and nuclei. *Int. J. Mod. Phys. E4*, 193–346. doi:10.1142/S0218301395000092
- [13] Bernard, V. (2008). Chiral Perturbation Theory and Baryon Properties. *Prog. Part. Nucl. Phys.* 60, 82–160. doi:10.1016/j.pnpnp.2007.07.001
- [14] Bijmans, J. and Ecker, G. (2014). Mesonic low-energy constants. *Ann. Rev. Nucl. Part. Sci.* 64, 149–174. doi:10.1146/annurev-nucl-102313-025528
- [15] Epelbaum, E., Gegelia, J., and Meißner, U.-G. (2017). Wilsonian renormalization group versus subtractive renormalization in effective field theories for nucleon–nucleon scattering. *Nucl. Phys. B925*, 161–185. doi:10.1016/j.nuclphysb.2017.10.008
- [16] Entem, D. R., Kaiser, N., Machleidt, R., and Nosyk, Y. (2015). Peripheral nucleon-nucleon scattering at fifth order of chiral perturbation theory. *Phys. Rev. C91*, 014002. doi:10.1103/PhysRevC.91.014002
- [17] Epelbaum, E., Krebs, H., and Meißner, U.-G. (2015). Precision nucleon-nucleon potential at fifth order in the chiral expansion. *Phys. Rev. Lett.* 115, 122301. doi:10.1103/PhysRevLett.115.122301
- [18] Entem, D. R., Machleidt, R., and Nosyk, Y. (2017). High-quality two-nucleon potentials up to fifth order of the chiral expansion. *Phys. Rev. C96*, 024004. doi:10.1103/PhysRevC.96.024004
- [19] Reinert, P., Krebs, H., and Epelbaum, E. (2018). Semilocal momentum-space regularized chiral two-nucleon potentials up to fifth order. *Eur. Phys. J. A54*, 86. doi:10.1140/epja/i2018-12516-4
- [20] Kaplan, D. B., Savage, M. J., and Wise, M. B. (1998). A New expansion for nucleon-nucleon interactions. *Phys. Lett. B424*, 390–396. doi:10.1016/S0370-2693(98)00210-X
- [21] Nogga, A., Timmermans, R. G. E., and van Kolck, U. (2005). Renormalization of one-pion exchange and power counting. *Phys. Rev. C72*, 054006. doi:10.1103/PhysRevC.72.054006
- [22] Birse, M. C. (2006). Power counting with one-pion exchange. *Phys. Rev. C74*, 014003. doi:10.1103/PhysRevC.74.014003
- [23] Valderrama, M. P. (2011). Perturbative renormalizability of chiral two pion exchange in nucleon-nucleon scattering. *Phys. Rev. C83*, 024003. doi:10.1103/PhysRevC.83.024003
- [24] Long, B. and Yang, C. J. (2012). Short-range nuclear forces in singlet channels. *Phys. Rev. C86*, 024001. doi:10.1103/PhysRevC.86.024001



- [25] Epelbaum, E. and Gegelia, J. (2012). Weinberg's approach to nucleon–nucleon scattering revisited. *Phys. Lett.* B716, 338–344. doi:10.1016/j.physletb.2012.08.025
- [26] Lepage, G. P. (1997). How to renormalize the Schrodinger equation. In *Nuclear physics. Proceedings, 8th Jorge Andre Swieca Summer School, Sao Jose dos Campos, Campos do Jordao, Brazil, January 26-February 7, 1997*. 135–180
- [27] Epelbaum, E. and Meißner, U.-G. (2013). On the Renormalization of the One-Pion Exchange Potential and the Consistency of Weinberg's Power Counting. *Few Body Syst.* 54, 2175–2190. doi:10.1007/s00601-012-0492-1
- [28] Epelbaum, E. and Gegelia, J. (2009). Regularization, renormalization and 'peratization' in effective field theory for two nucleons. *Eur. Phys. J.* A41, 341–354. doi:10.1140/epja/i2009-10833-3
- [29] Valderrama, M. P. (2016). Power Counting and Wilsonian Renormalization in Nuclear Effective Field Theory. *Int. J. Mod. Phys.* E25, 1641007. doi:10.1142/S021830131641007X
- [30] Epelbaum, E., Gasparyan, A. M., Gegelia, J., and Meißner, U.-G. (2018). How (not) to renormalize integral equations with singular potentials in effective field theory. *Eur. Phys. J.* A54, 186. doi:10.1140/epja/i2018-12632-1
- [31] Hammer, H. W., König, S., and van Kolck, U. (2019). Nuclear effective field theory: status and perspectives, ArXiv:1906.12122
- [32] Bedaque, P. F. and van Kolck, U. (2002). Effective field theory for few nucleon systems. *Ann. Rev. Nucl. Part. Sci.* 52, 339–396. doi:10.1146/annurev.nucl.52.050102.090637
- [33] Hammer, H.-W. and Platter, L. (2010). Efimov States in Nuclear and Particle Physics. *Ann. Rev. Nucl. Part. Sci.* 60, 207–236. doi:10.1146/annurev.nucl.012809.104439
- [34] Ramsey-Musolf, M. J. and Page, S. A. (2006). Hadronic parity violation: A New view through the looking glass. *Ann. Rev. Nucl. Part. Sci.* 56, 1–52. doi:10.1146/annurev.nucl.54.070103.181255
- [35] Hertzog, D. and Ramsey-Musolf, M. J. (2013). Parity- and Time-Reversal Tests in Nuclear Physics. In *100 Years of Subatomic Physics*, eds. E. M. Henley and S. D. Ellis. 155–170. doi:10.1142/9789814425810\_0006
- [36] Schindler, M. R. and Springer, R. P. (2013). The Theory of Parity Violation in Few-Nucleon Systems. *Prog. Part. Nucl. Phys.* 72, 1–43. doi:10.1016/j.pnpnp.2013.05.002
- [37] Haxton, W. C. and Holstein, B. R. (2013). Hadronic Parity Violation. *Prog. Part. Nucl. Phys.* 71, 185–203. doi:10.1016/j.pnpnp.2013.03.009
- [38] de Vries, J. and Meißner, U.-G. (2016). Violations of discrete space–time symmetries in chiral effective field theory. *Int. J. Mod. Phys.* E25, 1641008. doi:10.1142/S0218301316410081
- [39] Gardner, S., Haxton, W. C., and Holstein, B. R. (2017). A New Paradigm for Hadronic Parity Nonconservation and its Experimental Implications. *Ann. Rev. Nucl. Part. Sci.* 67, 69–95. doi:10.1146/annurev-nucl-041917-033231
- [40] Zhu, S.-L., Maekawa, C. M., Holstein, B. R., Ramsey-Musolf, M. J., and van Kolck, U. (2005). Nuclear parity-violation in effective field theory. *Nucl. Phys.* A748, 435–498. doi:10.1016/j.nuclphysa.2004.10.032
- [41] de Vries, J., Meißner, U.-G., Epelbaum, E., and Kaiser, N. (2013). Parity violation in proton-proton scattering from chiral effective field theory. *Eur. Phys. J.* A49, 149. doi:10.1140/epja/i2013-13149-9
- [42] Viviani, M., Baroni, A., Girlanda, L., Kievsky, A., Marcucci, L. E., and Schiavilla, R. (2014). Chiral effective field theory analysis of hadronic parity violation in few-nucleon systems. *Phys. Rev.* C89, 064004. doi:10.1103/PhysRevC.89.064004

- [43] Adelberger, E. G. and Haxton, W. C. (1985). Parity Violation in the Nucleon-Nucleon Interaction. *Ann. Rev. Nucl. Part. Sci.* 35, 501–558. doi:10.1146/annurev.ns.35.120185.002441
- [44] Girlanda, L. (2008). On a redundancy in the parity-violating 2-nucleon contact Lagrangian. *Phys. Rev. C* 77, 067001. doi:10.1103/PhysRevC.77.067001
- [45] Danilov, G. S. (1965). . *Phys. Lett.* 18, 40
- [46] de Vries, J., Li, N., Meißner, U.-G., Kaiser, N., Liu, X. H., and Zhu, S. L. (2014). A study of the parity-odd nucleon-nucleon potential. *Eur. Phys. J. A* 50, 108. doi:10.1140/epja/i2014-14108-8
- [47] Schindler, M. R., Springer, R. P., and Vanasse, J. (2016). Large- $N_c$  limit reduces the number of independent few-body parity-violating low-energy constants in pionless effective field theory. *Phys. Rev. C* 93, 025502. doi:10.1103/PhysRevC.97.059901,10.1103/PhysRevC.93.025502. [Erratum: *Phys. Rev. C* 97, no. 5, 059901 (2018)]
- [48] Phillips, D. R., Samart, D., and Schat, C. (2015). Parity-Violating Nucleon-Nucleon Force in the  $1/N_c$  Expansion. *Phys. Rev. Lett.* 114, 062301. doi:10.1103/PhysRevLett.114.062301
- [49] Vanasse, J. (2019). Parity-violating three-nucleon interactions at low energies and large  $N_C$ . *Phys. Rev. C* 99, 054001. doi:10.1103/PhysRevC.99.054001
- [50] Desplanques, B., Donoghue, J. F., and Holstein, B. R. (1980). Unified Treatment of the Parity Violating Nuclear Force. *Annals Phys.* 124, 449. doi:10.1016/0003-4916(80)90217-1
- [51] 't Hooft, G. (1976). Symmetry Breaking Through Bell-Jackiw Anomalies. *Phys. Rev. Lett.* 37, 8–11. doi:10.1103/PhysRevLett.37.8. [226(1976)]
- [52] Pospelov, M. and Ritz, A. (2005). Electric dipole moments as probes of new physics. *Annals Phys.* 318, 119–169. doi:10.1016/j.aop.2005.04.002
- [53] Sakharov, A. D. (1967). Violation of CP Invariance, C asymmetry, and baryon asymmetry of the universe. *Pisma Zh. Eksp. Teor. Fiz.* 5, 32–35. doi:10.1070/PU1991v034n05ABEH002497. [Usp. Fiz. Nauk 161, no. 5, 61 (1991)]
- [54] Cohen, A. G., Kaplan, D. B., and Nelson, A. E. (1993). Progress in electroweak baryogenesis. *Ann. Rev. Nucl. Part. Sci.* 43, 27–70. doi:10.1146/annurev.ns.43.120193.000331
- [55] Czarnecki, A. and Krause, B. (1997). Neutron electric dipole moment in the standard model: Valence quark contributions. *Phys. Rev. Lett.* 78, 4339–4342. doi:10.1103/PhysRevLett.78.4339
- [56] Mannel, T. and Uraltsev, N. (2012). Loop-Less Electric Dipole Moment of the Nucleon in the Standard Model. *Phys. Rev. D* 85, 096002. doi:10.1103/PhysRevD.85.096002
- [57] Mannel, T. and Uraltsev, N. (2013). Charm CP Violation and the Electric Dipole Moments from the Charm Scale. *JHEP* 03, 064. doi:10.1007/JHEP03(2013)064
- [58] Wirzba, A., Bsaisou, J., and Nogga, A. (2017). Permanent Electric Dipole Moments of Single-, Two-, and Three-Nucleon Systems. *Int. J. Mod. Phys. E* 26, 1740031. doi:10.1142/S0218301317400316
- [59] Seng, C.-Y. (2015). Reexamination of The Standard Model Nucleon Electric Dipole Moment. *Phys. Rev. C* 91, 025502. doi:10.1103/PhysRevC.91.025502
- [60] Baker, C. A. et al. (2006). An Improved experimental limit on the electric dipole moment of the neutron. *Phys. Rev. Lett.* 97, 131801. doi:10.1103/PhysRevLett.97.131801
- [61] Pendlebury, J. M. et al. (2015). Revised experimental upper limit on the electric dipole moment of the neutron. *Phys. Rev. D* 92, 092003. doi:10.1103/PhysRevD.92.092003
- [62] Graner, B., Chen, Y., Lindahl, E. G., and Heckel, B. R. (2016). Reduced Limit on the Permanent Electric Dipole Moment of Hg199. *Phys. Rev. Lett.* 116, 161601. doi:10.1103/PhysRevLett.119.119901,10.1103/PhysRevLett.116.161601. [Erratum: *Phys. Rev. Lett.* 119, no. 11, 119901 (2017)]
- [63] Dmitriev, V. F. and Sen'kov, R. A. (2003). Schiff moment of the mercury nucleus and the proton dipole moment. *Phys. Rev. Lett.* 91, 212303. doi:10.1103/PhysRevLett.91.212303

- [64] Andreev, V. et al. (2018). Improved limit on the electric dipole moment of the electron. *Nature* 562, 355–360. doi:10.1038/s41586-018-0599-8
- [65] Mereghetti, E., Hockings, W. H., and van Kolck, U. (2010). The Effective Chiral Lagrangian From the Theta Term. *Annals Phys.* 325, 2363–2409. doi:10.1016/j.aop.2010.03.005
- [66] Bsaisou, J., de Vries, J., Hanhart, C., Liebig, S., Meißner, U.-G., Minossi, D., et al. (2015). Nuclear Electric Dipole Moments in Chiral Effective Field Theory. *JHEP* 03, 104. doi:10.1007/JHEP03(2015)104,10.1007/JHEP05(2015)083. [Erratum: JHEP05,083(2015)]
- [67] Grzadkowski, B., Iskrzynski, M., Misiak, M., and Rosiek, J. (2010). Dimension-Six Terms in the Standard Model Lagrangian. *JHEP* 10, 085. doi:10.1007/JHEP10(2010)085
- [68] de Vries, J., Mereghetti, E., Timmermans, R. G. E., and van Kolck, U. (2013). The Effective Chiral Lagrangian From Dimension-Six Parity and Time-Reversal Violation. *Annals Phys.* 338, 50–96. doi:10.1016/j.aop.2013.05.022
- [69] Bsaisou, J., Meißner, U.-G., Nogga, A., and Wirzba, A. (2015). P- and T-Violating Lagrangians in Chiral Effective Field Theory and Nuclear Electric Dipole Moments. *Annals Phys.* 359, 317–370. doi:10.1016/j.aop.2015.04.031
- [70] de Vries, J., Mereghetti, E., Timmermans, R. G. E., and van Kolck, U. (2011). Parity- and Time-Reversal-Violating Form Factors of the Deuteron. *Phys. Rev. Lett.* 107, 091804. doi:10.1103/PhysRevLett.107.091804
- [71] Dekens, W., de Vries, J., Bsaisou, J., Bernreuther, W., Hanhart, C., Meißner, U.-G., et al. (2014). Unraveling models of CP violation through electric dipole moments of light nuclei. *JHEP* 07, 069. doi:10.1007/JHEP07(2014)069
- [72] Maekawa, C. M., Mereghetti, E., de Vries, J., and van Kolck, U. (2011). The Time-Reversal- and Parity-Violating Nuclear Potential in Chiral Effective Theory. *Nucl. Phys.* A872, 117–160. doi:10.1016/j.nuclphysa.2011.09.020
- [73] Bsaisou, J., Hanhart, C., Liebig, S., Meißner, U.-G., Nogga, A., and Wirzba, A. (2013). The electric dipole moment of the deuteron from the QCD  $\theta$ -term. *Eur. Phys. J.* A49, 31. doi:10.1140/epja/i2013-13031-x
- [74] Epelbaum, E., Glockle, W., and Meißner, U.-G. (2005). The Two-nucleon system at next-to-next-to-next-to-leading order. *Nucl. Phys.* A747, 362–424. doi:10.1016/j.nuclphysa.2004.09.107
- [75] Gnech, A. and Viviani, M. (2019). Time Reversal Violation in Light Nuclei, arXiv:1906.09021
- [76] Dobaczewski, J., Engel, J., Kortelainen, M., and Becker, P. (2018). Correlating Schiff moments in the light actinides with octupole moments. *Phys. Rev. Lett.* 121, 232501. doi:10.1103/PhysRevLett.121.232501
- [77] Orlov, Y. F., Morse, W. M., and Semertzidis, Y. K. (2006). Resonance method of electric-dipole-moment measurements in storage rings. *Phys. Rev. Lett.* 96, 214802. doi:10.1103/PhysRevLett.96.214802
- [78] Semertzidis, Y. K. (2011). A Storage Ring proton Electric Dipole Moment experiment: most sensitive experiment to CP-violation beyond the Standard Model. In *Particles and fields. Proceedings, Meeting of the Division of the American Physical Society, DPF 2011, Providence, USA, August 9-13, 2011*
- [79] Lehrach, A., Lorentz, B., Morse, W., Nikolaev, N., and Rathmann, F. (2012). Precursor Experiments to Search for Permanent Electric Dipole Moments (EDMs) of Protons and Deuterons at COSY, arXiv:1201.5773
- [80] Pretz, J. (2013). Measurement of Permanent Electric Dipole Moments of Charged Hadrons in Storage Rings. *Hyperfine Interact.* 214, 111–117. doi:10.1007/s10751-013-0799-4

- [81] Rathmann, F., Saleev, A., and Nikolaev, N. N. (2013). The search for electric dipole moments of light ions in storage rings. *J. Phys. Conf. Ser.* 447, 012011. doi:10.1088/1742-6596/447/1/012011
- [82] Abusaif, F. et al. (2019). Storage Ring to Search for Electric Dipole Moments of Charged Particles – Feasibility Study, arXiv:1912.07881
- [83] Wu, C. S., Ambler, E., Hayward, R. W., Hoppes, D. D., and Hudson, R. P. (1957). Experimental Test of Parity Conservation in Beta Decay. *Phys. Rev.* 105, 1413–1414. doi:10.1103/PhysRev.105.1413
- [84] Prescott, C. Y. et al. (1978). Parity Nonconservation in Inelastic Electron Scattering. *Phys. Lett.* B77, 347–352. doi:10.1016/0370-2693(78)90722-0. [,6.31(1978)]
- [85] Androić, D. et al. (2018). Precision measurement of the weak charge of the proton. *Nature* 557, 207–211. doi:10.1038/s41586-018-0096-0
- [86] Tiburzi, B. C. (2012). Hadronic Parity Violation at Next-to-Leading Order. *Phys. Rev.* D85, 054020. doi:10.1103/PhysRevD.85.054020
- [87] Buchmuller, W. and Wyler, D. (1986). Effective Lagrangian Analysis of New Interactions and Flavor Conservation. *Nucl. Phys.* B268, 621–653. doi:10.1016/0550-3213(86)90262-2
- [88] Kaplan, D. B. and Savage, M. J. (1993). An Analysis of parity violating pion - nucleon couplings. *Nucl. Phys.* A556, 653–671. doi:10.1016/0375-9474(93)90475-D,10.1016/0375-9474(94)90787-0,10.1016/0375-9474(94)90086-8. [Erratum: Nucl. Phys.A580,679(1994)]
- [89] Christenson, J. H., Cronin, J. W., Fitch, V. L., and Turlay, R. (1964). Evidence for the  $2\pi$  Decay of the  $K_2^0$  Meson. *Phys. Rev. Lett.* 13, 138–140. doi:10.1103/PhysRevLett.13.138
- [90] Abouzaid, E. et al. (2011). Precise Measurements of Direct CP Violation, CPT Symmetry, and Other Parameters in the Neutral Kaon System. *Phys. Rev.* D83, 092001. doi:10.1103/PhysRevD.83.092001
- [91] Batley, J. R. et al. (2002). A Precision measurement of direct CP violation in the decay of neutral kaons into two pions. *Phys. Lett.* B544, 97–112. doi:10.1016/S0370-2693(02)02476-0
- [92] Aubert, B. et al. (2001). Observation of CP violation in the  $B^0$  meson system. *Phys. Rev. Lett.* 87, 091801. doi:10.1103/PhysRevLett.87.091801
- [93] Abe, K. et al. (2001). Observation of large CP violation in the neutral  $B$  meson system. *Phys. Rev. Lett.* 87, 091802. doi:10.1103/PhysRevLett.87.091802
- [94] Aaij, R. et al. (2019). Observation of  $CP$  violation in charm decays. *Phys. Rev. Lett.* 122, 211803. doi:10.1103/PhysRevLett.122.211803
- [95] Khriplovich, I. B. and Zhitnitsky, A. R. (1982). What Is the Value of the Neutron Electric Dipole Moment in the Kobayashi-Maskawa Model? *Phys. Lett.* 109B, 490–492. doi:10.1016/0370-2693(82)91121-2
- [96] Pospelov, M. E. and Khriplovich, I. B. (1991). Electric dipole moment of the W boson and the electron in the Kobayashi-Maskawa model. *Sov. J. Nucl. Phys.* 53, 638–640. [Yad. Fiz.53,1030(1991)]
- [97] Booth, M. J. (1993). The Electric dipole moment of the W and electron in the Standard Model, arXiv:hep-ph/9301293
- [98] Pospelov, M. and Ritz, A. (2014). CKM benchmarks for electron electric dipole moment experiments. *Phys. Rev.* D89, 056006. doi:10.1103/PhysRevD.89.056006
- [99] Callan, C. G., Jr., Dashen, R. F., and Gross, D. J. (1976). The Structure of the Gauge Theory Vacuum. *Phys. Lett.* B63, 334–340. doi:10.1016/0370-2693(76)90277-X. [,357(1976)]
- [100] 't Hooft, G. (1976). Computation of the Quantum Effects Due to a Four-Dimensional Pseudoparticle. *Phys. Rev.* D14, 3432–3450. doi:10.1103/PhysRevD.14.3432. [,70(1976)]

- [101] Baluni, V. (1979). CP Violating Effects in QCD. *Phys. Rev. D*19, 2227–2230. doi:10.1103/PhysRevD.19.2227
- [102] Crewther, R. J., Di Vecchia, P., Veneziano, G., and Witten, E. (1979). Chiral Estimate of the Electric Dipole Moment of the Neutron in Quantum Chromodynamics. *Phys. Lett.* 88B, 123. doi:10.1016/0370-2693(80)91025-4,10.1016/0370-2693(79)90128-X. [Erratum: *Phys. Lett.*91B,487(1980)]
- [103] Dragos, J., Luu, T., Shindler, A., de Vries, J., and Yousif, A. (2019). Confirming the Existence of the strong CP Problem in Lattice QCD with the Gradient Flow, arXiv:1902.03254
- [104] Gavela, M. B., Hernandez, P., Orloff, J., and Pene, O. (1994). Standard model CP violation and baryon asymmetry. *Mod. Phys. Lett.* A9, 795–810. doi:10.1142/S0217732394000629
- [105] Gavela, M. B., Lozano, M., Orloff, J., and Pene, O. (1994). Standard model CP violation and baryon asymmetry. Part 1: Zero temperature. *Nucl. Phys.* B430, 345–381. doi:10.1016/0550-3213(94)00409-9
- [106] Gavela, M. B., Hernandez, P., Orloff, J., Pene, O., and Quimbay, C. (1994). Standard model CP violation and baryon asymmetry. Part 2: Finite temperature. *Nucl. Phys.* B430, 382–426. doi:10.1016/0550-3213(94)00410-2
- [107] Huet, P. and Sather, E. (1995). Electroweak baryogenesis and standard model CP violation. *Phys. Rev. D*51, 379–394. doi:10.1103/PhysRevD.51.379
- [108] Khriplovich, I. B. and Lamoreaux, S. K. (1997). *CP violation without strangeness: Electric dipole moments of particles, atoms, and molecules [Berlin, Germany: Springer (1997)]*
- [109] Dekens, W. and de Vries, J. (2013). Renormalization Group Running of Dimension-Six Sources of Parity and Time-Reversal Violation. *JHEP* 05, 149. doi:10.1007/JHEP05(2013)149
- [110] Engel, J., Ramsey-Musolf, M. J., and van Kolck, U. (2013). Electric Dipole Moments of Nucleons, Nuclei, and Atoms: The Standard Model and Beyond. *Prog. Part. Nucl. Phys.* 71, 21–74. doi:10.1016/j.pnnp.2013.03.003
- [111] Jenkins, E. E., Manohar, A. V., and Stoffer, P. (2018). Low-Energy Effective Field Theory below the Electroweak Scale: Operators and Matching. *JHEP* 03, 016. doi:10.1007/JHEP03(2018)016
- [112] Mereghetti, E. (2018). Electric dipole moments: a theory overview. In *13th Conference on the Intersections of Particle and Nuclear Physics (CIPANP 2018) Palm Springs, California, USA, May 29-June 3, 2018*
- [113] Weinberg, S. (1989). Larger Higgs Exchange Terms in the Neutron Electric Dipole Moment. *Phys. Rev. Lett.* 63, 2333. doi:10.1103/PhysRevLett.63.2333
- [114] Fuyuto, K., Ramsey-Musolf, M., and Shen, T. (2019). Electric Dipole Moments from CP-Violating Scalar Leptoquark Interactions. *Phys. Lett.* B788, 52–57. doi:10.1016/j.physletb.2018.11.016
- [115] Dekens, W., de Vries, J., Jung, M., and Vos, K. K. (2019). The phenomenology of electric dipole moments in models of scalar leptoquarks. *JHEP* 01, 069. doi:10.1007/JHEP01(2019)069
- [116] Ng, J. and Tulin, S. (2012). D versus d: CP Violation in Beta Decay and Electric Dipole Moments. *Phys. Rev. D*85, 033001. doi:10.1103/PhysRevD.85.033001
- [117] Jenkins, E. E. and Manohar, A. V. (1991). Baryon chiral perturbation theory using a heavy fermion Lagrangian. *Phys. Lett.* B255, 558–562. doi:10.1016/0370-2693(91)90266-S
- [118] Baroni, A., Girlanda, L., Pastore, S., Schiavilla, R., and Viviani, M. (2016). Nuclear Axial Currents in Chiral Effective Field Theory. *Phys. Rev.* C93, 015501. doi:10.1103/PhysRevC.93.049902,10.1103/PhysRevC.93.015501,10.1103/PhysRevC.95.059901. [Erratum: *Phys. Rev.*C95,no.5,059901(2017)]

- [119] Kaplan, D. B., Savage, M. J., Springer, R. P., and Wise, M. B. (1999). An Effective field theory calculation of the parity violating asymmetry in  $\vec{n} + p \rightarrow d + \gamma$ . *Phys. Lett.* B449, 1–5. doi:10.1016/S0370-2693(99)00032-5
- [120] Manohar, A. and Georgi, H. (1984). Chiral Quarks and the Nonrelativistic Quark Model. *Nucl. Phys.* B234, 189–212. doi:10.1016/0550-3213(84)90231-1
- [121] Michel, F. C. (1964). Parity Nonconservation in Nuclei. *Phys. Rev.* 133, B329–B349. doi:10.1103/PhysRev.133.B329
- [122] Donoghue, J. F., Golowich, E., and Holstein, B. R. (1992). Dynamics of the standard model. *Camb. Monogr. Part. Phys. Nucl. Phys. Cosmol.* 2, 1–540. doi:10.1017/CBO9780511524370. [Camb. Monogr. Part. Phys. Nucl. Phys. Cosmol.35(2014)]
- [123] McKellar, B. H. J. (1967). The one pion exchange contribution to the weak parity violating nucleon-nucleon potential. *Phys. Lett.* 26B, 107–108. doi:10.1016/0370-2693(67)90561-8
- [124] Fischbach, E. (1968). Application of Current Algebra and Partially Conserved Axial-Vector Current to the Weak BB $\pi$  Vertex. *Phys. Rev.* 170, 1398–1400. doi:10.1103/PhysRev.170.1398
- [125] Tadic, D. (1968). Weak parity-nonconserving potentials. *Phys. Rev.* 174, 1694–1703. doi:10.1103/PhysRev.174.1694
- [126] Kummer, W. and Schweda, M. (1968). An SU(6) estimate of the effective nonleptonic parity-violating coupling in strangeness-conserving weak processes. *Acta Phys. Austriaca* 28, 303–308
- [127] McKellar, B. H. J. and Pick, P. (1972). Pion-pole dominance of the divergence of the weak parity-nonconserving  $n n \rho$  amplitude. *Phys. Rev.* D6, 2184–2188. doi:10.1103/PhysRevD.6.2184
- [128] Dubovik, V. M. and Zenkin, S. V. (1986). Formation of Parity Nonconserving Nuclear Forces in the Standard Model SU(2)(l) X U(1) X SU(3)(c). *Annals Phys.* 172, 100–135. doi:10.1016/0003-4916(86)90021-7
- [129] Feldman, G. B., Crawford, G. A., Dubach, J., and Holstein, B. R. (1991). Delta contributions to the parity violating nuclear interaction. *Phys. Rev.* C43, 863–874. doi:10.1103/PhysRevC.43.863
- [130] Meißner, U. G. and Weigel, H. (1999). The Parity violating pion nucleon coupling constant from a realistic three flavor Skyrme model. *Phys. Lett.* B447, 1–7. doi:10.1016/S0370-2693(98)01569-X
- [131] Haeberli, W. and Holstein, B. R. (1995). Parity violation and the nucleon-nucleon system, arXiv:nucl-th/9510062 doi:10.1142/9789812831446\_0002
- [132] Wasem, J. (2012). Lattice QCD Calculation of Nuclear Parity Violation. *Phys. Rev.* C85, 022501. doi:10.1103/PhysRevC.85.022501
- [133] Cheng, H.-Y. (1991). Reanalysis of strong CP violating effects in chiral perturbation theory. *Phys. Rev.* D44, 166–174. doi:10.1103/PhysRevD.44.166
- [134] Pich, A. and de Rafael, E. (1991). Strong CP violation in an effective chiral Lagrangian approach. *Nucl. Phys.* B367, 313–333. doi:10.1016/0550-3213(91)90019-T
- [135] Cho, P. L. (1993). Chiral estimates of strong CP violation revisited. *Phys. Rev.* D48, 3304–3309. doi:10.1103/PhysRevD.48.3304
- [136] Borasoy, B. (2000). The Electric dipole moment of the neutron in chiral perturbation theory. *Phys. Rev.* D61, 114017. doi:10.1103/PhysRevD.61.114017
- [137] Ottnad, K., Kubis, B., Meißner, U.-G., and Guo, F. K. (2010). New insights into the neutron electric dipole moment. *Phys. Lett.* B687, 42–47. doi:10.1016/j.physletb.2010.03.005
- [138] Liu, C. P., de Vries, J., Mereghetti, E., Timmermans, R. G. E., and van Kolck, U. (2012). Deuteron Magnetic Quadrupole Moment From Chiral Effective Field Theory. *Phys. Lett.* B713, 447–452. doi:10.1016/j.physletb.2012.06.024

- [139] Peccei, R. D. and Quinn, H. R. (1977). CP Conservation in the Presence of Instantons. *Phys. Rev. Lett.* 38, 1440–1443. doi:10.1103/PhysRevLett.38.1440. [328(1977)]
- [140] Mereghetti, E. and van Kolck, U. (2015). Effective Field Theory and Time-Reversal Violation in Light Nuclei. *Ann. Rev. Nucl. Part. Sci.* 65, 215–243. doi:10.1146/annurev-nucl-102014-022344
- [141] Cirigliano, V., Dekens, W., de Vries, J., and Mereghetti, E. (2017). An  $\epsilon'$  improvement from right-handed currents. *Phys. Lett.* B767, 1–9. doi:10.1016/j.physletb.2017.01.037
- [142] Liu, C. P. and Timmermans, R. G. E. (2004). P- and T-odd two-nucleon interaction and the deuteron electric dipole moment. *Phys. Rev.* C70, 055501. doi:10.1103/PhysRevC.70.055501
- [143] de Vries, J., Higa, R., Liu, C. P., Mereghetti, E., Stetcu, I., Timmermans, R. G. E., et al. (2011). Electric Dipole Moments of Light Nuclei From Chiral Effective Field Theory. *Phys. Rev.* C84, 065501. doi:10.1103/PhysRevC.84.065501
- [144] de Vries, J., Mereghetti, E., and Walker-Loud, A. (2015). Baryon mass splittings and strong CP violation in SU(3) Chiral Perturbation Theory. *Phys. Rev.* C92, 045201. doi:10.1103/PhysRevC.92.045201
- [145] Borsanyi, S. et al. (2015). Ab initio calculation of the neutron-proton mass difference. *Science* 347, 1452–1455. doi:10.1126/science.1257050
- [146] Brantley, D. A., Joo, B., Mastropas, E. V., Mereghetti, E., Monge-Camacho, H., Tiburzi, B. C., et al. (2016). Strong isospin violation and chiral logarithms in the baryon spectrum
- [147] de Vries, J., Mereghetti, E., Seng, C.-Y., and Walker-Loud, A. (2017). Lattice QCD spectroscopy for hadronic CP violation. *Phys. Lett.* B766, 254–262. doi:10.1016/j.physletb.2017.01.017
- [148] Seng, C.-Y. and Ramsey-Musolf, M. (2017). Parity-violating and time-reversal-violating pion-nucleon couplings: Higher order chiral matching relations. *Phys. Rev.* C96, 065204. doi:10.1103/PhysRevC.96.065204
- [149] Pospelov, M. and Ritz, A. (2001). Neutron EDM from electric and chromoelectric dipole moments of quarks. *Phys. Rev.* D63, 073015. doi:10.1103/PhysRevD.63.073015
- [150] Samart, D., Schat, C., Schindler, M. R., and Phillips, D. R. (2016). Time-reversal-invariance-violating nucleon-nucleon potential in the  $1/N_c$  expansion. *Phys. Rev.* C94, 024001. doi:10.1103/PhysRevC.94.024001
- [151] Guo, F. K., Horsley, R., Meißner, U.-G., Nakamura, Y., Perlt, H., Rakow, P. E. L., et al. (2015). The electric dipole moment of the neutron from 2+1 flavor lattice QCD. *Phys. Rev. Lett.* 115, 062001. doi:10.1103/PhysRevLett.115.062001
- [152] Abramczyk, M., Aoki, S., Blum, T., Izubuchi, T., Ohki, H., and Syritsyn, S. (2017). Lattice calculation of electric dipole moments and form factors of the nucleon. *Phys. Rev.* D96, 014501. doi:10.1103/PhysRevD.96.014501
- [153] Gupta, R., Jang, Y.-C., Yoon, B., Lin, H.-W., Cirigliano, V., and Bhattacharya, T. (2018). Isovector Charges of the Nucleon from 2+1+1-flavor Lattice QCD. *Phys. Rev.* D98, 034503. doi:10.1103/PhysRevD.98.034503
- [154] Aoki, S. et al. (2019). FLAG Review 2019, arXiv:1902.08191
- [155] Kim, J., Dragos, J., Shindler, A., Luu, T., and de Vries, J. (2019). Towards a determination of the nucleon EDM from the quark chromo-EDM operator with the gradient flow. *PoS LATTICE2018*, 260. doi:10.22323/1.334.0260
- [156] Rizik, M., Monahan, C., and Shindler, A. (2018). Renormalization of CP-Violating Pure Gauge Operators in Perturbative QCD Using the Gradient Flow. *PoS LATTICE2018*, 215. doi:10.22323/1.334.0215

- [157] Mereghetti, E., de Vries, J., Hockings, W. H., Maekawa, C. M., and van Kolck, U. (2011). The Electric Dipole Form Factor of the Nucleon in Chiral Perturbation Theory to Sub-leading Order. *Phys. Lett. B* 696, 97–102. doi:10.1016/j.physletb.2010.12.018
- [158] Haisch, U. and Hala, A. (2019). Sum rules for CP-violating operators of Weinberg type, arXiv:1909.08955
- [159] Epelbaum, E., Meißner, U.-G., and Glöckle, W. (2003). Nuclear forces in the chiral limit. *Nucl. Phys. A* 714, 535–574. doi:10.1016/S0375-9474(02)01393-3
- [160] Krebs, H., Epelbaum, E., and Meißner, U. G. (2017). Nuclear axial current operators to fourth order in chiral effective field theory. *Annals Phys.* 378, 317–395. doi:10.1016/j.aop.2017.01.021
- [161] Pastore, S., Schiavilla, R., and Goity, J. L. (2008). Electromagnetic two-body currents of one- and two-pion range. *Phys. Rev. C* 78, 064002. doi:10.1103/PhysRevC.78.064002
- [162] Pastore, S., Girlanda, L., Schiavilla, R., and Viviani, M. (2011). The two-nucleon electromagnetic charge operator in chiral effective field theory ( $\chi$ EFT) up to one loop. *Phys. Rev. C* 84, 024001. doi:10.1103/PhysRevC.84.024001
- [163] Krebs, H., Epelbaum, E., and Meißner, U.-G. (2020). Box diagram contribution to the axial two-nucleon current, arXiv:2001.03904
- [164] Fukuda, N., Sawada, K., and Taketani, M. (1954). On the construction of potential in field theory. *Prog. Theor. Phys.* 12, 156. doi:10.1143/PTP.12.156
- [165] Okubo, S. (1954). Diagonalization of Hamiltonian and Tamm-Dancoff Equation. *Prog. Theor. Phys.* 12, 603. doi:10.1143/PTP.12.603
- [166] Epelbaum, E., Glöckle, W., and Meißner, U.-G. (1998). Nuclear forces from chiral Lagrangians using the method of unitary transformation. 1. Formalism. *Nucl. Phys. A* 637, 107–134. doi:10.1016/S0375-9474(98)00220-6
- [167] Epelbaum, E. (2007). Four-nucleon force using the method of unitary transformation. *Eur. Phys. J. A* 34, 197–214. doi:10.1140/epja/i2007-10496-0
- [168] Epelbaum, E. (2006). Four-nucleon force in chiral effective field theory. *Phys. Lett. B* 639, 456–461. doi:10.1016/j.physletb.2006.06.046
- [169] Bernard, V., Epelbaum, E., Krebs, H., and Meißner, U.-G. (2008). Subleading contributions to the chiral three-nucleon force. I. Long-range terms. *Phys. Rev. C* 77, 064004. doi:10.1103/PhysRevC.77.064004
- [170] Bernard, V., Epelbaum, E., Krebs, H., and Meißner, U.-G. (2011). Subleading contributions to the chiral three-nucleon force II: Short-range terms and relativistic corrections. *Phys. Rev. C* 84, 054001. doi:10.1103/PhysRevC.84.054001
- [171] Krebs, H., Gasparyan, A., and Epelbaum, E. (2012). Chiral three-nucleon force at  $N^4$ LO I: Longest-range contributions. *Phys. Rev. C* 85, 054006. doi:10.1103/PhysRevC.85.054006
- [172] Krebs, H., Gasparyan, A., and Epelbaum, E. (2013). Chiral three-nucleon force at  $N^4$ LO II: Intermediate-range contributions. *Phys. Rev. C* 87, 054007. doi:10.1103/PhysRevC.87.054007
- [173] de Vries, J., Li, N., Meißner, U.-G., Nogga, A., Epelbaum, E., and Kaiser, N. (2015). Parity violation in neutron capture on the proton: Determining the weak pion–nucleon coupling. *Phys. Lett. B* 747, 299–304. doi:10.1016/j.physletb.2015.05.074
- [174] Gnech, A. (2016). *Parity and Time Reversal Violation in Two Nucleons Systems*. Master’s thesis, University of Pisa, Pisa, Italy
- [175] Kaiser, N. (2007). Parity-violating two-pion exchange nucleon-nucleon interaction. *Phys. Rev. C* 76, 047001. doi:10.1103/PhysRevC.76.047001



- [176] Epelbaum, E., Glöckle, W., and Meißner, U.-G. (2004). Improving the convergence of the chiral expansion for nuclear forces. 1. Peripheral phases. *Eur. Phys. J. A*19, 125–137. doi:10.1140/epja/i2003-10096-0
- [177] Friar, J. L. (1996). Dimensional regularization and nuclear potentials. *Mod. Phys. Lett. A*11, 3043–3048. doi:10.1142/S0217732396003027
- [178] Kaiser, N., Brockmann, R., and Weise, W. (1997). Peripheral nucleon-nucleon phase shifts and chiral symmetry. *Nucl. Phys. A*625, 758–788. doi:10.1016/S0375-9474(97)00586-1
- [179] Epelbaum, E., Krebs, H., and Meißner, U.-G. (2015). Improved chiral nucleon-nucleon potential up to next-to-next-to-next-to-leading order. *Eur. Phys. J. A*51, 53. doi:10.1140/epja/i2015-15053-8
- [180] Krebs, H. (2019). Electroweak Current Operators in Chiral Effective Field Theory, arXiv:1908.01538. In *9th International Workshop on Chiral Dynamics (CD18) Durham, NC, USA, September 17-21, 2018*
- [181] Epelbaum, E. (2019). Towards high-precision nuclear forces from chiral effective field theory, arXiv:1908.09349. In *6th International Conference Nuclear Theory in the Supercomputing Era (NTSE-2018) Daejeon, Korea, October 29-November 2, 2018*
- [182] Epelbaum, E., Krebs, H., and Reinert, P. (2019). High-precision nuclear forces from chiral EFT: State-of-the-art, challenges and outlook, arXiv:1911.11875
- [183] Maekawa, C. M., Veiga, J. S., and van Kolck, U. (2000). The Nucleon anapole form-factor in chiral perturbation theory to subleading order. *Phys. Lett. B*488, 167–174. doi:10.1016/S0370-2693(00)00851-0
- [184] Epelbaum, E., Glöckle, W., and Meißner, U.-G. (2000). Nuclear forces from chiral Lagrangians using the method of unitary transformation. 2. The two nucleon system. *Nucl. Phys. A*671, 295–331. doi:10.1016/S0375-9474(99)00821-0
- [185] Girlanda, L., Pastore, S., Schiavilla, R., and Viviani, M. (2010). Relativity constraints on the two-nucleon contact interaction. *Phys. Rev. C*81, 034005. doi:10.1103/PhysRevC.81.034005
- [186] Kaplan, D. B., Savage, M. J., and Wise, M. B. (1999). A Perturbative calculation of the electromagnetic form-factors of the deuteron. *Phys. Rev. C*59, 617–629. doi:10.1103/PhysRevC.59.617
- [187] Savage, M. J. and Springer, R. P. (1998). Parity violation in effective field theory and the deuteron anapole moment. *Nucl. Phys. A*644, 235–244. doi:10.1016/S0375-9474(98)80013-4,10.1016/S0375-9474(99)00341-3. [Erratum: *Nucl. Phys. A*657,457(1999)]
- [188] Phillips, D. R., Schindler, M. R., and Springer, R. P. (2009). An Effective-field-theory analysis of low-energy parity-violation in nucleon-nucleon scattering. *Nucl. Phys. A*822, 1–19. doi:10.1016/j.nuclphysa.2009.02.011
- [189] Vanasse, J. and David, A. (2019). Time-Reversal-Invariance Violation in the  $Nd$  System and Large- $N_C$ , arXiv:1910.03133
- [190] 't Hooft, G. (1974). A Planar Diagram Theory for Strong Interactions. *Nucl. Phys. B*72, 461. doi:10.1016/0550-3213(74)90154-0. [,337(1973)]
- [191] Witten, E. (1979). Baryons in the  $1/n$  Expansion. *Nucl. Phys. B*160, 57–115. doi:10.1016/0550-3213(79)90232-3
- [192] Dashen, R. F., Jenkins, E. E., and Manohar, A. V. (1995). Spin flavor structure of large  $N(c)$  baryons. *Phys. Rev. D*51, 3697–3727. doi:10.1103/PhysRevD.51.3697
- [193] Kaplan, D. B. and Savage, M. J. (1996). The Spin flavor dependence of nuclear forces from large  $n$  QCD. *Phys. Lett. B*365, 244–251. doi:10.1016/0370-2693(95)01277-X

- [194] Kaplan, D. B. and Manohar, A. V. (1997). The Nucleon-nucleon potential in the  $1/N(c)$  expansion. *Phys. Rev. C* 56, 76–83. doi:10.1103/PhysRevC.56.76
- [195] Nagels, M. M., Rijken, T. A., and de Swart, J. J. (1975). Baryon Baryon Scattering in an OBEP Approach. 1. Nucleon-Nucleon Scattering. *Phys. Rev. D* 12, 744. doi:10.1103/PhysRevD.12.744
- [196] Nagels, M. M., Rijken, T. A., and de Swart, J. J. (1977). Baryon Baryon Scattering in a One Boson Exchange Potential Approach. 2. Hyperon-Nucleon Scattering. *Phys. Rev. D* 15, 2547. doi:10.1103/PhysRevD.15.2547
- [197] Sakurai, J. J. (1960). Theory of strong interactions. *Annals Phys.* 11, 1–48. doi:10.1016/0003-4916(60)90126-3
- [198] Barton, G. (1961). Notes on the static parity nonconserving internucleon potential. *Nuovo Cim.* 19, 512–527. doi:10.1007/BF02733247
- [199] Holstein, B. R. (1981). Nuclear parity violation parameter  $h_\rho^{(1)'}$ . *Phys. Rev. D* 23, 1618–1623. doi:10.1103/PhysRevD.23.1618
- [200] Herczeg, P. (1987). T violating effects in neutron physics and cp violation in gauge models. In *Workshop on Time Reversal Invariance in Neutron Physics Chapel Hill, North Carolina, April 17-19, 1987*
- [201] Schiavilla, R., Viviani, M., Girlanda, L., Kievsky, A., and Marcucci, L. E. (2008). Neutron spin rotation in n-polarized - d scattering. *Phys. Rev. C* 78, 014002. doi:10.1103/PhysRevC.78.014002, 10.1103/PhysRevC.83.029902. [Erratum: *Phys. Rev. C* 83, 029902(2011)]
- [202] Haxton, W. C. and Henley, E. M. (1983). ENHANCED T VIOLATING NUCLEAR MOMENTS. *Phys. Rev. Lett.* 51, 1937. doi:10.1103/PhysRevLett.51.1937
- [203] Gudkov, V. P., He, X.-G., and McKellar, B. H. J. (1993). On the CP odd nucleon potential. *Phys. Rev. C* 47, 2365–2368. doi:10.1103/PhysRevC.47.2365
- [204] Towner, I. S. and Hayes, A. C. (1994). P, T violating nuclear matrix elements in the one meson exchange approximation. *Phys. Rev. C* 49, 2391–2397. doi:10.1103/PhysRevC.49.2391
- [205] Song, Y.-H., Lazauskas, R., and Gudkov, V. (2013). Nuclear electric dipole moment of three-body systems. *Phys. Rev. C* 87, 015501. doi:10.1103/PhysRevC.87.015501
- [206] Yamanaka, N. (2017). Review of the electric dipole moment of light nuclei. *Int. J. Mod. Phys. E* 26, 1730002. doi:10.1142/S0218301317300028
- [207] Blyth, D. et al. (2018). First Observation of  $P$ -odd  $\gamma$  Asymmetry in Polarized Neutron Capture on Hydrogen. *Phys. Rev. Lett.* 121, 242002. doi:10.1103/PhysRevLett.121.242002
- [208] Schiavilla, R., Carlson, J., and Paris, M. W. (2004). Parity violating interaction effects in the np system. *Phys. Rev. C* 70, 044007. doi:10.1103/PhysRevC.70.044007
- [209] Hyun, C. H., Park, T.-S., and Min, D.-P. (2001). Asymmetry in polarized  $n + p \rightarrow d + \gamma$ . *Phys. Lett. B* 516, 321–326. doi:10.1016/S0370-2693(01)00917-0
- [210] Schiavilla, R., Carlson, J., and Paris, M. W. (2003). Parity violating interactions and currents in the deuteron. *Phys. Rev. C* 67, 032501. doi:10.1103/PhysRevC.67.032501
- [211] Desplanques, B. (1975). Study of parity-violating effects in the neutron capture  $n + p \rightarrow d + \gamma$ . *Nucl. Phys. A* 242, 423–428. doi:10.1016/0375-9474(75)90105-0
- [212] McKellar, B. H. J. (1975). Parity Nonconservation in the Low-Energy Nucleon-Nucleon System: Evidence for an Isotensor Weak Interaction? *Nucl. Phys. A* 254, 349–352. doi:10.1016/0375-9474(75)90221-3
- [213] Desplanques, B. (1980). Parity nonconserving nuclear forces. *Nucl. Phys. A* 335, 147–167. doi:10.1016/0375-9474(80)90174-8

- [214] Eversheim, P. D. et al. (1991). Parity violation in proton proton scattering at 13.6-MeV. *Phys. Lett.* B256, 11–14. doi:10.1016/0370-2693(91)90209-9
- [215] Kistryn, S. et al. (1987). Precision Measurement of Parity Violation in Proton Proton Scattering at 45-MeV. *Phys. Rev. Lett.* 58, 1616. doi:10.1103/PhysRevLett.58.1616
- [216] Berdoz, A. R. et al. (2003). Parity violation in proton proton scattering at 221-MeV. *Phys. Rev.* C68, 034004. doi:10.1103/PhysRevC.68.034004
- [217] Hoferichter, M., Ruiz de Elvira, J., Kubis, B., and Meißner, U.-G. (2015). Matching pion-nucleon Roy-Steiner equations to chiral perturbation theory. *Phys. Rev. Lett.* 115, 192301. doi:10.1103/PhysRevLett.115.192301
- [218] Carlson, J., Schiavilla, R., Brown, V. R., and Gibson, B. F. (2002). Parity violating interaction effects 1: The Longitudinal asymmetry in pp elastic scattering. *Phys. Rev.* C65, 035502. doi:10.1103/PhysRevC.65.035502
- [219] Desplanques, B. (2001). About the parity nonconserving asymmetry in  $n + p \rightarrow d + \gamma$ . *Phys. Lett.* B512, 305–313. doi:10.1016/S0370-2693(01)00713-4
- [220] Song, Y.-H., Lazauskas, R., and Gudkov, V. (2011). Parity violation in low energy neutron deuteron scattering. *Phys. Rev.* C83, 015501. doi:10.1103/PhysRevC.83.015501
- [221] Walecka, J. D. (1995). *Theoretical nuclear and subnuclear physics*, vol. 16
- [222] Yamanaka, N. and Hiyama, E. (2015). Enhancement of the CP-odd effect in the nuclear electric dipole moment of  ${}^6\text{Li}$ . *Phys. Rev.* C91, 054005. doi:10.1103/PhysRevC.91.054005
- [223] Lebedev, O., Olive, K. A., Pospelov, M., and Ritz, A. (2004). Probing CP violation with the deuteron electric dipole moment. *Phys. Rev.* D70, 016003. doi:10.1103/PhysRevD.70.016003
- [224] Hoferichter, M., Ruiz de Elvira, J., Kubis, B., and Meißner, U.-G. (2016). Roy–Steiner-equation analysis of pion–nucleon scattering. *Phys. Rept.* 625, 1–88. doi:10.1016/j.physrep.2016.02.002
- [225] Siemens, D., Ruiz de Elvira, J., Epelbaum, E., Hoferichter, M., Krebs, H., Kubis, B., et al. (2017). Reconciling threshold and subthreshold expansions for pion–nucleon scattering. *Phys. Lett.* B770, 27–34. doi:10.1016/j.physletb.2017.04.039
- [226] Guo, F.-K. and Seng, C.-Y. (2019). Effective Field Theory in The Study of Long Range Nuclear Parity Violation on Lattice. *Eur. Phys. J.* C79, 22. doi:10.1140/epjc/s10052-018-6529-y
- [227] Bass, C. D. et al. (2009). A Liquid helium target system for a measurement of parity violation in neutron spin rotation. *Nucl. Instrum. Meth.* A612, 69–82. doi:10.1016/j.nima.2009.10.055
- [228] Lang, J., Maier, T., Muller, R., Nessi-Tedaldi, F., Roser, T., Simonius, M., et al. (1985). Parity nonconservation in elastic p alpha scattering and the determination of the weak meson - nucleon coupling constants. *Phys. Rev. Lett.* 54, 170–173. doi:10.1103/PhysRevLett.54.170
- [229] Guidoboni, G. et al. (2016). How to Reach a Thousand-Second in-Plane Polarization Lifetime with 0.97-GeV/c Deuterons in a Storage Ring. *Phys. Rev. Lett.* 117, 054801. doi:10.1103/PhysRevLett.117.054801
- [230] Yamanaka, N., Yamada, T., and Funaki, Y. (2019). Nuclear electric dipole moment in the cluster model with a triton:  ${}^7\text{Li}$  and  ${}^{11}\text{B}$ . *Phys. Rev.* C100, 055501. doi:10.1103/PhysRevC.100.055501
- [231] Kabir, P. K. (1982). Test of  $T$  Invariance in Neutron Optics. *Phys. Rev.* D25, 2013. doi:10.1103/PhysRevD.25.2013
- [232] Stodolsky, L. (1982). Parity Violation in Threshold Neutron Scattering. *Nucl. Phys.* B197, 213–227. doi:10.1016/0550-3213(82)90287-5
- [233] Bunakov, V. E. and Gudkov, V. P. (1983). Parity Violation and Related Effects in Neutron Induced Reactions. *Nucl. Phys.* A401, 93–116. doi:10.1016/0375-9474(83)90338-X

- 
- [234] Gudkov, V. P. (1992). On CP violation in nuclear reactions. *Phys. Rept.* 212, 77–105. doi:10.1016/0370-1573(92)90121-F
- [235] Bowman, J. D. and Gudkov, V. (2014). Search for time reversal invariance violation in neutron transmission. *Phys. Rev. C*90, 065503. doi:10.1103/PhysRevC.90.065503
- [236] Shimizu, H. et al. (2017). Discrete Symmetry Tests In Neutron-induced Compound States. *PoS INPC2016*, 187. doi:10.22323/1.281.0187
- [237] Gudkov, V. and Shimizu, H. M. (2018). Nuclear spin dependence of time reversal invariance violating effects in neutron scattering. *Phys. Rev. C*97, 065502. doi:10.1103/PhysRevC.97.065502
- [238] Uzikov, Yu. N. and Haidenbauer, J. (2016). Polarized proton-deuteron scattering as a test of time-reversal invariance. *Phys. Rev. C*94, 035501. doi:10.1103/PhysRevC.94.035501
- [239] Murata, J. et al. (2017). The MTV Experiment: from T-violation to Lorentz-violation. *PoS INPC2016*, 185. doi:10.22323/1.281.0185